



universität
wien

MASTERARBEIT

Titel der Masterarbeit

Differential effects of TbSec24 isoforms on Golgi protein localization

angestrebter akademischer Grad

Master of Science (MSc)

Verfasserin / Verfasser:

Michael Melak

Studienrichtung (lt.
Studienblatt):

Masterstudium Genetik und Entwicklungsbiologie

Betreuerin / Betreuer:

Prof. Graham Warren

Wien, im Dezember 2010

Contents

Abstract	5
Zusammenfassung	7
Abbreviations	9
1. Introduction	11
1.1 Vesicular transport.....	11
1.2 COPII-coated vesicles: formation and function.....	14
1.3 The Golgi.....	18
1.4 Duplication of the Golgi.....	21
1.5 Golgi matrix proteins.....	24
1.6 The parasitic protist <i>T. brucei</i>	27
1.6.1 Cell architecture of <i>T. brucei</i>	28
1.6.2 The cell cycle of <i>T. brucei</i>	30
1.6.3 Characteristics of the secretory system in <i>T. brucei</i>	33
1.6.4 Golgi duplication in <i>T. brucei</i>	35
2. Rationale	38
3. Results	39
3.1 Effects of TbSec24 isoforms on the growth rate and cell cycle progression.....	39
3.2 Specificity and efficiency of TbSec24 RNAi.....	41
3.3 The differential effects of TbSec24 isoforms on the localization of Golgi resident proteins.....	43
3.4 The effect of TbSec24 isoforms on the protein level of TbGRIP70 and TbGRASP.....	50
3.5 The effect of TbSec24 isoforms on the total number of Golgi.....	51
3.5.1 The effect of TbSec24 isoforms on the total number of TbGRIP70 labeled Golgi.....	52
3.5.2 The effect of TbSec24 isoforms on the total number of TbGRASP labeled Golgi.....	55
3.6 The effects of TbSec24.1 RNAi on bilobe and non-bilobe Golgi.....	59
3.6.1 The effect of TbSec24.1 RNAi on TbGRIP70 labeled bilobe and non-bilobe Golgi.....	60
3.6.2 The effect of TbSec24.1RNAi on TbGRASP labeled bilobe and non-bilobe Golgi.....	64
3.7 The effect of TbSec24.1 RNAi on the formation of the paraflagellar rod....	67
3.8 Cell recovery after TbSec24.1RNAi and TbSec24.2 RNAi.....	68

3.8.1	The effect of switching off RNAi on the growth rate and cell cycle stages of <i>T. brucei</i>	69
3.8.2	The effect of switching off TbSec24.1 RNAi and TbSec24.2 RNAi on protein levels.....	71
3.8.3	The effect of switching off TbSec24.1 RNAi on the total number of TbGRIP70 and TbGRASP labeled Golgi.....	72
3.8.4	The effect of switching off TbSec24.1 RNAi on TbGRIP70 and TbGRASP labeled bilobe and non bilobe Golgi	73
3.9	Biochemical analysis of TbGRASP interaction with TbGolgin63.....	75
4.	Discussion.....	78
4.1	Both isoforms of the COPII component TbSec24 are essential	78
4.2	Golgi components are differentially selected by COPII vesicles	79
4.3	Depletion of both TbSec24 isoforms shows differential effects on Golgi labeling and the number of discriminative Golgi populations	82
5.	Material and Methods	85
5.1	Buffers and Solutions.....	85
5.2	Antibody list.....	86
5.3	<i>E. coli</i> transformation	86
5.4	Plasmid DNA Purification.....	87
5.5	DNA extraction and purification from agarose gels in TAE buffer	87
5.6	<i>T. brucei</i> cell lines	87
5.7	Selection markers	88
5.8	Vectors and constructs.....	88
5.9	Silencing of TbSec24.1 and TbSec24.2 expression by RNA interference (RNAi).....	88
5.10	Transfection of Trypanosomes.....	89
5.11	Immunofluorescence microscopy.....	89
5.12	Co-Immunoprecipitation	90
5.13	GST-pulldown	91
5.14	Cell lysate	91
5.15	SDS-PAGE and Immunoblotting (wet blot)	91
5.16	Immunoblot stripping.....	92
	References	93
	Acknowledgements.....	105
	Curriculum Vitae.....	107

Abstract

Despite intense research, the precise mechanisms of Golgi biogenesis are still unclear. In the simple eukaryote *Trypanosoma brucei*, Golgi biogenesis was suggested to require a coordinated supply of components from both the old Golgi and the new ER exit site. These components are then delivered to the site of the new Golgi. For studying further aspects of building a new Golgi in *T. brucei*, it is crucial to know how Golgi resident proteins are selected for transport to the Golgi.

ER-to-Golgi transport is mediated by COPII vesicles. *T. brucei* has two different isoforms of the COPII component TbSec24 (TbSec24.1 and TbSec24.2). In this study RNA interference (RNAi) is used to silence expression of either TbSec24 isoform in the procyclic form of *T. brucei*. Cells show decelerated cell growth after depletion of either TbSec24.1 or TbSec24.2, but reveal no obvious abnormalities in terms of cell cycle progression. It is shown by immunofluorescence microscopy that TbSec24.1 depletion leads to a particularly striking mislocalization of the Golgi marker TbGRASP, whereas the localization of TbGRASP after depletion of TbSec24.2 remains unaffected. TbGRIP70 and Tb ϵ -COP maintain their distinct Golgi localization after induction of RNAi to either TbSec24.1 or TbSec24.2, though TbGRIP70 is lost from non-bilobe Golgi upon depletion of TbSec24.1. The bilobe is a novel structure thought to be involved in Golgi biogenesis. The observed phenotypic effects are fully reversible upon relaxation of the RNAi silencing. These data provide evidence for a TbSec24 isoform-specific selective mechanism of sorting Golgi resident proteins in the early secretory pathway.

Zusammenfassung

Trotz intensiver Erforschung des Golgi Apparates konnte der genaue Mechanismus für dessen Biogenese und Duplizierung sowie für dessen Vererbung an die Tochterzellen noch nicht vollständig entschlüsselt werden. Bisherige Untersuchungen am einzelligen Parasiten *Trypanosoma brucei* haben ergeben, daß in diesem Organismus die Komponenten des neuen Golgi sowohl vom bereits bestehenden Golgi, als auch von der neu gebildeten ER Austrittsstelle abstammen. Die einzelnen Golgi-Bestandteile lagern sich dabei geordnet an jener Stelle zusammen, an welcher der neue Golgi gebildet werden soll. Die vorliegende Arbeit soll weitere Aspekte der Synthese und Vererbung des Golgi Apparates in der prozyklischen Form von *T. brucei* aufzeigen. Im Speziellen wird hier untersucht, ob verschiedene Golgi-Komponenten selektiv für ihren Transport zum Golgi ausgewählt werden.

Der Transport vom Endoplasmatischen Retikulum zum Golgi erfolgt mittels COPII Transportvesikel. Ein wesentlicher Bestandteil dieser Vesikel ist das Protein Sec24, von dem *T. brucei* zwei Isoformen, nämlich TbSec24.1 und TbSec24.2, besitzt. In dieser Studie wird jeweils eine der beiden TbSec24 Isoformen mittels RNA-Interferenz ausgeschaltet. Es zeigt sich, daß sowohl das Fehlen von TbSec24.1, als auch von TbSec24.2, zu einer verlangsamten Zellteilung, bis hin zu einem kompletten Arrest des Zellzyklus führt. Dabei kommt es jedoch zu keinerlei Abnormitäten in Bezug auf die einzelnen Stadien des Zellzyklus. Mittels Immunfluoreszenz-Mikroskopie wird klar, daß beide TbSec24 Isoformen einen selektiven Einfluß auf die Rekrutierung der Golgi Proteine TbGRIP70, Tb ϵ -COP und TbGRASP zum Golgi Komplex ausüben. Eine Abnahme von TbSec24.1 in der Zelle führt dazu, daß TbGRASP nicht mehr am Golgi Apparat detektiert werden kann. Umgekehrt jedoch zeigt eine verminderte Expression von TbSec24.2 keinerlei derartigen Auswirkungen. Die Untersuchung des Aufenthaltsortes der Golgi Marker TbGRIP70 und Tb ϵ -COP ergibt keine Veränderung, weder nach beeinträchtigter Expression von TbSec24.1, noch von TbSec24.2. Eine Detektion von TbGRIP70 ist nach verminderter TbSec24.1 Expression allerdings nur noch an jenen Golgi Apparaten möglich, welche mit einer kürzlich entdeckten ‚Bilobe‘-förmigen Struktur assoziiert vorliegen. Zusätzlich zeigen wir noch die Reversibilität sämtlicher aufgetretener Phänotypen nach dem Abschalten der RNA-Interferenz.

Abbreviations

AB	antibody
BSD	blasticidin S deaminase
CGN	cis-Golgi network
DAPI	4',6'-Diamino-2-phenylindol
DIC	differential interference contrast microscopy
Dox	doxycycline
ER	endoplasmatic reticulum
ERES	ER exit site
ERGIC	ER-Golgi intermediate compartment
F	flagellum
FAZ	flagellum attachment zone
FBS	foetal bovine serum
GAP	GTPase activating protein
GEF	guanine nucleotide exchange factor
GPI	glycosylphosphatidylinositol
GST	glutathione S-transferase
HRP	horseradish peroxidase
K	kinetoplast
N	nucleus
NPT	neomycin phosphotransferase
NSF	N-ethylmaleimide-sensitive factor
PBS	phosphate buffered saline
PFR	paraflagellar rod
PFRA	paraflagellar rod protein A
RNAi	RNA interference

RT	room temperature
SB	sample buffer
SN	supernatant
SNAP	soluble NSF attachment protein
SNARE	soluble NSF attachment protein receptor
<i>T. brucei</i>	<i>Trypanosoma brucei</i>
TAP	tandem affinity purification
Tet	tetracycline
TGN	trans-Golgi network
VSG	variable surface glycoprotein
VTC	vesicular tubular clusters

1. Introduction

The Golgi is an essential component of the eukaryotic secretory system [1]. It plays an important role in post translational protein modifications, sorting, and transport of proteins [2]. Therefore, replicating cells must ensure that the biogenesis of the new Golgi is executed precisely to guarantee a fully functional Golgi in each daughter cell.

Studying Golgi biogenesis and partitioning in higher eukaryotes is very difficult, as for example in mammalian cells the Golgi consists of many stacks which are assembled into a higher order Golgi ribbon [3]. However, the monoflagellated parasitic protist *Trypanosoma brucei* (*T. brucei*) harbors only a single Golgi stack that duplicates during the cell cycle [4]. Therefore, *T. brucei* is an ideal model system as the single Golgi can be visualized directly during the duplication process.

1.1 Vesicular transport

Vesicular transport is necessary in eukaryotic cells to carry soluble macromolecules, membrane-spanning and soluble proteins as well as membrane components from one chemically distinct, membrane-enclosed compartment to another. Thereby, a selective, precise and continual flux of cargo is maintained [5, 6]. Movement of cargo between the different compartments occurs by small, membrane-enclosed carrier vesicles which bud from a donor compartment [6]. The budding process is initiated by recruitment of vesicle coat proteins which assemble around the donor membrane in the cytoplasm [7]. Coat assembly is controlled by members of the monomeric family of GTPases [8-10]. The coat proteins then mediate selective accumulation and incorporation of cargo as well as subsequent membrane deformation. Afterwards, the vesicles are separated from the donor compartment [7]. They are transported to their destination by diffusion or by transport mediated by motor proteins along a cytoskeletal track [11]. During the transport to the target compartment, the coat proteins are removed from the vesicles and recycled for reuse. After reaching the target organelle, the uncoated vesicles tether and fuse with the target membrane whereupon cargo is released into the acceptor compartment [7].

At least three major vesicle coats have been identified so far which are used for transport between the distinct organelles of the vesicular transport system: COPI [12], COPII [8] and Clathrin [13, 14]. A schematic overview of the major membrane traffic pathways using COPI, COPII and clathrin coated carrier vesicles is shown in Figure 1.

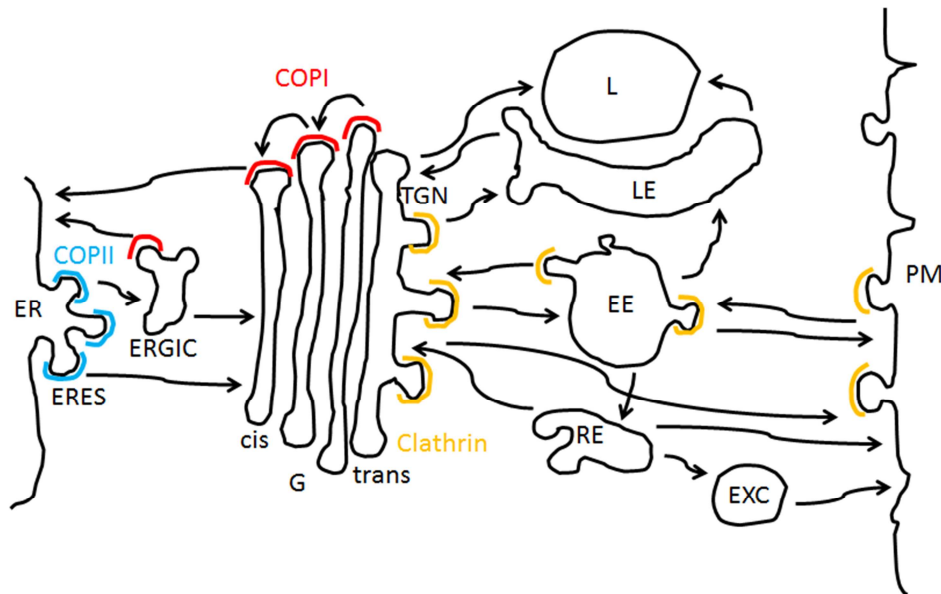


Figure 1: Intracellular transport pathways. The scheme shows the major routes of the biosynthetic, lysosomal, and endocytic pathways in mammalian cells. The colors show the locations of COPI (red), COPII (blue), and clathrin (yellow) coated vesicles. The single transport steps are indicated by arrows. EE: early endosome, ER: endoplasmic reticulum, ERES: ER exit site, ERGIC: ER-Golgi intermediate compartment, EXC: exocytic carrier, G: Golgi, L: lysosome, LE: late endosome, PM: plasma membrane, RE: recycling endosome, TGN: *trans* Golgi network. Adapted from [7].

Proteins destined for the cell surface or lysosomes, as well as transmembrane proteins, are assembled in the endoplasmic reticulum (ER) membrane [15]. The proteins exit the ER in COPII-coated carrier vesicles [8], budding at special sites for transport, called ER exit sites (ERES) [16, 17]. These vesicles are delivered either to interconnected ER-Golgi intermediate compartments (ERGIC) (also known as vesicular tubular cluster – VTCs) in mammalian cells [18, 19] or directly to the *cis*-face of the Golgi, where membrane fusion takes place [8]. These ERGICs (or VTCs) are cargo-rich compartments mediating the transport of secretory cargo between the ER and the Golgi [20, 21].

COPI-coated retrograde transport vesicles recycle proteins from the Golgi or the ERGIC back to the ER [12, 22]. These vesicles are also responsible for transport within the Golgi [23].

Clathrin-coated vesicles are involved in two major routes of the vesicular transport system: the transfer of molecules between the *trans*-Golgi network (TGN) and the endosome, as well as the transport between the plasma membrane and the early endosome [13, 14, 24].

The different coats also play a role in cargo selection by directly recognizing sorting signals at transmembrane cargo proteins. Soluble luminal cargoes are recognized by interaction with the luminal domains of transmembrane cargo adaptor proteins. These adaptor proteins bind to components of the vesicle coat through their cytosolic domain [25-29]. By means of these sorting signals, the distinct routes through the vesicular transport system are determined [30].

Specificity in membrane targeting is ensured by assortative types of surface markers on both, transport vesicles and target membranes. This specificity depends on three types of proteins: members of the Rab GTPase family [31], tethering factors [32] as well as the so called soluble N-ethylmaleimide-sensitive factor attachment protein receptors (SNAREs) [33].

Rab proteins form the largest family of monomeric GTPases. In their active, GTP bound state, Rabs are localized to transport vesicles and target membranes. These proteins execute regulatory functions in all major steps of membrane traffic: vesicle budding, transport and tethering leading to vesicle fusion [34]. Rab family members are selectively distributed in distinct membranes and their regulatory function is restricted to the compartment where they are localized. Hence, these proteins play a role in maintaining the specificity of vesicular transport and organelle identity. Activated Rabs bind specifically to a variety of soluble factors, called Rab effectors, which show a high structural heterogeneity. Rab effectors transduce the signals of an activated Rab protein to facilitate specific functions of membrane transport, such as protein sorting in vesicle formation, vesicle motility and tethering. [31, 34-36].

Mostly, tethering factors are either long coiled-coil proteins, which can form long homodimeric coiled coils, or multisubunit complexes [37]. These proteins are required to implement the specific initial interaction between a transport vesicle and its target

membrane. Tethering factors are thought to form long physical bridges to bring vesicles and their target compartment in close proximity before they can fuse [32].

SNARE proteins catalyze the membrane fusion reactions in vesicular transport [33]. According to the SNARE hypothesis, a v-SNARE on the vesicle membrane forms a specific pair with a t-SNARE on the membrane of the target organelle [38]. V-SNAREs are single polypeptide chains, whereas t-SNAREs are composed of three chains. Both SNARE types have characteristic helical domains which form a stable helical-bundle when a v-SNARE and a t-SNARE interact. Upon interaction, fusion of the lipid bilayers is initiated [39].

1.2 COPII-coated vesicles: formation and function

The export of proteins from the ER to the Golgi occurs in most eukaryotic cells at the ERES [16], facing the *cis*-side of the Golgi [40]. Among several organisms, the number and location of the ERES is different. *Saccharomyces cerevisiae* for example does not show a well-organized ERES, budding seems to occur across the entire ER membrane. However, the yeast *Pichia pastoris* shows between two and five well defined ERES [41, 42]. In mammalian cells there are several hundred ERES distributed throughout the cytoplasm with an accumulation of ERES in the region directly adjacent to a stacked Golgi [17].

Transport of proteins from the ER is mediated by COPII-coated vesicles [8]. The COPII machinery consists of a multi-subunit complex comprised mainly of five components: the small GTPase Sar1 [43], as well as the heterodimers Sec23/Sec24 [44] and Sec13/Sec31 [45, 46]. For a simplified schematic of a fully assembled COPII-coated vesicle see Figure 2.

The large peripheral membrane protein Sec16 stably binds to the ER membrane at the ERES. Originally identified in *S. cerevisiae*, Sec16 seems to prevent the coat from premature disassembly and it might play a role as a membrane bound scaffold for the organized assembly of COPII components [58-60]. Yeast two-hybrid and other direct binding experiments have shown in yeast that Sec16 interacts directly with the COPII coat subunits Sec23, Sec24 and Sec31 [61, 62]. Studies indicated that overexpression of Sec16 is lethal in *S. cerevisiae* [61]. Depletion of Sec16 in *P. pastoris* and *Drosophila* leads to a disruption of the ERES and inhibits ER export [58, 63]. In mammalian cells, two orthologues of Sec16 have been identified, Sec16A and the shorter Sec16B [64]. Overexpression of Sec16A, which seems to contain the most similarities to Sec16 in other organisms, leads to an inhibition of ER to Golgi transfer [65], whereas siRNA depletion of Sec16A results in a delayed transport [64-66].

Export of cargo from the ER is directed by a large variety of export signals. These signals are located in the polypeptide chain of integral membrane cargo proteins or of transmembrane adaptor proteins [30]. Several different types of transport signals in cargo proteins have been identified, for example di-acidic, di-aromatic or di-hydrophobic motifs [67-70].

As denoted above, direct interactions between components of the COPII coat and secretory proteins are essential for cargo inclusion into the transport vesicle. However, not all secretory cargo can bind directly to the coat proteins. For example, soluble proteins interact via transmembrane adaptors [30]. Several potential transmembrane adaptor proteins have been identified, including for example the protein ERGIC53 [71-73] and the p24 proteins [74-76]. These adaptors are thought to cycle between compartments of the ER and the Golgi. After arriving at the target compartment, the adaptor protein releases the cargo and is recycled back to the ER in COPI vesicles [30]. Adaptor proteins contain a luminal domain for recognizing sorting signals on soluble secretory proteins and a cytoplasmic domain including the sorting signals required for anterograde transport in COPII vesicles and retrograde COPI dependent movement [77-80].

Sec24 is the major responsible component for efficient recruitment of specific cargo into newly forming COPII vesicles [52]. The ER export signals on transmembrane cargo or transmembrane adaptor proteins can be directly recognized and bound by

multiple independent cargo binding sites on the Sec24 subunit. These multiple independent binding sites expand the repertoire of cargo proteins to be selectively captured into COPII transport vesicles [53, 81].

Another intrinsic method for extending the range and selectivity of cargo proteins is the fact that most organisms contain multiple isoforms of Sec24. *S. cerevisiae* has three Sec24 isoforms, Sec24p, Lss1p, and Lst1p, of which only Sec24p is essential for growth [82, 83]. *P. pastoris* contains two Sec24 homologues, PpSec24 and PpLst1. Of these, only PpSec24 is essential [84]. The human genome expresses four Sec24 isoforms (Sec24A – Sec24D), which are all nonessential for cell growth, at least in vitro [70, 85, 86].

The different Sec24 isoforms were shown to have distinct affinity for ER export signals on secretory cargo [53, 86], accompanied by a high level of functional redundancy [70]. For example, it has been described in *S. cerevisiae* that optimal packaging of the plasma membrane ATPase Pma1p requires a mixture of both heterodimers Sec23p/Sec24p and Sec23p/Lst1p. However, only deletion of Lst1p leads to defects in the packaging and transport of Pma1p [83, 87]. A variety of knockdown and *in vitro* experiments indicated that the four human Sec24 isoforms have distinct selectivity within a series of aromatic and hydrophobic signals. For instance, Sec24A is selectively required for the ER to Golgi transport of proteins containing a dileucine motif but not for cargo transport mediated by other signals. However, double knockdown of Sec24A with one of the other three Sec24 isoforms restricted transport of all proteins containing aromatic or hydrophobic signals. In contrast, the four isoforms show partially overlapping transport signal specificity as for example the combination of Sec24B, Sec24C and Sec24D are able to rescue the depletion of Sec24A [70]. Recently, it has been demonstrated in mice *in vivo* that Sec24B is specifically required for ER exit and secretion of Vangl2, a key component of the Wnt signaling pathway. The inability to secrete Vangl2 results in a lethal failure of neural tube closure [88]. Furthermore, the incorporation of several SNARE proteins in yeast and mammals into COPII vesicles depends on the specific binding to a specific Sec24 isoform [52, 53, 89].

Transmembrane adaptor proteins are also selected differentially by Sec24 isoforms. Among others, proteins containing a Glycosylphosphatidylinositol (GPI) anchor are dependent on binding to p24 adaptor proteins to be packaged into COPII vesicles.

For example, the yeast GPI-anchored protein Gas1p requires the p24 protein Emp24p for COPII mediated transport [75, 90]. Furthermore, Gas1p transport to the cell surface is delayed upon deletion of Lst1p [91]. Additionally, it has recently been shown that the mammalian GPI-anchored protein CD59 is preferentially transported from the ER to the Golgi in COPII vesicles containing the isoforms Sec24C and Sec24D. Thereby, transport of CD59 is also dependent on the p24-p23 complex. p24-p23 is a putative cargo receptor for GPI-anchored proteins, as the complex interacts with CD59 and features the same Sec24C and Sec24D dependence as CD59 [92].

1.3 The Golgi

Electron microscopy studies demonstrated that in most eukaryotic cells the Golgi is comprised of a characteristic series of four to six ordered, flattened cisternal membrane structures and associated vesicles [93, 94]. Each Golgi stack shows two distinct faces: a *cis*-face and a *trans*-face (Figure 3). The *cis*-face is the site, where proteins and lipids arrive from the ER and enter the Golgi [94]. Cargo is transported then from the *cis*- via the medial- to the *trans*-cisternae. The *trans*-face of the Golgi is connected to a special compartment, composed of an interconnected tubular network, named the *trans*-Golgi network (TGN) [95]. A constant flow of multiple types of transport carriers from and to the TGN occurs. For example, clathrin coated vesicles deliver material to the endosomal/lysosomal system [96]. Additionally, larger, uncoated carrier vesicles can emerge from the TGN and travel to the plasma membrane [97]. Moreover, vesicles involved in endocytic and recycling pathways fuse with the TGN [98].

The presence of a Golgi with its characteristic morphology is often said to be a fundamental feature of eukaryotic cells. However, there are some differences within the broad field of eukaryotes, even within distinct cell types of the same organism. These differences can concern number, size, structure or enzymatic composition of the Golgi stack. The Golgi in vertebrate cells for instance is organized into a single continuous ribbon-like structure, at least in interphase cells (Figure 3). Plants and flies on the other hand contain multiple single stacks [18, 94]. The yeast *P. pastoris* contains two to six stacked Golgi per cell [41], whereas the protozoa *Toxoplasma*

gondii contains only a single Golgi [99]. An example for an atypical morphology is the Golgi in *S. cerevisiae*. Here, the Golgi consists of unstacked, individual cisternae, which are dispersed randomly throughout the cytoplasm [100]. Additionally, some parasitic unicellular eukaryotes without visible Golgi structures have been described [1].

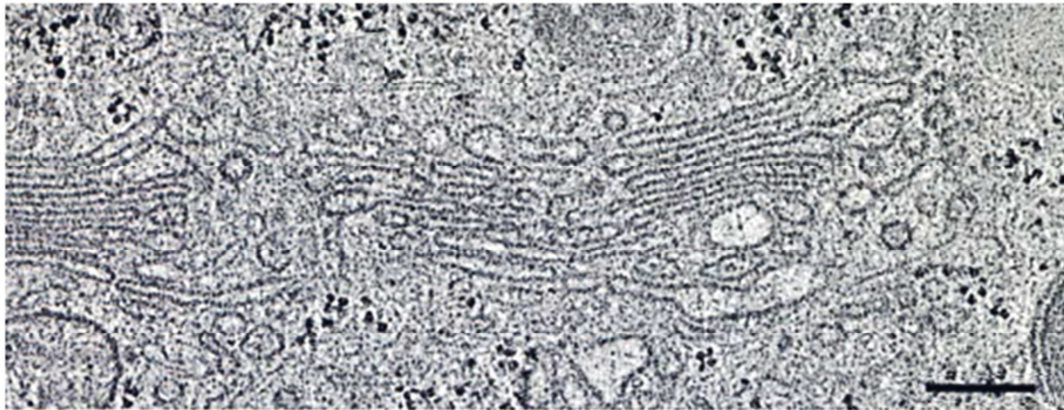


Figure 3: Morphology of a significant part of the mammalian Golgi on an ultrastructural level.

The image shows the characteristic membranes of multiple individual Golgi cisternae in a normal rat kidney cell. Two compact Golgi regions separated by a non-compact region can be seen. Bar = 250 nm. [18]

The Golgi lies on the track between the ER and other compartments of the vesicular transport system [6]. There, it has to fulfill two major functions: First, the Golgi is the site of several complex carbohydrate modifications, which are found on many proteins and lipids [94, 101-103]. For example, inside the ER, an N-linked oligosaccharide is attached to many secretory proteins on asparagine residues [103]. This glycosylation plays an important role in correct folding and recognition of misfolded proteins [104]. Upon arrival at the Golgi, proteins containing an N-linked oligosaccharide are processed successively on their way through the Golgi. Thereby, several glycosyl transferases and glycosidases add or remove a variety of sugars at various positions leading to the formation of glycoproteins [105, 106]. Additionally, O-linked glycosylation occurs in the lumen of the Golgi. Here, proteins are modified on serine or threonine residues by glycosyl transferase enzymes to produce proteoglycans [107, 108]. Second, the Golgi is the central organizing organelle of the membrane-trafficking system. It plays a major role in sorting of proteins and lipids for delivery to other subcellular compartments [6]. At the *cis*-side, proteins are divided into either components for ongoing transport through the Golgi or for being

transported back into the ER [94]. At the *trans*-side and the TGN, proteins are sorted for further delivery to their subcellular destinations [95].

There are two proposed mechanisms for anterograde transport through the cisternal stack: The stable compartments model and the cisternal maturation model [109], (Figure 4).

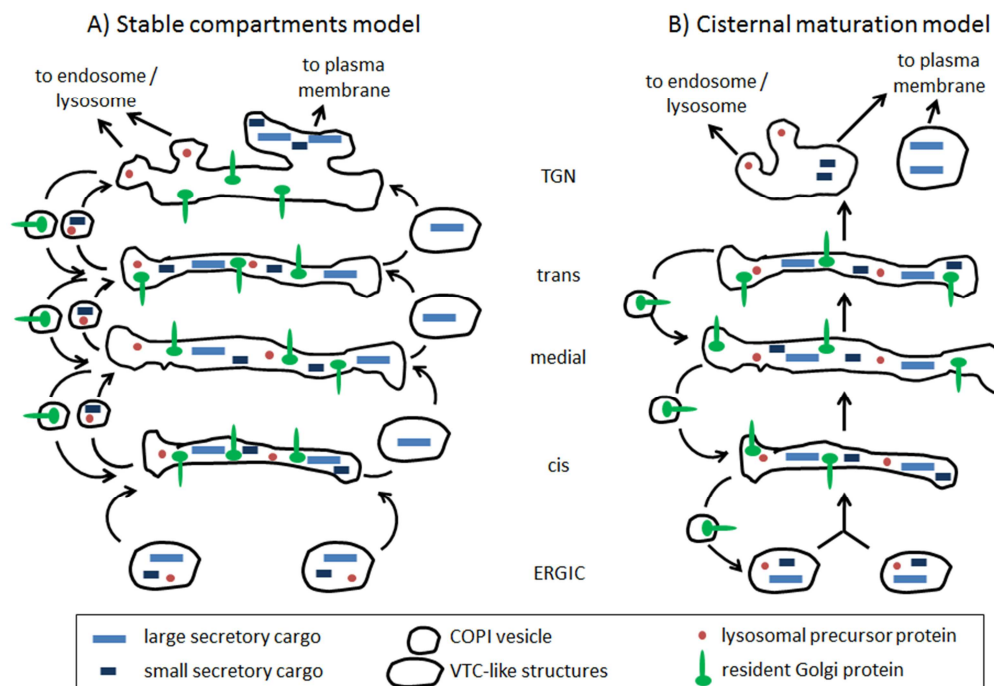


Figure 4: Two models for transport through the Golgi. A) In the stable compartments model cargo is transported through the static Golgi compartments in anterograde COPI vesicles and/or VTC-like structures. Additionally, escaped Golgi resident proteins can be recycled by retrograde COPI vesicles. B) In the cisternal maturation model ER derived vesicles fuse homotypically and create a new *cis*-cisterna. This new cisterna progresses from the *cis*-face to the *trans*-face. Thereby, anterograde cargo remains inside the cisterna. Maturation of the cisterna occurs through the recycling of resident Golgi enzymes by retrograde moving COPI vesicles. The figure was adapted from [2, 110].

The stable compartments model was suggested after executing *in vitro* transport assays in which it was shown that COPI coated vesicles carry cargo in an anterograde way across the Golgi stack [111-116]. This model proposes that the Golgi is composed of a series of relatively static, pre-existing compartments, which each contain a characteristic complement of resident enzymes. Transport vesicles derived from the ER are thought to fuse with the *cis*-face of the Golgi and release their cargoes into the *cis*-cisterna. Different cargoes which have to be delivered to distinct destinations within the cell are transported among the Golgi compartments from the *cis*-face to the *trans*-face by anterograde COPI vesicles [105, 117-119].

Large secretory cargo might be carried through the Golgi by VTC-like structures, which were shown in vertebrate cells. However, their exact composition and the distinction to Golgi cisternae are still unknown [18]. In addition to anterograde COPI vesicles, retrograde COPI coated vesicles were identified, which transport escaped Golgi and ER resident proteins to their preceding compartments [12, 119].

In the cisternal maturation model, the Golgi itself is thought to be rather a dynamic than a static structure [120, 121]. Transport carriers from the ER fuse constantly and homotypically to build a new *cis*-cisterna. This *cis*-cisterna then matures progressively and migrates through the stack where it subsequently becomes a medial-cisterna and ends up as *trans*-cisterna [122]. During the maturation process, secretory cargo as well as Golgi enzymes are carried forward by the entire cisternae. However, appropriate Golgi resident proteins and lipids, which belong to earlier compartments, are transported back by COPI coated vesicles. Finally, after becoming part of the TGN, the cargo is delivered in various types of vesicles to its final destination [109, 122-126].

1.4 Duplication of the Golgi

When a cell replicates it has to be ensured that both daughter cells obtain a complete and fully functional subset of essential cellular contents [127].

Several different, yet not mutually exclusive scenarios have been proposed on how new organelles are formed during cell division. The main difference between the models is the issue whether organelles can form *de novo* or are inherited from the mother cell. *De novo* formation occurs when an organelle can be formed without requirement of a pre-existing template or copy. The whole necessary information about structure and function of the self-organizing organelle is obtained from its constitutive components [128]. Alternatively, the organelles are considered to be autonomously replicating and are maintained by inheritance of progenitors [128]. For example, the progenitor organelle might form a template and provides new material for the formation of a new copy alongside the original. Another alternative is that the progenitor organelle grows until it reaches a certain size and undergoes fission afterwards [129].

Organelles present in multiple copies can theoretically be distributed by a passive, stochastic process during cell division. Single copy organelles however have to be duplicated and segregated prior to cytokinesis by an active and ordered mechanism. Another possibility for partitioning of single copy organelles is to break down into multiple subunits, which are then dispersed through the cytoplasm and partitioned into the nascent daughter cells afterwards [128].

One of the main controversial issues in the research field of organelle duplication is the question if the Golgi is synthesized *de novo* by a self-organizing process, or if its assembly is dependent of a pre-existing template [130].

In agreement with the maturation model, it has been proposed that the Golgi can form *de novo* (Figure 5A) [41, 42, 122]. ER derived COPII vesicles, containing Golgi membrane components and enzymes, bud from the ERES and fuse homotypically to generate a new *cis*-compartment. Simultaneously, retrograde COPI coated vesicles return components from later Golgi compartments to the corresponding ones. By means of this retrograde transport, the Golgi stack becomes polarized [122, 123]. For completion of the Golgi, cytosolic peripheral membrane proteins are recruited to the cisternal membrane [131], and Golgi destined components are returned from later secretory compartments, for example endosomes [132].

Confocal video microscopy studies of the dynamics of ERES and Golgi structures in *P. pastoris* have shown that the ERES forms *de novo* in the newly forming bud. Shortly after the formation of a new ERES, new Golgi structures appear adjacent to it. Both, the new ERES and the new Golgi arise at locations which previously lacked detectable structures. This leads to the conclusion that the newly formed ERES might give rise to COPII vesicles which fuse and form a new *cis*-Golgi cisterna. Thereby, inheritance of the old Golgi does not seem to be essential for maintaining a new Golgi in the new daughter cell [41].

In an alternative scenario, new Golgi components assemble around a pre-existing and permanent template [130]. For example, it has been described in the protists *Trichomonas vaginalis* and *Tritrichomonas foetus* as well as in *T. gondii* that these organisms inherit their single copy Golgi by a lateral growth process followed by medial fission (Figure 5B) [133, 134].

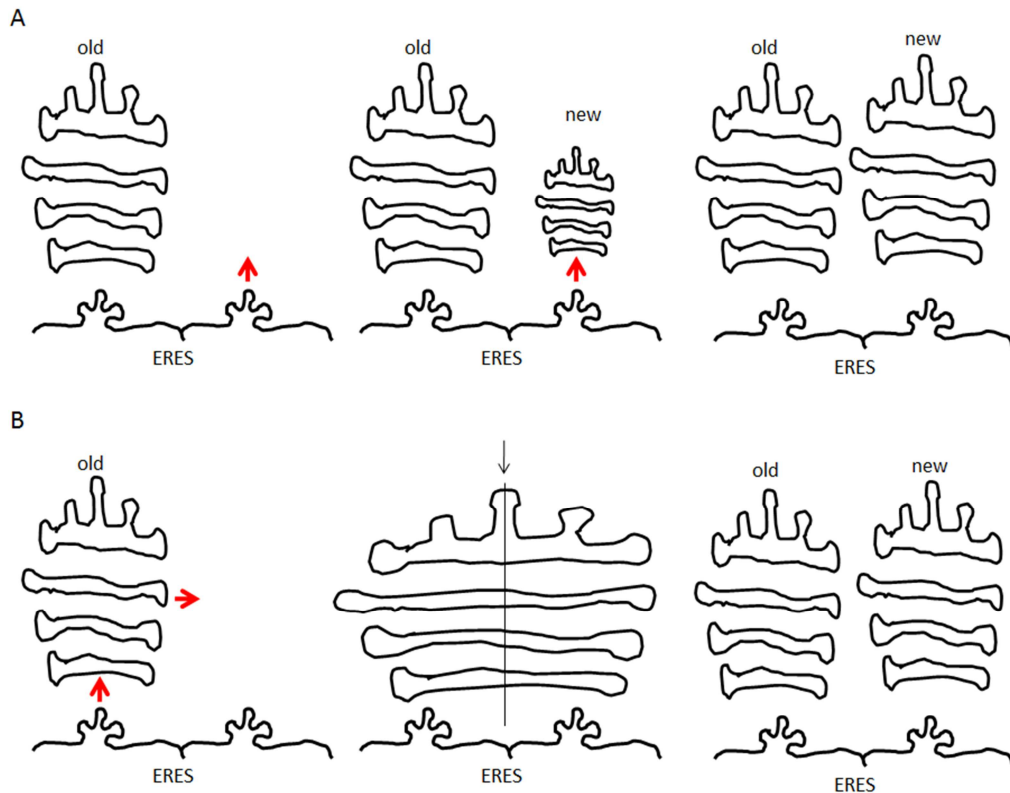


Figure 5: Two different scenarios of Golgi biogenesis. A) *De novo* biogenesis of the Golgi: The new Golgi appears at the site of the new ERES. Thereby the old Golgi plays no role in the formation of the new one. B) Growth and fission: The Golgi duplicates by lateral cysternal growth, followed by medial fission.

The inheritance of the Golgi in mammalian cells is different from the scenarios shown above. During the S-phase, material is delivered to the existing Golgi until it reaches a certain size [135]. At the beginning of mitosis, the lateral tubular connections, which crosslink the Golgi stacks during the interphase, disappear. The lateral rupture is followed by a loss of stacking of the cisternae and the Golgi fragments into small vesicular and tubular clusters [136, 137]. However, is still not completely unraveled what happens exactly during the dispersion process of the Golgi compartments. The most widely accepted model suggests that membrane fusion is blocked in mitosis. For this reason, continued COPI vesicle budding creates an accumulation of vesicles and tubules (Golgi haze) containing Golgi enzymes and structural components. Thereby, these vesicles remain independent from the ER [138-142], and might be partitioned by a stochastic process into the daughter cells [143]. Other studies also suggest a role of the mitotic spindle in Golgi partitioning between the daughter cells, as the Golgi fragments accumulate at the spindle poles and along spindle microtubules [144, 145]. After partitioning, the Golgi reassembles by fusion of the

vesicles and tubules into Golgi cisternae [146], followed by cisternal restacking [147]. Thereby it is not entirely known if all the Golgi fragments can completely self-assemble, or if they stringently need a template to attach.

1.5 Golgi matrix proteins

The Golgi is known to be a highly dynamic organelle. It has to manage the permanent exchange of membranes as well as correct and spatially ordered sorting and modification of proteins and lipids [148]. These complex features of the Golgi led to the assumption of existing mechanisms and components for maintaining the correct stacking of the particular Golgi cisternae. Research conducted in order to prove this supposition showed the presence of crosslinking proteins connecting adjacent Golgi cisternae [149-151]. Other studies revealed a detergent-insoluble structural scaffold termed Golgi matrix in a cell free system [152, 153]. This matrix is thought to serve as a template for the reassembling Golgi enzymes containing membranes during cytokinesis. [154, 155]. It also seems to maintain the characteristic Golgi structure [154, 156, 157].

By now, several components of the putative Golgi matrix have been identified. The majority of the Golgi located matrix proteins are members of the Golgi reassembly and stacking protein family (GRASP) and of the golgin protein family [158].

GRASP proteins were first identified in cell free assays for post-mitotic reassembly of Golgi stacks. These assays revealed two isoforms of GRASP in mammals: GRASP55 and GRASP65 [159, 160]. GRASP proteins occur as homodimers, interacting via their N-terminal GRASP domain [159-161]. Generally, GRASPs are peripherally attached to the cytoplasmic surface of the *cis*- and medial-cisternae of the Golgi membrane by an N-terminal myristic acid anchor [159, 160]. Although GRASP proteins are thought to be well conserved in evolution [158], the yeast orthologue of GRASP65, Grh1p, shows some fundamental differences to GRASP proteins in most other organisms [162]. Instead of a myristic acid anchor, Grh1 contains an N-terminal amphipathic helix which mediates *cis*-Golgi association after N-terminal acetylation [162].

The specific targeting of GRASP proteins to the Golgi membrane is still unclear [163]. The myristoylation alone was shown not to be sufficient for localization of GRASP to the Golgi. Additional factors, such as integral membrane proteins at the *cis*- and medial Golgi, are thought to act as a receptor for direct recruiting of GRASP proteins to their correct location at the Golgi [163].

It was also demonstrated that GRASP requires interaction with members of the Golgin protein family for their Golgi localization. In mammalian cells, GRASP55 is associated with Golgin45 [156], whereas GRASP65 interacts with GM130 [161]. In yeast, the recruitment of Grh1p to the Golgi is dependent on the interaction with Bug1p. Bug1p shows comparable structural features of GM130 in mammals but a different primary sequence of amino acids [162].

All golgins contain a characteristic motif, namely large regions of coiled-coil alpha helical rod-like structures [164, 165]. These proteins interact either peripherally with the cytoplasmic surface of the Golgi membrane, or they are integral membrane proteins, containing a transmembrane domain near the C-terminus [165]. Many members of the peripheral golgin proteins interact with small GTPases of the Rab-, Arf- or Arl-families. The GTPases thereby function as adaptor proteins to recruit peripheral membrane golgins to the Golgi membrane. An example is the golgin p115, which binds through its coiled-coil region to Rab1 at the *cis*-Golgi and Golgi intermediates [166].

Different regions of the Golgi contain a distinct subset of golgins [165]. For example, GM130 is mainly found at the *cis*-face of the Golgi [167], whereas Golgin245 is localized to the *trans*-face [168]. Golgins also differ in their location within a single cisterna. The golgin Giantin is associated with the edges [169] whereas GM130 localizes to the center of the *cis*-cisterna [167].

The different Golgi matrix proteins were shown to fulfill functions in various aspects of maintaining Golgi structure and dynamics. *In vitro* assays indicated that mammalian GRASP homologues mediate direct stacking interactions of the adjacent compartments during Golgi reassembly [159, 170]. More recent studies showed unaffected Golgi stacking but defects in Golgi ribbon formation after depletion of GRASP55 or GRASP65 *in vivo*. Therefore, a function of GRASPs in laterally linking of Golgi cisternae was suggested to be more likely [171, 172].

Both GRASP isoforms in mammalian cells might also play a role in regulating mitotic disassembly of the Golgi as they are heavily phosphorylated after mitotic entry. It is thought that phosphorylation leads to disruption of the oligomerisation of GRASPs, followed by disruption of cisternal stacking [170]. Thereby, GRASP65 is phosphorylated at the C-terminus by the polo-like kinase 1 [170, 173], whereas GRASP55 is a substrate of ERK2 in mitosis [174]. Furthermore, GRASP65 was suggested to have a function in signal transduction during cell growth, as it is phosphorylated by ERK in interphase cells [175]. Additional functions of GRASP have been described. For example, in mammalian cells GRASP65 was shown to play a role in apoptosis, where the protein is a target for caspase cleavage, leading to fragmentation of the Golgi ribbon [176].

Generally, it can be stated that golgin proteins are responsible for maintaining the structure and function of the Golgi. Thereby, the roles of distinct golgins seem to differ within the large protein family, also due to their diverse localization at the Golgi. As known so far, the main function of golgins are tethering interactions. The well-studied golgin GM130 for example binds to the golgin p115 [177]. Both proteins were shown to play a role in tethering COPII vesicles either directly to the *cis*-face of the Golgi or to Golgi intermediates [178]. Golgin84 in turn is located at the Golgi rims, playing a role in tethering retrograde COPI vesicles [179].

Additionally to tethering actions, golgins might also mediate membrane fusion events. To enable an interaction of SNARE proteins, the golgins have to bring the membrane of the acceptor and the donor compartment in close proximity. Therefore, conformational changes in Golgins may be necessary, which could be promoted by binding to Rab GTPases [163]. Also direct interactions of golgins with SNAREs have been observed, which would argue for combined tethering and fusion actions [178, 180].

A third major function of golgins is the formation and maintenance of the Golgi structure by providing an external scaffold which is linked to Golgi membranes [153]. For example GM130, p115 and giantin are required for cisternae stacking during Golgi assembly as shown in *in vitro* experiments [147].

1.6 The parasitic protist *Trypanosoma brucei*

The parasitic protist *Trypanosoma brucei*, including the subspecies *Trypanosoma brucei brucei* and the human infective forms *T. b. rhodesiense* and *T. b. gambiense* are the cause for African sleeping sickness, which leads to about 70,000 deaths per year. The parasite also causes the disease 'nagana' in cattle, leading to serious agricultural problems in developing countries [4].

T. brucei reside in two different hosts: mammals and the tsetse fly *Glossina* ssp [4], which is the only known vector for transmission of trypanosomes [181]. After uptake of the parasite by a tsetse fly sucking blood from an infected mammal, it is located in the midgut of the fly. Later, *T. brucei* migrates to the salivary glands of *Glossina*, from where it is transmitted by biting to a new mammalian host [181].

During this transmission cycle, the parasites undergo several life cycle stages which differ in terms of morphology, gene expression and proliferation [182]. In the mammalian bloodstream, trypanosomes proliferate as morphologically slender forms. After the number of parasites increases, they change into a non-proliferative stumpy form [182]. Both bloodstream forms express variable surface glycoproteins (VSG), covering densely the entire surface of the parasite [183, 184]. These VSGs are linked to the surface membrane by a GPI anchor [185]. A part of the *T. brucei* population within a mammalian host periodically changes the molecular composition of the VSGs, which allows them to avoid antibody responses and to survive in the mammalian bloodstream, leading to a chronic infection [186, 187]. The trypanosome genome contains several hundreds of different VSG genes. Thereof, only one VSG gene is expressed at a time [188].

After the translocation into the midgut of the tsetse fly, the parasites differentiate into the procyclic form of *T. brucei* [4]. Thereby, VSG synthesis is repressed rapidly [189], and the VSG coat is replaced by a new surface coat composed of GPI-anchored procyclins [190, 191]. Procyclin is thought to protect the cells from hydrolases in the tsetse fly midgut [192]. In the midgut, the procyclic form proliferates and migrates afterwards to the salivary gland. There, *T. brucei* is attached to the salivary gland wall by the flagellar membrane as a so called epimastigote form [4]. After continuing proliferation, cells differentiate into the non-proliferative metacyclic form. In this stage, *T. brucei* expresses a new VSG coat and detaches from the gland wall. Upon being

released into the salivary gland lumen, the parasites can be transmitted to a new mammalian host [4].

1.6.1 Cell architecture of *T. brucei*

The cell shape of *T. brucei*, which differs between the life cycle stages, is defined by the highly ordered, membrane-associated microtubule cytoskeleton. These subpellicular microtubules are positioned underneath the plasma membrane and are connected to each other and the plasma membrane. They are arranged along the anterior-posterior axis of the cell, with their plus ends at the posterior part of the cell [193, 194].

Most organelles in *T. brucei* exist as a single copy, making it a helpful model organism in molecular cell biology. Within the cell, the organelles are positioned precisely between the center and the posterior end of the cell [195] (Figure 6). This clearly defined polarized organization might be regulated by the subpellicular microtubules [193].

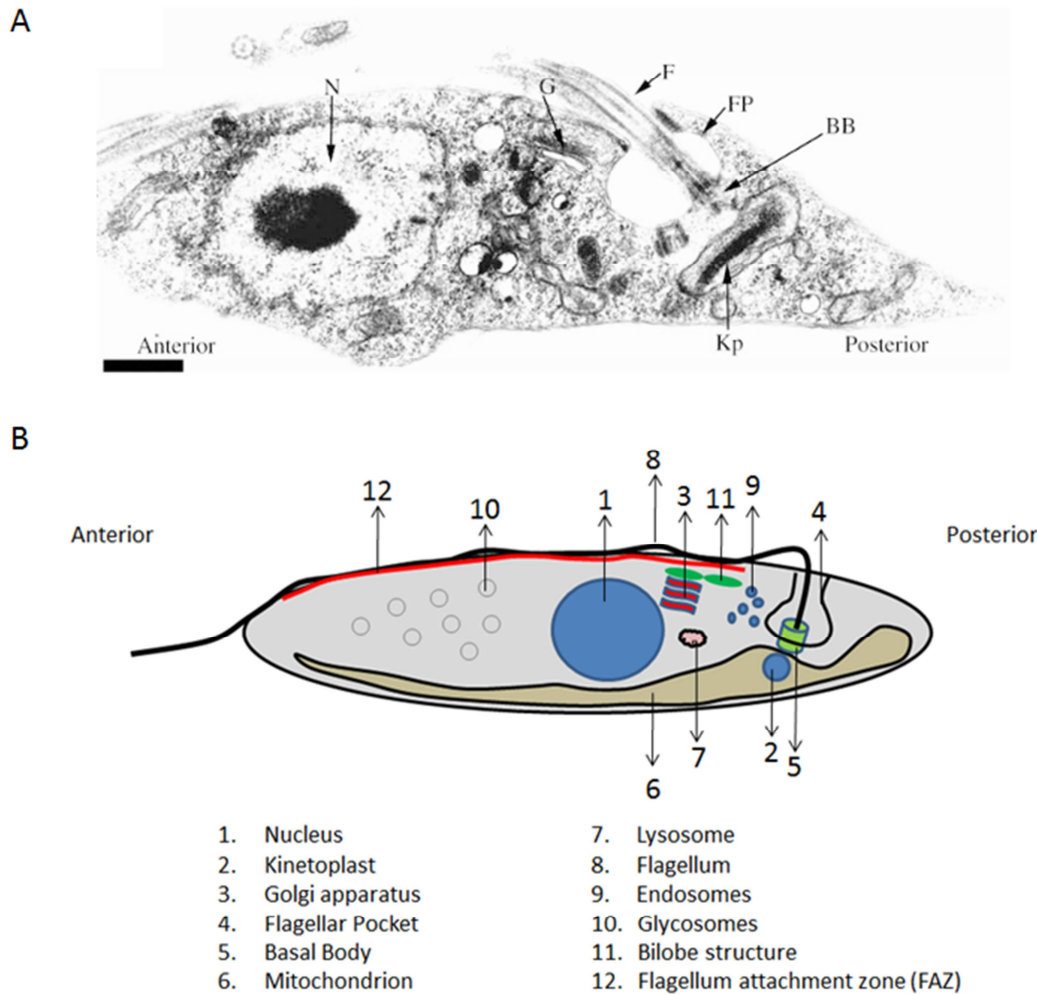


Figure 6: A) **Ultrastructural morphology of *T. brucei*.** The picture shows the arrangement of the posterior end of the cell. The kinetoplast (Kp) is linked to the basal bodies (BB) that are located at the base of the flagellar pocket (FP). The basal bodies nucleate the flagellum (F). The Golgi (G) is located between the flagellar pocket and the nucleus (N). Bar = 1 μm . Image A was taken from [196]. B) **Cell architecture of *T. brucei*.** It shows a simplified schematic of the location of the major organelles of the cell. The schematic (B) was adapted from [4].

Early in the cell cycle, trypanosomes have a single Golgi stack which is positioned between the nucleus and the flagellar pocket [4], closely associated with the ERES [197]. Recently, a TbCentrin2/TbCentrin4 positive bilobe-shaped structure was identified adjacent to the Golgi and the ERES. The bilobe is thought to act as a scaffold for the regulation of the position and size of the new Golgi [198].

The flagellar pocket was shown to be the exit point for the flagellum [199]. Trypanosomal motility is dependent upon its single flagellum, comprising a conventional axonemal structure [200] plus an associated paraflagellar rod (PFR) [201]. A complex transmembrane crosslinking attaches the flagellum to the cell body

along the flagellum attachment zone (FAZ) [202]. The FAZ itself is composed of a cytoplasmic filament complex and a set of four specialized microtubules adjacent to it [193, 200]. These four microtubules differ from other subpellicular microtubules in the way that they originate near the basal bodies and are thought to have antipodal polarity. Additionally they were shown to be more stable compared to other microtubules of the corset [193].

The flagellum originates from the basal body, which is a short cylindrical structure related to centrioles. It forms the microtubule-organising centre (MTOC) for the flagellar axonemal microtubules [203]. Through the mitochondrial membrane, the basal body is linked to the kinetoplast [204], which contains the microtubular DNA [205].

The nuclear genome of *T. brucei* harbors 11 'megabase' chromosomes (~1 – 6 Mb) and more than 100 minichromosomes (~50 - 150 Kb) [206]. Minichromosomes contain non-transcribed copies of VSG genes and expand the VSG gene pool [207].

1.6.2 The cell cycle of *T. brucei*

The typical eukaryotic cell cycle consists of four phases: G1, S, G2, and M. Broadly, the cell division cycle in *T. brucei* follows this scheme. The parasite contains a number of single copy organelles and structures which have to be accurately duplicated and segregated in a precise order (Figure 7). In procyclic *T. brucei*, the cell cycle typically lasts about 8.5 hours. The basal body is the first duplicating organelle [208]. Thereby, the new basal body first matures from the old existing probasal body and then it initiates the growth of the new flagellum [209, 210]. Coinciding with formation of a new ERES, the Golgi duplicates next. Golgi duplication is followed by duplication of the bilobe structure [198, 211]. Throughout the cell cycle, additional Golgi appear and disappear which are not associated to the bilobe structure [211]. More details about Golgi duplication and the bilobe structure are given in chapter 1.6.4.

At about the same time the bilobe segregates, the flagellar pocket duplicates. Afterwards, the flagellum grows and the new FAZ starts to assemble [198, 212]. These events are followed by duplication and segregation of the kinetoplast [212],

which is mediated by the separating basal bodies [204]. In Trypanosomatides, the kinetoplast features a discrete S and G2 phase, which is coordinated with the nuclear genome replication and segregation [213]. Kinetoplast duplication begins and is completed considerably before nuclear division [212], which allows a clear discrimination between the different cell cycle stages. Upon kinetoplast duplication, cells contain 1 nucleus and 2 kinetoplasts (1N2K) [212]. After duplication of the kinetoplast, the division of the nucleus takes place [212] which results in a cell containing 2 kinetoplasts and 2 nuclei (2N2K).

Nuclear division is followed by cytokinesis along the entire longitudinal axis, which generates two daughters with the same complement of organelles [208, 212]. The site of furrow initiation is determined by the anterior end of the new flagellum and/or the FAZ [214]. After furrow ingression, duplicating cells remain joined at the posterior ends for some time. At least, flagellar beat seems to be required for their abscission [215]. However, the accurate mechanism of cytokinesis is yet unidentified.

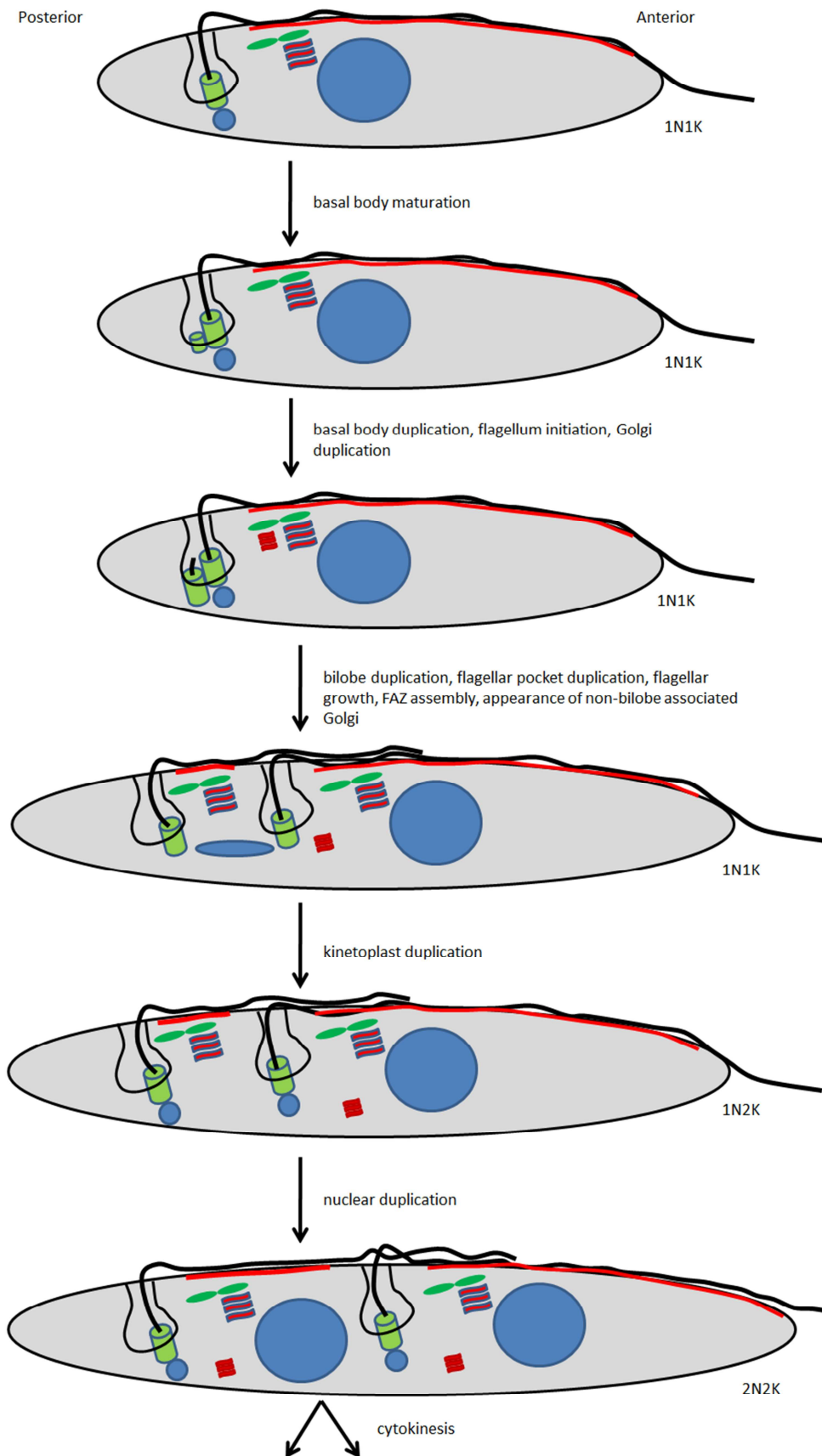


Figure 7: Cell cycle of *T. brucei*. The picture shows a simplified schematic illustration of the *T. brucei* cell cycle. See text for details. Legend see Figure 1. The figure was adapted from [4, 212, 216].

Compared to other eukaryotic cells, the cell division cycle of *T. brucei* shows some unique features. During the cell cycle the organelles are strictly positioned within the posterior end of the cell [217]. However, the position of the organelles relative to the posterior end of the cell differs between the life cycle stages [217]. Furthermore, some cell cycle checkpoints and regulatory proteins are known to be absent in particular life cycle stages [217]. For example, it was shown that correct cytokinesis is not dependent upon the completion of nuclear mitosis. Disruption of the mitotic spindle generates cells with a mitochondrial genome but no nucleus. These cells are termed zoids [195].

1.6.3 Characteristics of the secretory pathway in *T. brucei*

Generally, the basic features of the secretory pathway have been highly conserved between trypanosomatids and other eukaryotes [197]. This includes, among other things, the structure, composition and function of diverse membrane enclosed compartments, the transport routes, as well as the molecular machinery for cargo selection, budding, targeting, tethering and fusion processes. Nevertheless, *T. brucei* provides several special features compared to other eukaryotic cells [197, 218].

One of the most extraordinary characteristics of the trypanosomal secretory pathway is that both endocytosis as well as exocytosis are restricted at the plasma membrane to the flagellar pocket [218]. The reason is thought to be the fact that the flagellar pocket lacks subpellicular microtubules, which probably inhibit vesicular traffic at the rest of the plasma membrane [197].

The early secretory pathway of *T. brucei* broadly follows the mechanism of ER to Golgi transport by COPII vesicles in other organisms [219]. The COPII machinery of *T. brucei* contains two paralogues of each TbSec23 and TbSec24 subunit, namely TbSec23.1, TbSec23.2, as well as TbSec24.1 and TbSec24.2. Both TbSec23 and TbSec24 isoforms are essential for cell growth in the bloodstream form [219].

Two distinct heterodimers (TbSec23.1/TbSec24.2 and TbSec23.2/TbSec24.1) are used in trypanosomal COPII vesicle assembly [219]. It was shown in the bloodstream form of *T. brucei* that the heterodimers differ in their redundancy of transporting cargo from the ER to the Golgi. Several transmembrane and soluble cargos can be sorted

into COPII vesicles by both of the TbSec23/TbSec24 heterodimers [219]. On the other hand for example, the transport of GPI-anchored proteins is restricted to TbSec23.2/TbSec24.1. It was observed that depletion of either TbSec23.2 or TbSec24.1 leads to a delay in transport of GPI-anchored VSG to the cell surface [219].

In the bloodstream form of *T. brucei*, the ERES is located close to the FAZ [219]. This particular part of the ER associates with the specialized subpellicular microtubule quartet and the FAZ filament [193, 219, 220]. Adjacent to the ERES lies the *cis*-face of the Golgi [211]. The bilobe structure is located alongside to the ERES and the Golgi, close to the FAZ and the flagellar pocket [198, 221]. A schematic overview of the early secretory pathway arrangement is shown in Figure 8.

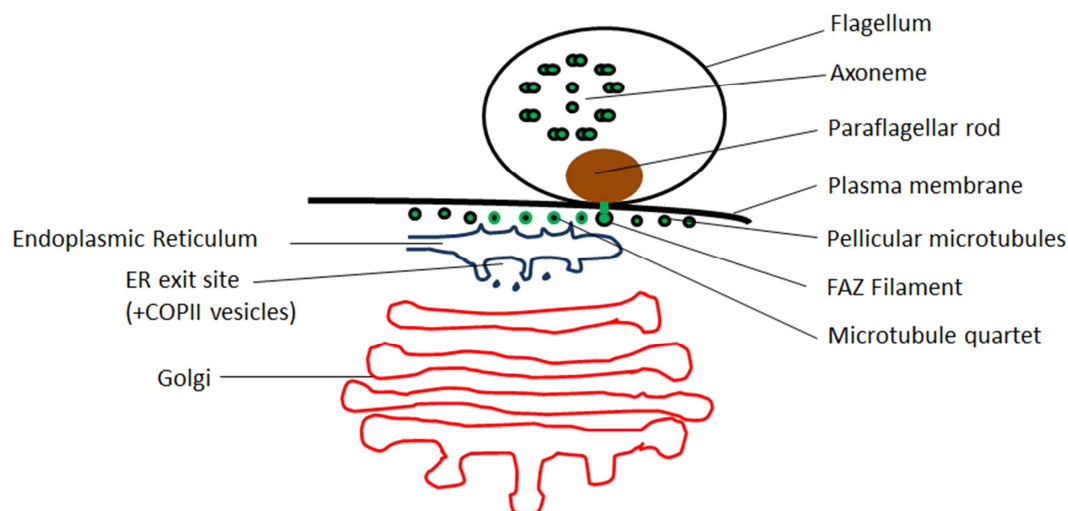


Figure 8: Simplified diagram of the ERES and Golgi location in the bloodstream form of *T. brucei*. The picture shows a cross section through the FAZ, ERES and Golgi region of the cell. The diagram was inspired and adapted from [193, 219].

The Golgi in *T. brucei* shows the common polarized organization into *cis*-, medial-, and *trans*-Golgi face. It is composed of three to four flattened cisternae and a more frayed TGN [196, 197]. Two different types of Golgi can be distinguished within *T. brucei* cells. The first form is composed of a single stack of cisternae, located between the nucleus and the flagellar pocket, closely related to the ERES [197, 211]. Additionally, the Golgi is closely associated with the anterior lobe of the previously discovered bilobe structure [198], therefore it will be named ‘bilobe Golgi’ in this study. This Golgi type is regarded as stacked, transport competent ‘main Golgi’.

On the other hand, further Golgi appear and disappear during progression of the cell cycle [211]. They were shown to be smaller in size and are not located proximate the bilobe structure [196]. Although these type of Golgi are accompanied by an ERES, their formation and function is still unclear [196, 211]. Ultrastructural studies have shown that these Golgi are structurally less organized compared to the bilobe associated Golgi [196].

1.6.4 Golgi duplication in *T. brucei*

Video fluorescence microscopy indicates that the onset of Golgi biogenesis starts about an hour after completion of the previous cytokinesis. The Golgi duplication process itself takes about two hours (Figure 9). Over this period of time, the new forming Golgi grows until it reaches about the same size of the old Golgi [211]. The process of Golgi biogenesis is chronologically and spatially exactly matched with the appearance of a new ERES. Both organelles start growing juxtaposed to each other at the same time and stay closely associated during segregation into the new daughter cells [211].

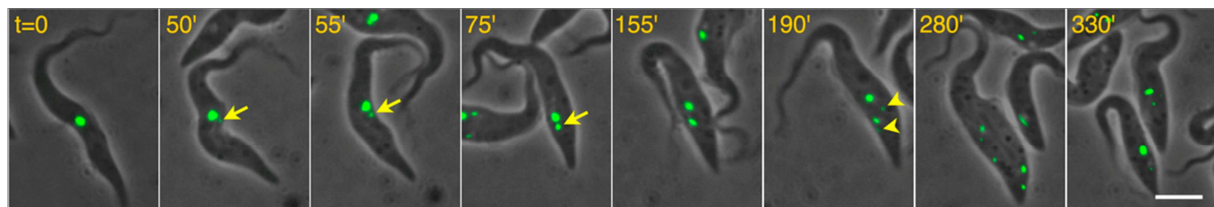


Figure 9: Golgi duplication in *T. brucei*. The video fluorescence microscopy images show a single procyclic *T. brucei* cell, which stably expresses the Golgi marker TbGRASP-GFP (green). The formation of a new Golgi (arrow) as well as additionally appearing and disappearing Golgi (arrowheads) were visualized during the period of a whole cell cycle. Bar = 5 μ m. The figure was taken from [211].

Immunofluorescence microscopy after costaining of the Golgi and the bilobe revealed that at the beginning of the cell cycle, the old Golgi is located close to the anterior lobe (Figure 10A). Simultaneously with the appearance of the new ERES at the posterior lobe [198], assembly of the new Golgi could be observed, also adjacent to the posterior lobe (Figure 10B). After the new Golgi has grown to a certain size, it moves away from the old Golgi (Figure 10C). During bilobe duplication, the old Golgi remains associated to the old bilobe, and the newly formed Golgi localizes close the

new one. Both Golgi are positioned at the anterior lobe (Figure 10C-E). The emergence of non-bilobe associated Golgi can be seen in Figure 10F. [198]

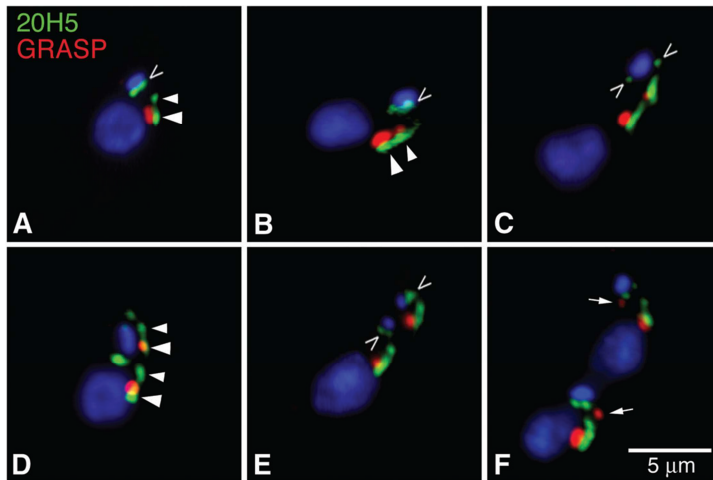


Figure 10: Duplication of the bilobe and the Golgi in *T. brucei*. Triple labeled cells (anti-GRASP – red, anti-Centrin – green, and DAPI – blue) show the chronologically ordered duplication of the Golgi (red), the basal body (green, open arrowheads) and the bilobe (green, solid arrowheads) during the cell cycle process. The Golgi can be distinguished between bilobe associated and non-bilobe associated (red, arrows) ones. Details are explained in the text. The picture was adapted from [198].

Fluorescence recovery after photobleaching experiments have shown that at least one component for assembly of the new Golgi in *T. brucei* is not supplied from the new ERES. Some of the material is transported directly from the old Golgi to the new one [211]. Taken together, these data indicate that Golgi duplication in *T. brucei* follows kind of a mixture of the duplication models denoted in Figure 5, with an additional role of the bilobe for defining the correct assembly site (Figure 11).

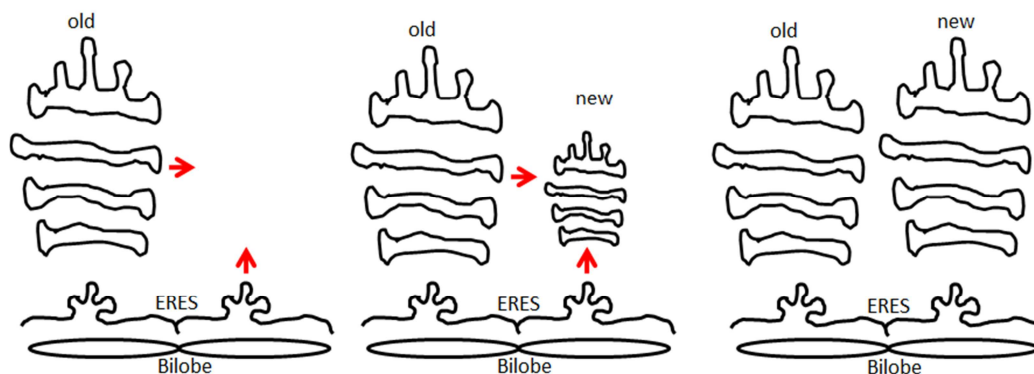


Figure 11: A model for Golgi biogenesis in *T. brucei*. The new Golgi is not the exclusive product of the new ERES. At least one Golgi component is supplied from the old Golgi [211]. The bilobe is thought to play a role in regulating the position and the size of the new Golgi [198, 216].

The assembly of the new Golgi in *T. brucei* seems to follow an accurately ordered mechanism. By investigation of several different Golgi markers, it was determined that Golgi growth is a process comprising at least two coordinated steps [222]. First, structural (TbGRASP) and enzymatic (TbGntB – a membrane spanning, putative Golgi enzyme) components assemble next to the newly forming ERES [222]. This assembly step is followed by the delivery of components which are necessary for transport of cargo within and from the Golgi (Tb ϵ -COP, TbGRIP70) [222]. Interestingly, the Golgi in *T. brucei* starts to operate after it reaches about 10 – 20 % of its final size, soon after initiation of the second step [222].

2. Rationale

The exact mechanisms and the relevant components needed for maintaining the structure and function of the Golgi as well as for its duplication and inheritance are still unclear at the present time.

The parasitic protist *T. brucei* is a good model system to study different aspects of intracellular vesicular traffic since most organelles appear in single-copy and are compactly organized in the posterior part of the cell. Several proteins involved in vesicular transport in *T. brucei* are highly conserved in more complex eukaryotes. It is believed that in *T. brucei* the new Golgi is assembled through the combined actions of the old Golgi and the new ERES [211] and that the components needed for assembly of the Golgi are delivered in a regulated process [222]. To obtain further information of Golgi biogenesis in *T. brucei*, it might be useful to know if several components needed to form a functional new Golgi are selectively delivered in different COPII vesicles from the ER to the Golgi.

T. brucei contains two different isoforms of the COPII vesicle component TbSec24, namely TbSec24.1 and TbSec24.2. First of all, it has to be investigated, if both TbSec24 isoforms are essential for cell growth in the procyclic form of *T. brucei*. Additionally, the influence of depletion of either TbSec24 isoforms on the cell cycle progression has to be established.

Recent studies have shown a disparity between the two isoforms in delivering GPI-anchored proteins such as VSG to the cell surface [219]. However, it is not clear if both TbSec24 isoforms also differ in their specificity of selecting Golgi associated proteins. Does depletion of either TbSec24 isoforms differentially impact Golgi recruitment of the Golgi markers TbGRIP70, Tb ϵ -COP and TbGRASP? What are the effects on these proteins after RNAi silencing of TbSec24.1 or TbSec24.2? Only very little is known about the frequently occurring non-bilobe associated Golgi. Does the ER to Golgi transport differentially influence bilobe Golgi and non-bilobe Golgi? Are non-bilobe Golgi synthesized the same way as the bilobe Golgi? As non-bilobe Golgi appear and disappear during the cell cycle, the question arises if they are less stable compared to bilobe Golgi?

3. Results

3.1 Effects of TbSec24 isoforms on the growth rate and cell cycle progression

In order to inhibit ER to Golgi transport by disrupting COPII vesicle formation, procyclic *T. brucei* 29-13 cells were transfected with either a TbSec24.1 RNAi or a TbSec24.2 RNAi construct.

Cells were counted every 24 hours after RNAi induction over six days to study whether depletion of TbSec24 isoforms has an influence on cell viability.

Both, the TbSec24.1 RNAi (Figure 12A) and TbSec24.2 RNAi (Figure 12B) cell line showed comparable growth defects after depletion of either TbSec24 isoform. A gradual decrease in the growth rate was observed and started to manifest itself two days after induction of RNAi.

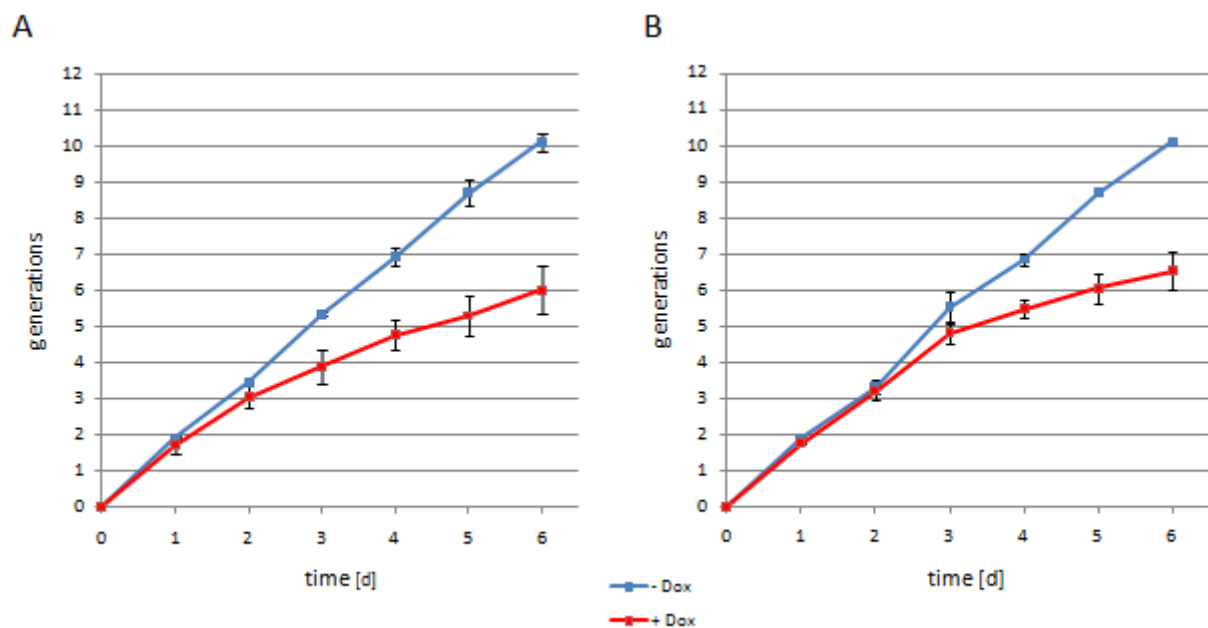


Figure 12: Cell growth after RNAi knockdown. TbSec24.1 RNAi cells (A) and TbSec24.2 RNAi cells (B) were grown in the absence or presence of doxycycline (Dox) to induce RNAi. Samples were counted every 24 hours. The results are presented as mean \pm SD, n = 3. The growth rate of untreated control cells is shown in blue; the red line indicates the RNAi induced cells.

The observed growth defects led to the question if cells arrested growth in a specific cell cycle stage. Immunofluorescence microscopy pictures were taken every 24 hours of RNAi induced cells and the uninduced control cells. Nucleus and kinetoplast of the

cells were stained with DAPI and the pictures were analyzed afterwards. Uninduced cells usually show a distribution of about 85 % cells with one nucleus and one kinetoplast (1N1K), about 10 % of cells with one nucleus and two kinetoplasts (1N2K), and about 5 % of cells with two nuclei and two kinetoplasts (2N2K). Abnormal cells with two nuclei and one kinetoplast (2N1K), zoids (0N1K), or cells with one nucleus and without any kinetoplast (1N0K) were very rarely observed (below 1.5 %). Comparing induced RNAi cells to control cells, no significant effects on the cell cycle stages could be seen over the course of the RNAi in neither TbSec24.1 RNAi (Figure 13A) nor TbSec24.2 RNAi cells (Figure 13B). To obtain a most accurate result, a large number of cells were analyzed (Figure 13C).

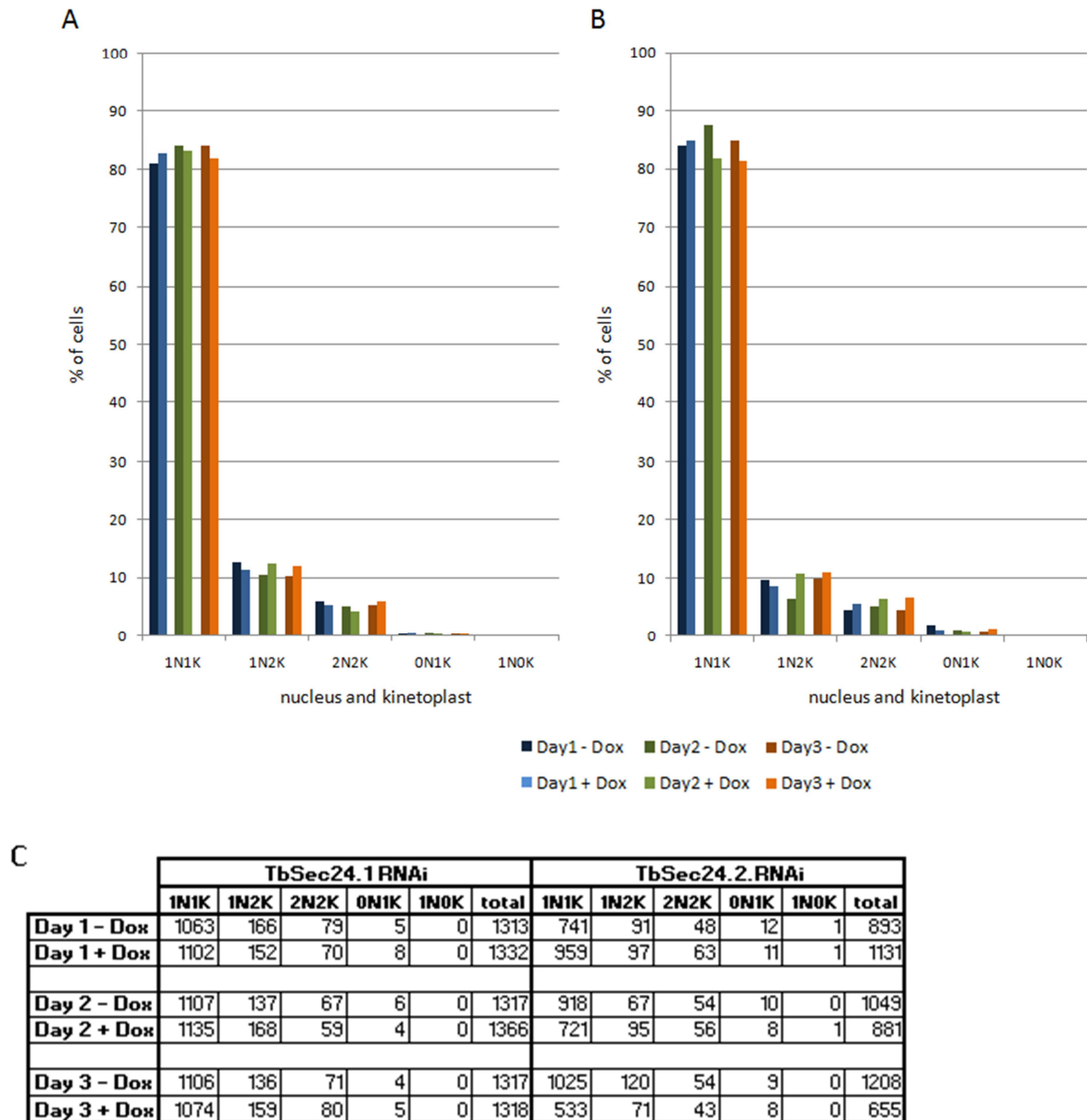


Figure 13: Effects of TbSec24 isoforms on cell cycle stages. Induced RNAi of both TbSec24 isoforms, TbSec24.1 (A) and TbSec24.2 (B) did not show significant effects on cell cycle stages compared to uninduced control cells after one, two and three days after depletion of either TbSec24 isoforms. C) The absolute numbers of analyzed cells are shown.

3.2 Specificity and efficiency of TbSec24 RNAi

Immunofluorescence microscopy data showed that TbSec24.1 RNAi led only to depletion of TbSec24.1 but not of TbSec24.2 (Figure 14A). Contrary, TbSec24.2 RNAi only depleted TbSec24.2 (Figure 14B). Immunoblotting confirmed the

specificity of either RNAi. A decrease in the protein level could only be detected in TbSec24.1 and not in TbSec24.2 after TbSec24.1 RNAi and vice versa (Figure 14C).

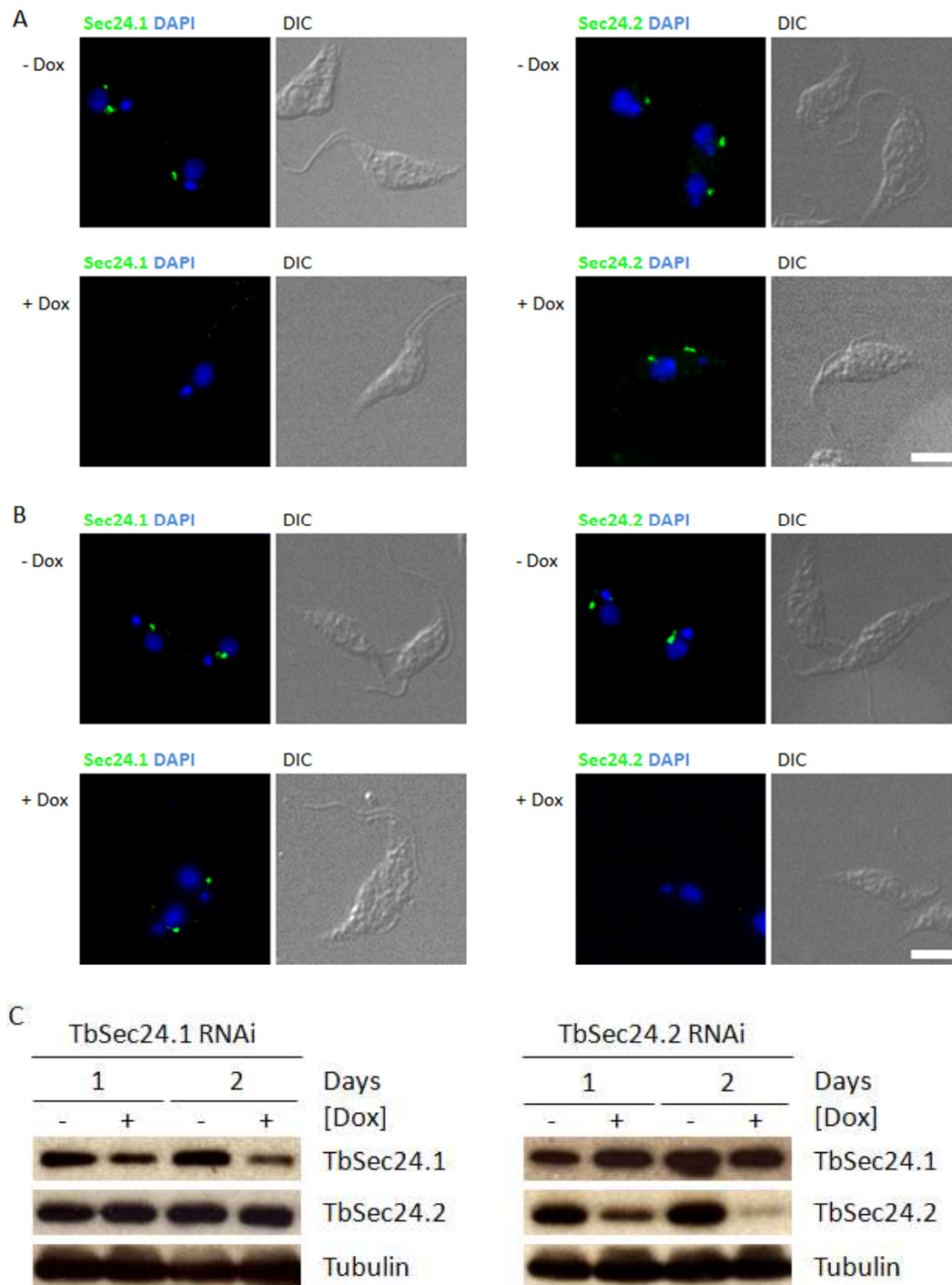


Figure 14: Specificity of TbSec24 RNAi. Fluorescence microscopy images of methanol fixed cells expressing TbSec24.1 RNAi (A) or TbSec24.2 RNAi (B) show the site of COPII vesicle formation (anti-TbSec24.1 or anti-TbSec24.2, green) and the nuclear and kinetoplast DNA (DAPI, blue). The pictures were taken two days after TbSec24 isoform depletion. TbSec24 RNAi induced cells showed depletion only of the corresponding TbSec24 isoform, but not of the other. Bar = 5 μ m. C) Immunoblotting of TbSec24.1. RNAi cells show increasing depletion of the TbSec24.1 protein levels after one and two

days of induction, whereas constant amounts of TbSec24.2 were detected. Blotting TbSec24.2 RNAi cells showed a reciprocal result. Lysate: 4×10^6 cells per lane. Anti-tubulin antibodies were used as loading control. The immunoblot was done by Lars Demmel.

TbSec24 RNAi efficiency in both cell lines was tested by semiquantitative immunoblotting (Figure 15). Both TbSec24 isoforms showed about similar levels of depletion. After one day, the protein level decreased to about 40 % and after two days to about 15 % of the level of uninduced cells.

It was shown in the bloodstream form that RNAi of one TbSec24 isoform leads to an upregulation of the other isoform at the mRNA level. TbSec24.1 mRNA increased at about 70 % after TbSec24.2 RNAi and TbSec24.2 mRNA at about 40 % after TbSec24.1 RNAi [219]. However, depletion of either TbSec24 isoform in procyclic *T. brucei* did not result in an upregulation of the other isoform at the protein level.

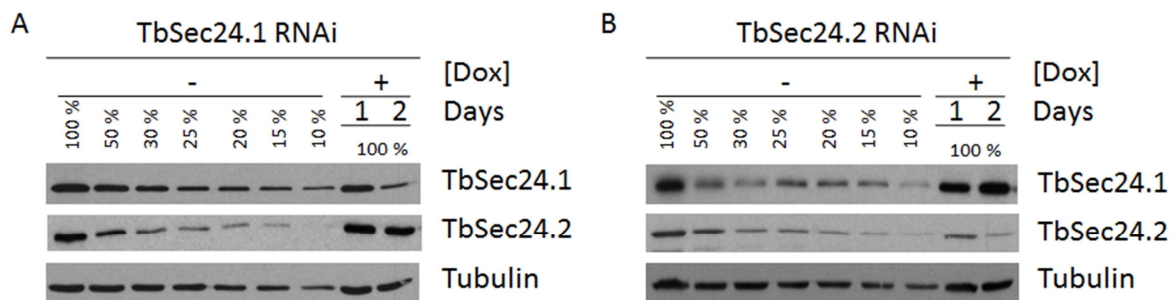


Figure 15: TbSec24 RNAi efficiency. Both TbSec24 isoforms showed a comparable decrease in the protein level over two days of RNAi. Depletion of either TbSec24.1 (A) or TbSec24.2 (B) to about 40 % after one day and to about 15 % after two days was obtained in TbSec24.1 RNAi cells (A) and TbSec24.2 RNAi cells (B). In both TbSec24 isoforms, no upregulation of the other isoform could be detected. Lysate: $100 \% \pm 6 \times 10^6$ cells. The lysate was diluted with 2 x SB. As loading control, anti-tubulin antibodies were used.

3.3 The differential effects of TbSec24 isoforms on the localization of Golgi resident proteins

Immunofluorescence microscopy was used to analyze the localization of three different Golgi markers, TbGRIP70, Tb ϵ -COP, and TbGRASP before and after depletion of either TbSec24 RNAi isoform. The 70 kDa large golgin TbGRIP70 is located at the TGN. Tb ϵ -COP (35 kDa) is a subunit of the COPI coatomer and

localizes to the rims of Golgi cisternae. TbGRASP is a marker for the *cis*- and *medial*-face of the Golgi with a molecular weight of about 55 kDa.

RNAi was induced in TbSec24.1 and TbSec24.2 RNAi cell lines, and samples were taken and prepared for immunofluorescence microscopy on day one, two and three after depletion of either TbSec24 isoforms. The percentage of cells with correct localized Golgi markers was determined. Thereby, the number of cells with visible Golgi observed by immunofluorescence microscopy was scored regardless of the number of Golgi foci per cell.

Both TbSec24 RNAi cells did not display any noticeable differences in cell morphology by differential interference contrast microscopy (DIC) when compared induced to control cells over a three day time course (Figures 16, 18, 20).

It was observed that TbGRIP70 still localized to distinct Golgi foci after depletion of TbSec24 isoforms. After removing the background signal, distinct Golgi could be found in both RNAi cell lines (Figure 16A,B).

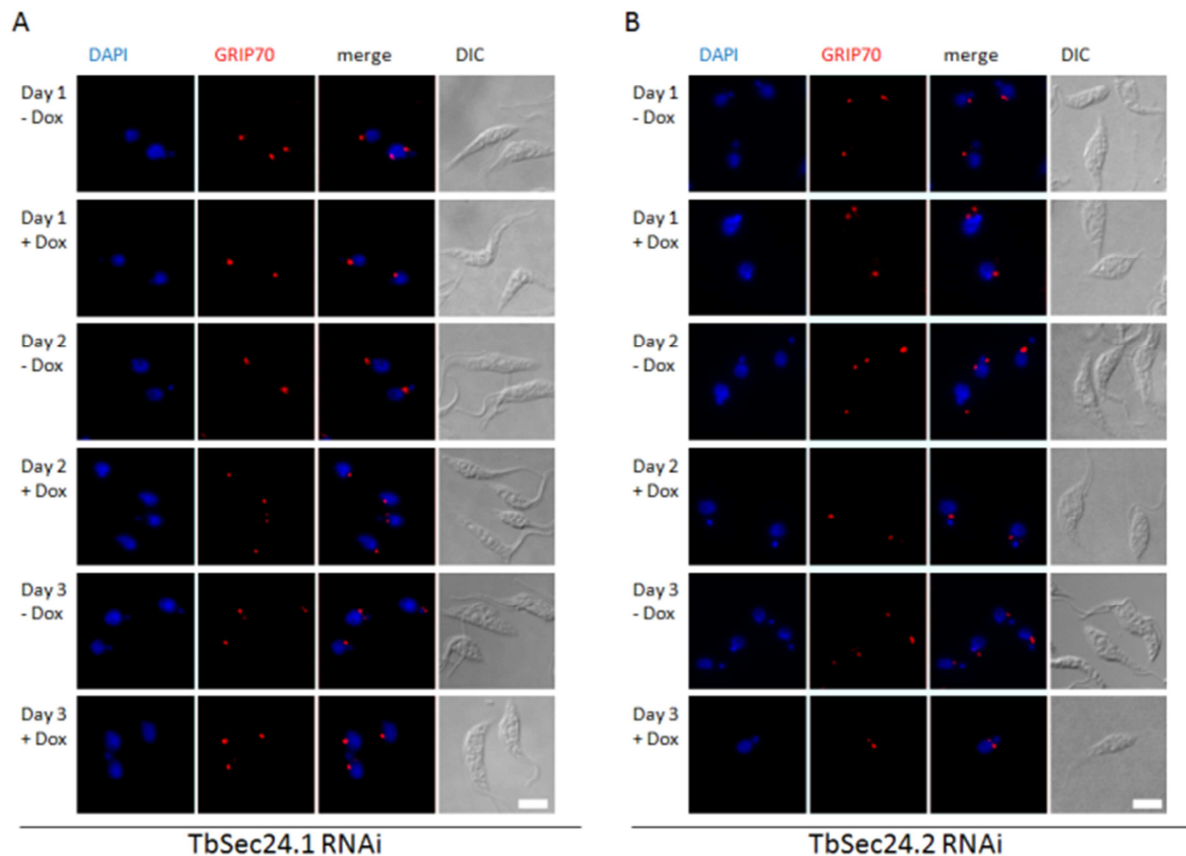


Figure 16: Effects of TbSec24 isoforms on TbGRIP70 localization. Immunofluorescence microscopy of methanol fixed TbSec24.1 (A) and TbSec24.2 (B) RNAi cells displayed Golgi structures (anti-GRIP70 antibody, red) as well as the nucleus and kinetoplast (DAPI, blue). Distinct Golgi structures could be seen in both RNAi cell lines, induced and uninduced, in all three days. No differences in morphology were observed using DIC. Bar = 5 μ m.

No increase in the number of cells with mislocalized TbGRIP70 after depletion of TbSec24.1 (Figure 17A) or TbSec24.2 RNAi (Figure 17B) could be observed. Only about 2 to 5 % of all cells showed TbGRIP70 not localized to the Golgi.

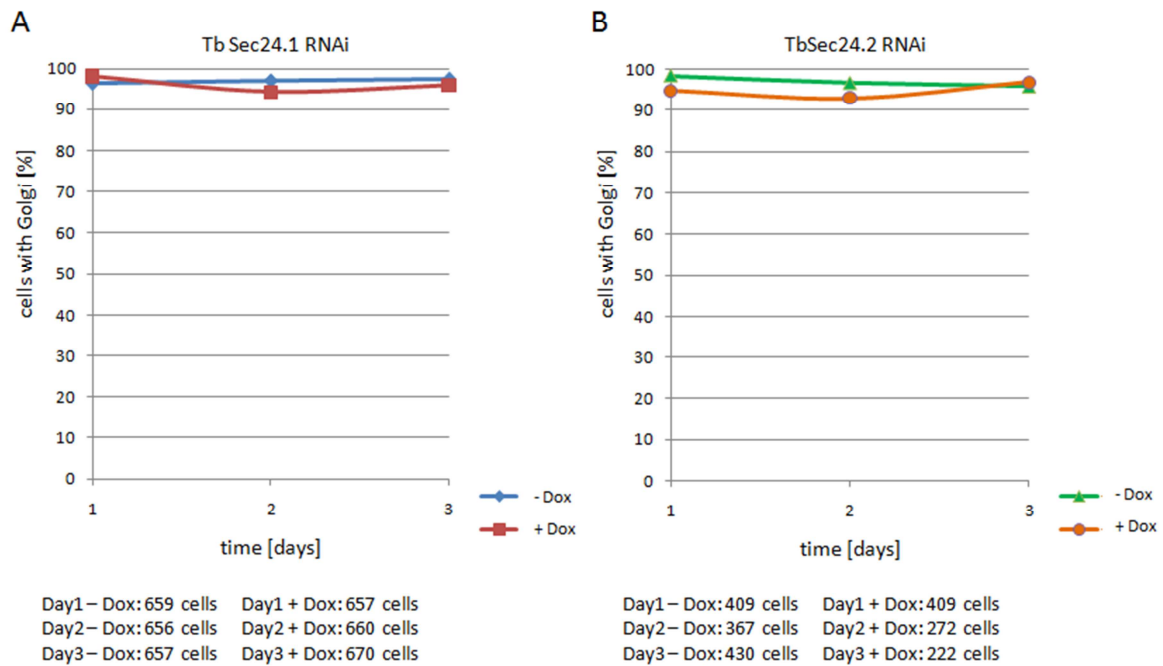


Figure 17: Quantification of TbGRIP70 localization. Cells were analyzed for TbGRIP70 localization to the Golgi, regardless of Golgi numbers. Induced and uninduced TbSec24.1 RNAi (A) and TbSec24.2 RNAi (B) cell lines showed TbGRIP70 localized to the TGN in about 95 to 98 % of all analyzed cells in all three days. Below the graph, the total numbers of analyzed cells are shown.

Immunofluorescence microscopy pictures did not illustrate a mislocalization of Tbε-COP in both, TbSec24.1 RNAi (Figure 18A) and TbSec24.2 RNAi (Figure 18B) cells after RNAi induction. The result was comparable to TbGRIP70 labeling (Figures 16, 17) after depletion of TbSec24.1 or TbSec24.2.

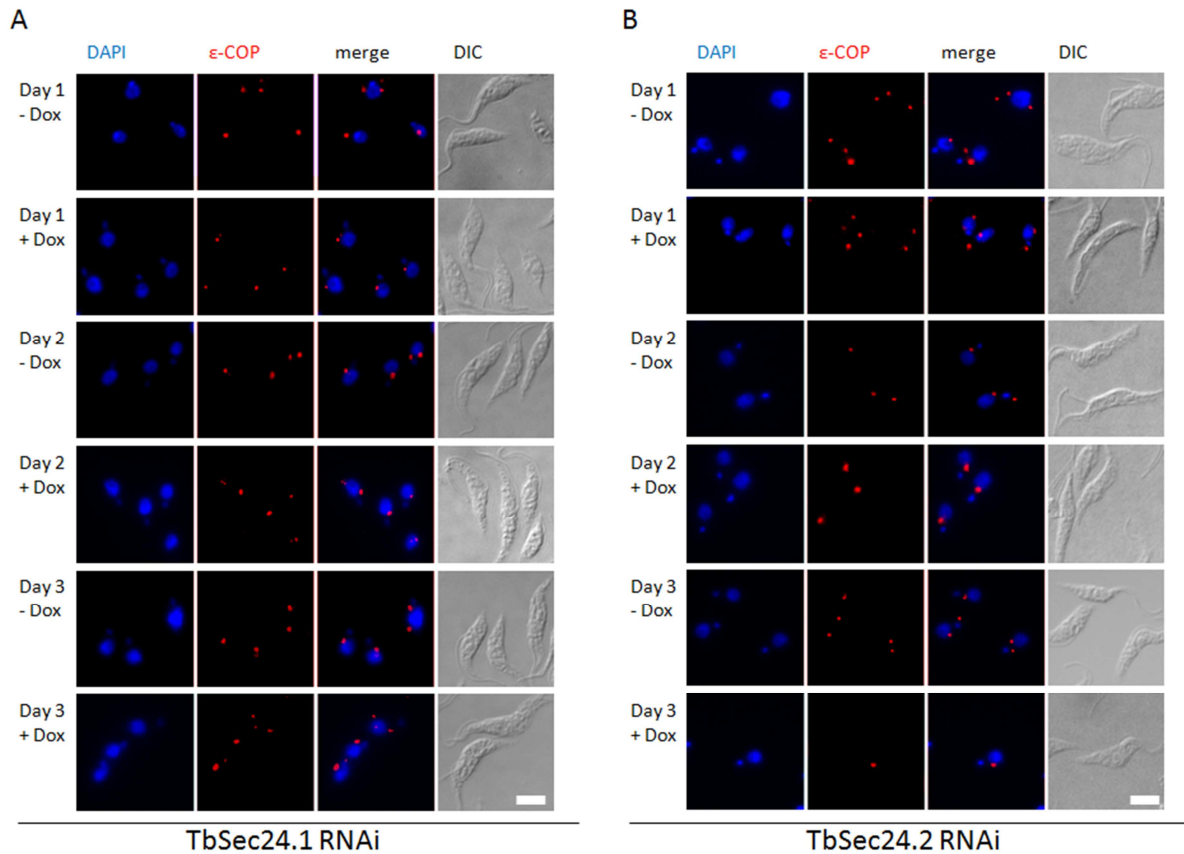


Figure 18: Effects of TbSec24 isoforms on Tb ϵ -COP localization. Golgi structures (anti- ϵ -COP antibody, red), as well as nucleus and kinetoplast (DAPI, blue) were shown by immunofluorescence microscopy of methanol fixed TbSec24.1 (A) and TbSec24.2 (B) RNAi cells. In all three days, distinct Golgi structures could be observed in both RNAi cell lines, induced and uninduced. Bar = 5 μ m.

It was determined that the number of cells with not Golgi associated Tb ϵ -COP did not increase after depletion of TbSec24.1 (Figure 19A) or TbSec24.2 (Figure 19B). Only about 2 to 5 % of all cells showed mislocalized Tb ϵ -COP.

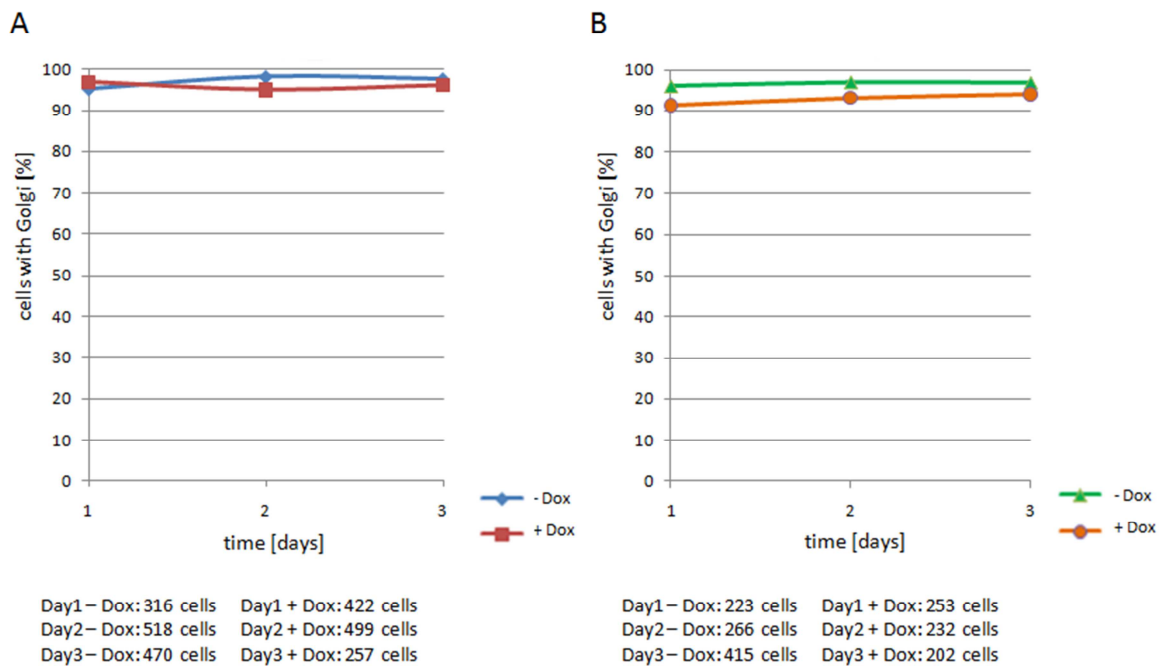


Figure 19: Quantification of correct Tb ϵ -COP localization. Cells were analyzed if Tb ϵ -COP localized to the Golgi. It showed Golgi localization in about 95 to 98 % of the cells on all three days after depletion of TbSec24.1 (A) or TbSec24.2 (B). The total numbers of analyzed cells are indicated below the graph.

TbGRASP labeling revealed localization of TbGRASP to the Golgi in control cell lines (Figure 20A, B). Images taken after TbSec24.2 RNAi (Figure 20B) showed TbGRASP still localized to distinct Golgi foci. However, TbSec24.1 RNAi led to a loss of TbGRASP Golgi labeling (Figure 20A). Three days after TbSec24.1 depletion, distinct TbGRASP labeled Golgi could only be detected in about 20 % of cells.

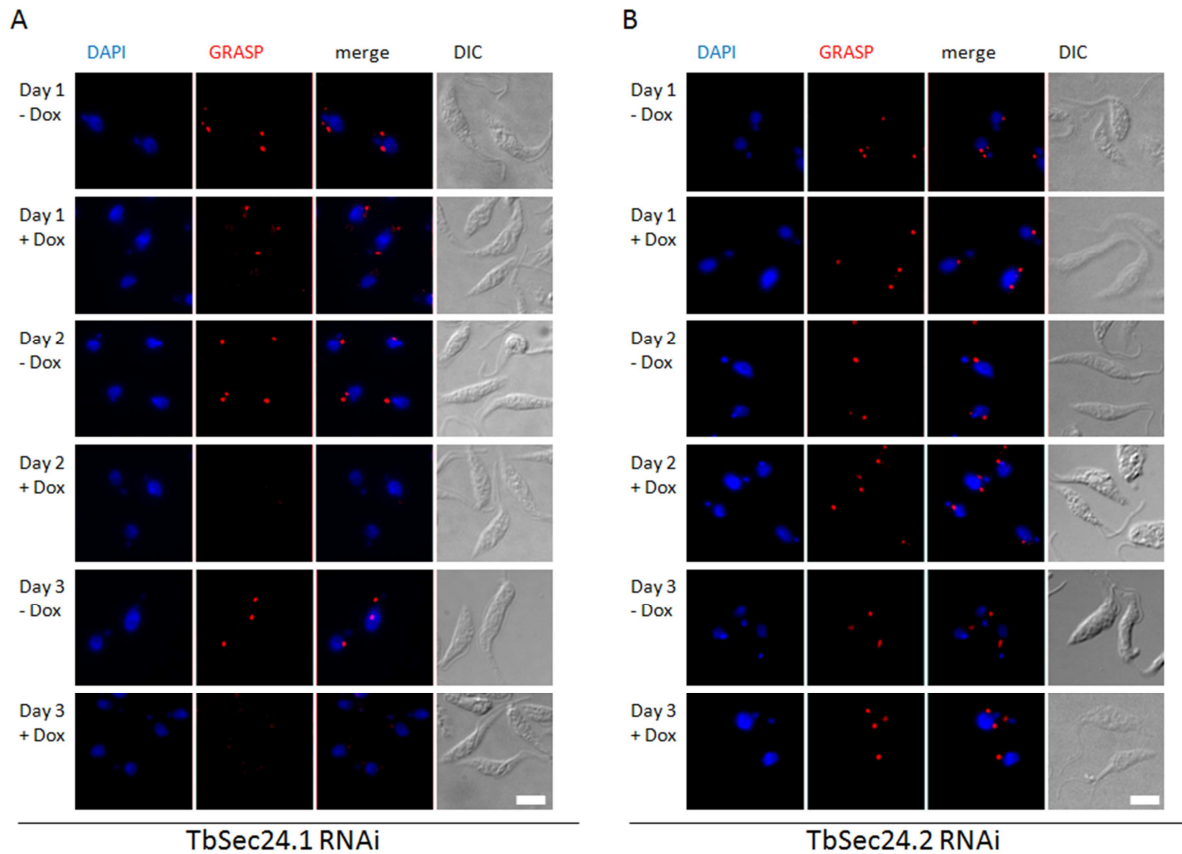


Figure 20: Effects of TbSec24 isoforms on TbGRASP localization. Immunofluorescence microscopy of methanol fixed TbSec24.1 (A) and TbSec24.2 (B) RNAi cells illustrated Golgi structures (anti-GRASP antibody, red) and the nucleus and kinetoplast (DAPI, blue). Distinct Golgi structures could be seen in TbSec24.2 RNAi cells, induced and uninduced, in all three days, However, TbGRASP showed displacement upon TbSec24.1 RNAi in all three days. Bar = 5 μ m.

The quantification of the localization of TbGRASP to the Golgi showed a decrease in cells with Golgi localized TbGRASP after depletion of TbSec24.1. One day after RNAi induction, about 85 % of cells show TbGRASP localized at the Golgi and the amount decreases to about 35 % on day two and 20 % on day three (Figure 21A). However, after depletion of TbSec24.2 RNAi, cells with Golgi localized TbGRASP remained constant in all three days (Figure 21B).

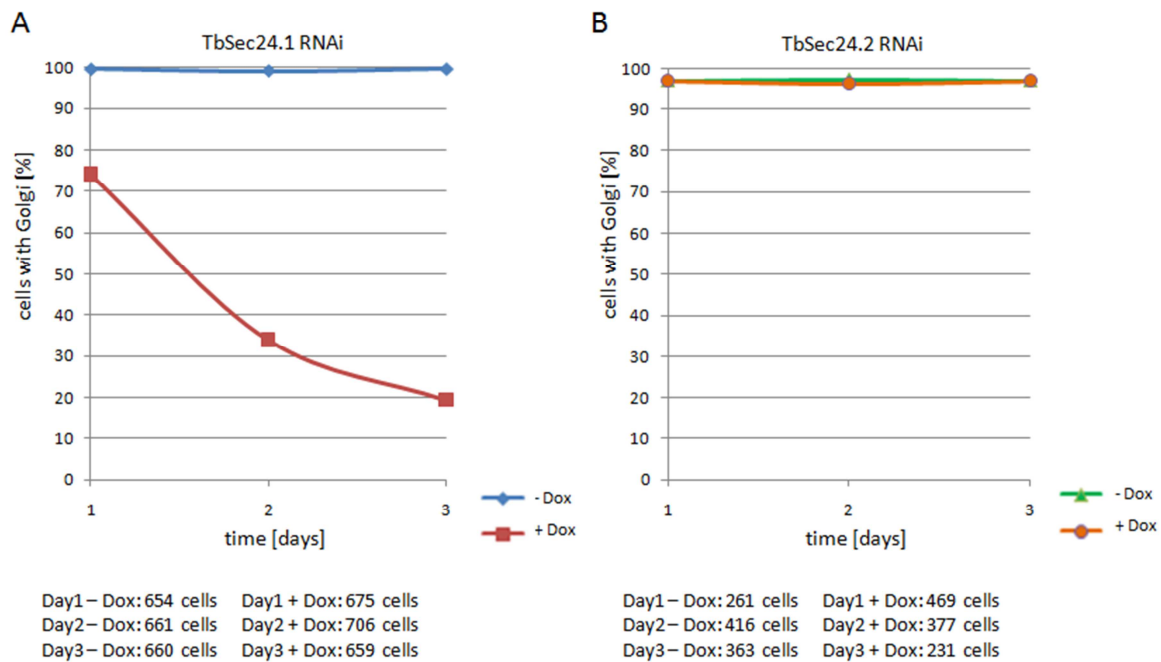


Figure 21: Quantification of TbGRASP localization. Cells were analyzed for TbGRASP localization to the Golgi. A) Continuous TbSec24.1 RNAi led to a strong decrease in cells with Golgi localized TbGRASP. After three days, only about 20 % of the cells showed TbGRASP correctly localized at the Golgi. B) No effect occurred after depletion of TbSec24.2. Below the graph, the total numbers of analyzed cells are displayed.

Taken together, the results suggest that the Golgi localization of TbGRASP depends on TbSec24.1 mediated selective cargo incorporation into COPII vesicles.

3.4 The effect of TbSec24 isoforms on the protein level of TbGRIP70 and TbGRASP

Lack of TbGRASP at the Golgi upon TbSec24.1 RNAi led to the question, if the mislocalization was the result of a downregulation of protein expression. Therefore, TbSec24.1 and TbSec24.2 RNAi cells were induced. The protein levels of TbGRIP70 and TbGRASP were determined by immunoblotting. The depletion of neither TbSec24 isoforms (Figure 22) caused a change in TbGRIP70 or TbGRASP protein levels.

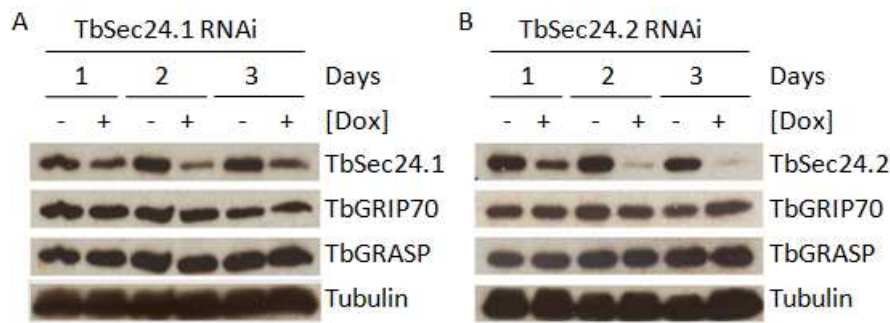


Figure 22: Effect of TbSec24 isoforms on protein levels of Golgi markers. A) Induction of TbSec24.1 RNAi resulted in increasing depletion of TbSec24.1 levels from day one to day three. RNAi induction did not affect the levels of Golgi markers TbGRIP70 and TbGRASP. B) Induction of TbSec24.2 RNAi led to an increasing depletion of TbSec24.2 levels. The levels of the Golgi markers TbGRIP70 and TbGRASP were not affected. Lysate: 4×10^6 cells were used per lane. Anti-tubulin antibodies were used as control for equal loading.

Equal levels of TbGRASP and TbGRIP70 after depletion of TbSec24 isoforms indicate that expression of both Golgi markers is unaltered. Therefore, the lack of detectable TbGRASP at the Golgi is not caused by downregulation of its expression in TbSec24.1 RNAi cells.

3.5 The effect of TbSec24 isoforms on the total number of Golgi

In chapter 3.3 it was shown that TbSec24 isoforms selectively influence the localization of at least one Golgi marker (TbGRASP). However, the quantification done before did not analyze the effect on the number of detectable Golgi per cell. Therefore, a detailed analysis on the impact of TbSec24 isoform RNAi on the number of visible Golgi was conducted.

Usually, wild type *T. brucei* have one or two main Golgi in the 1N1K cell cycle stage, whereas 1N2K and 2N2K cells have two. Throughout the cell cycle, additional Golgi appear and disappear [211].

The same cells as used in 3.3 were additionally examined for differences in the total number of visible Golgi. Anti-TbGRIP70 and anti-TbGRASP labeled cells were analyzed before and after depletion of TbSec24.1 or TbSec24.2 over three days. Tb ϵ -COP was not used as it showed similar effects in Golgi localization as TbGRIP70.

3.5.1 The effect of TbSec24 isoforms on the total number of TbGRIP70 labeled Golgi

Quantification of the total number of TbGRIP70 labeled Golgi in uninduced control cells indicated that the majority of cells contain one or two Golgi. RNAi induction led to a constant decrease of between 5 to 10 % in cells with two and three TbGRIP70 positive Golgi foci. A concomitant increase of between 10 to 15 % in cells with one TbGRIP70 labeled Golgi was also observed. As described before, no increase in cells without a TbGRIP70 positive Golgi could be detected. The effect occurred consistently on all three days. A comparable effect was observed in both cell lines, TbSec24.1 (Figure 23A) and TbSec24.2 RNAi (Figure 23B).

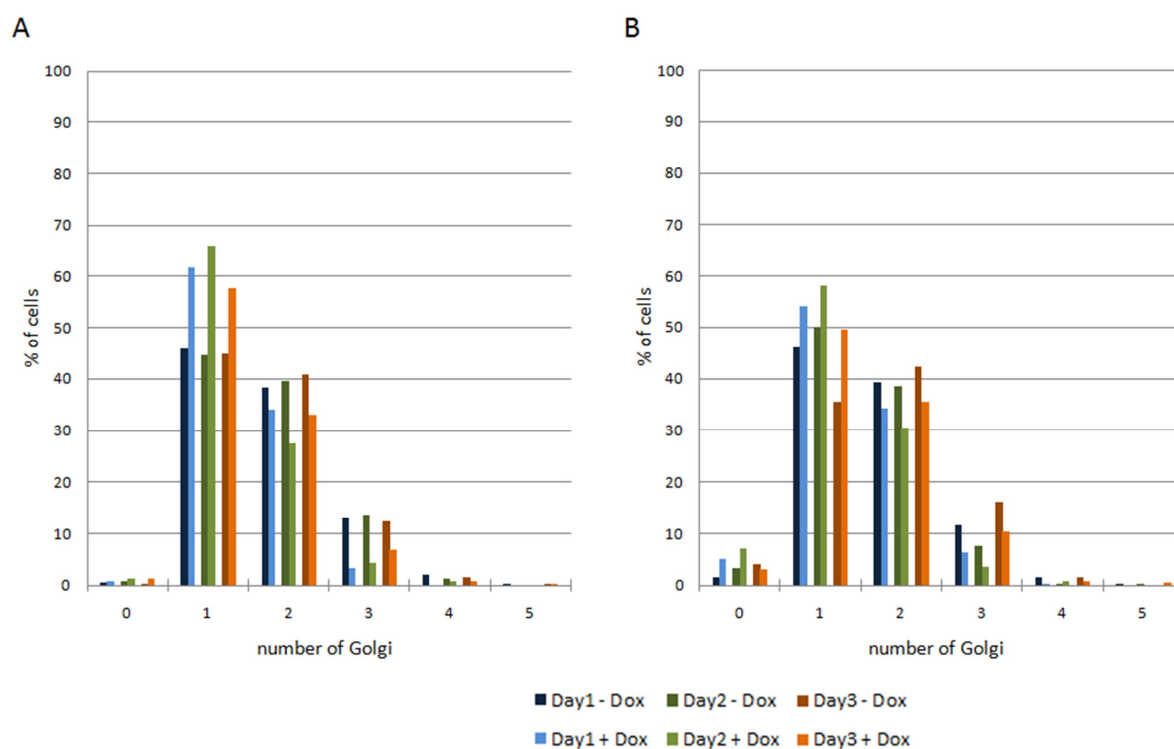
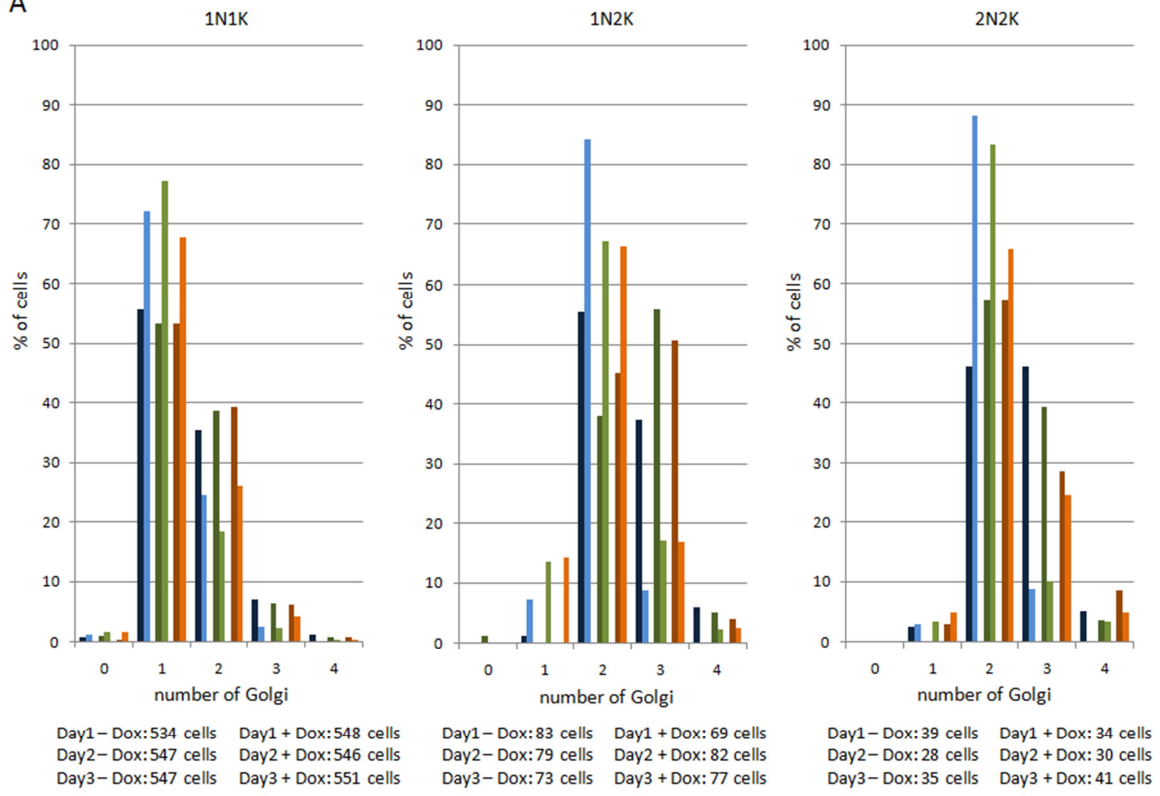


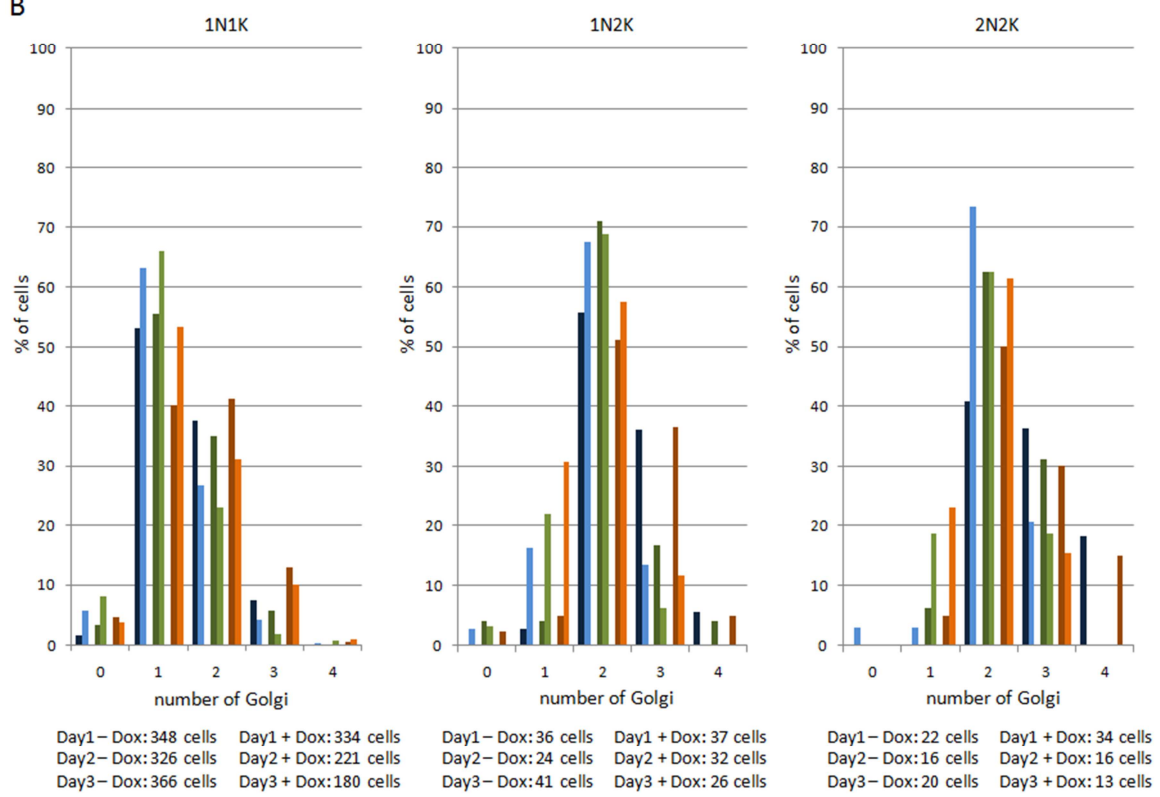
Figure 23: Quantification of TbSec24 isoform effects on total number of TbGRIP70 labeled Golgi. Cells were analyzed one, two and three days after RNAi induction. Depletion of TbSec24.1 (A) and TbSec24.2 (B) led to comparable results. An increase in cells with one TbGRIP70 labeled Golgi with simultaneous decrease of cells with two and three could be seen after depletion of either TbSec24 isoforms. The graph shows the pooled data of all cell cycle stages. The analyzed cells were the same as in Figure 16.

The total number of TbGRIP70 labeled Golgi was quantified after TbSec24.1 (Figure 24A) and TbSec24.2 (Figure 24B) RNAi with respect to different canonical cell cycle stages. It was observed that about 90 % of 1N1K cells contained one or two TbGRIP70 labeled Golgi structures. In 1N2K and 2N2K cells, the percentage of cells with two or three Golgi was also at about 90 %. Both, TbSec24.1 and TbSec24.2 RNAi cell lines showed a 10 to 20 % increase in 1N1K cells with one TbGRIP70 labeled Golgi and a simultaneous decrease in cells with two Golgi in the 1N1K cells after RNAi induction. 1N2K and 2N2K cells in both cell lines indicated an increase in cells with one and two TbGRIP70 positive Golgi foci and a strong decrease of cells with three (up to 40 %).

A



B



■ Day1 - Dox ■ Day2 - Dox ■ Day3 - Dox
■ Day1 + Dox ■ Day2 + Dox ■ Day3 + Dox

Figure 24: Effects of TbSec24 isoforms on total number of TbGRIP70 labeled Golgi in different cell cycle stages. Cells were analyzed one, two and three days after RNAi induction. TbSec24.1 (A) and TbSec24.2 (B) depletion led to comparable results. 1N1K cells indicated a constant increase in cells with one TbGRIP70 labeled Golgi and a decrease in cells with two and three. 1N2K and 2N2K cells showed an increase in cells with one and two and a decrease in cells with three TbGRIP70 positive Golgi. Cells lacking a TbGRIP70 labeled Golgi remained constant. Analyzed cells were the same as in Figure 16. The number of analyzed cells in each cell cycle stage is shown below the graph.

3.5.2 The effect of TbSec24 isoforms on the total number of TbGRASP labeled Golgi

A strong increase in cells with mislocalized TbGRASP was observed (Figure 25A). One day after RNAi induction, about 25 % of all cells did not exhibit TbGRASP labelled Golgi. After three days, this number increased to 80 %. This effect of TbSec24.1 RNAi occurred at the expense of cells with one, two and three TbGRASP labelled Golgi (up to 30 %), although on day one after TbSec24.1 depletion, a slight increase of about 7 % in cells with one TbGRASP positive Golgi could be seen. This finding was in striking contrast to the results obtained by TbGRIP70 labeling.

On the other hand, similar effects as TbGRIP70 labeling were observed after depletion of TbSec24.2 (Figure 23B, Figure 25B). A slight but constant decrease of cells with two, three and four TbGRASP labeled Golgi foci could be seen (about 5 to 10 %) while cells containing one Golgi increased by 15 %. No increase in cells without TbGRASP labelled Golgi was perceived after depletion of TbSec24.2.

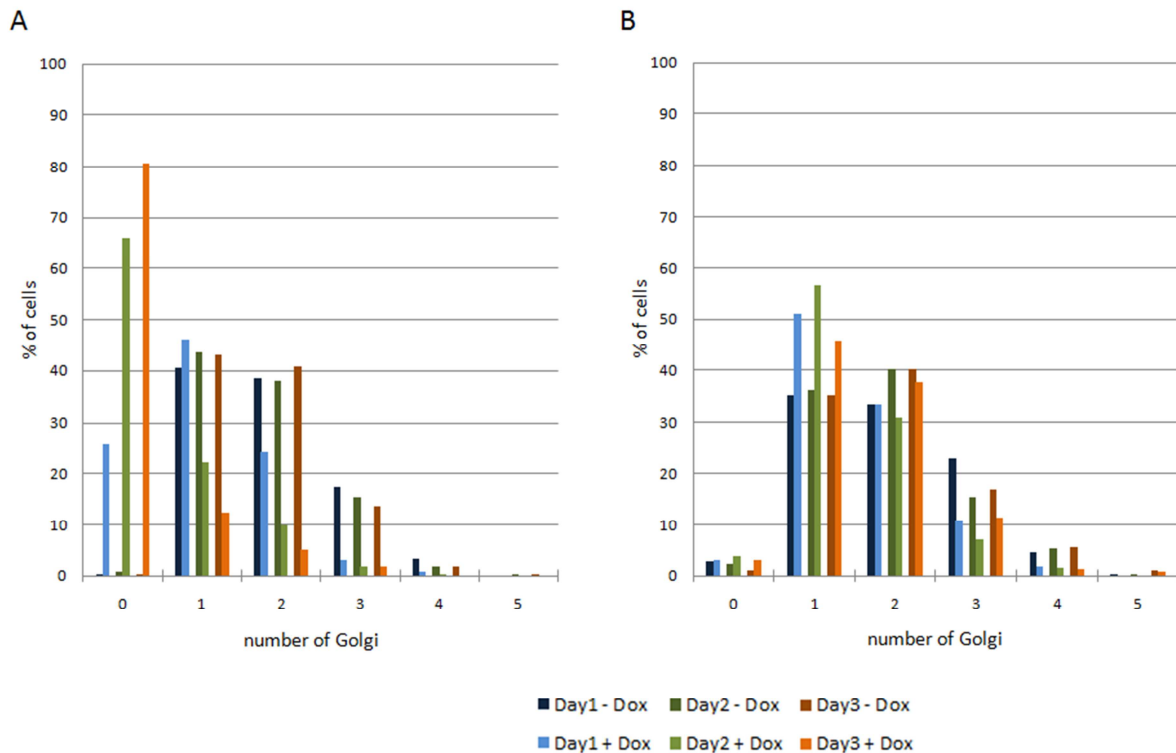


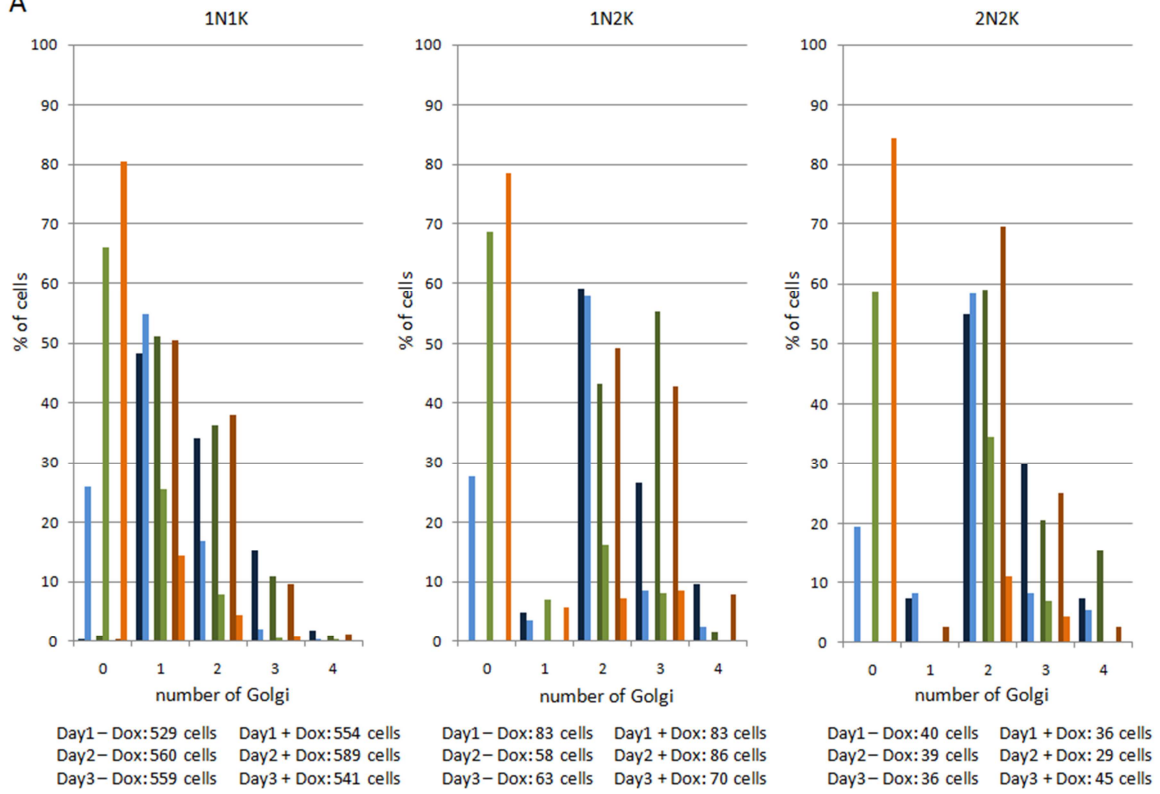
Figure 25: Quantification of TbSec24 isoform effects on total number of TbGRASP labeled Golgi. Cells were analyzed one, two and three days after induction of TbSec24.1 RNAi or TbSec24.2 RNAi. A) TbSec24.1 RNAi showed a strong increase from day one to day three in cells with mislocalized TbGRASP whereas the number of cells with one, two and three TbGRASP labeled Golgi decreased. B) TbSec24.2 RNAi indicated a constant increase in cells with one TbGRASP positive Golgi with simultaneous decrease of cells with two, three, and four. The graph illustrates the pooled data of all cell cycle stages. Analyzed cells were the same as in Figure 20.

An increase in cells with mislocalized TbGRASP was observed in all cell cycle stages after TbSec24.1 RNAi (Figure 26A). At the same time, the number of cells with Golgi localized TbGRASP decreased. One day after TbSec24.1 depletion, the number of cells without detectable TbGRASP labeled Golgi increased in 1N1K cells to about 25%. Three days after induction, a TbGRASP positive Golgi could be detected in only about 20 % of the cells. 1N1K cells containing one TbGRASP labeled Golgi remained stable one day after TbSec24.1depletion, but decreased drastically on day two and three. In addition, the number of cells with two and three TbGRASP positive Golgi foci decreased dramatically. 1N2K and 2N2K cells also showed an increase in cells without TbGRASP labeled Golgi. This result was comparable to 1N1K cells. In both, 1N2K and 2N2K cells no increase in cells containing a single TbGRASP positive Golgi was observed after TbSec24.1 RNAi. However, a strong progressive loss of cells with two and three TbGRASP labeled Golgi was obtained. Three days after

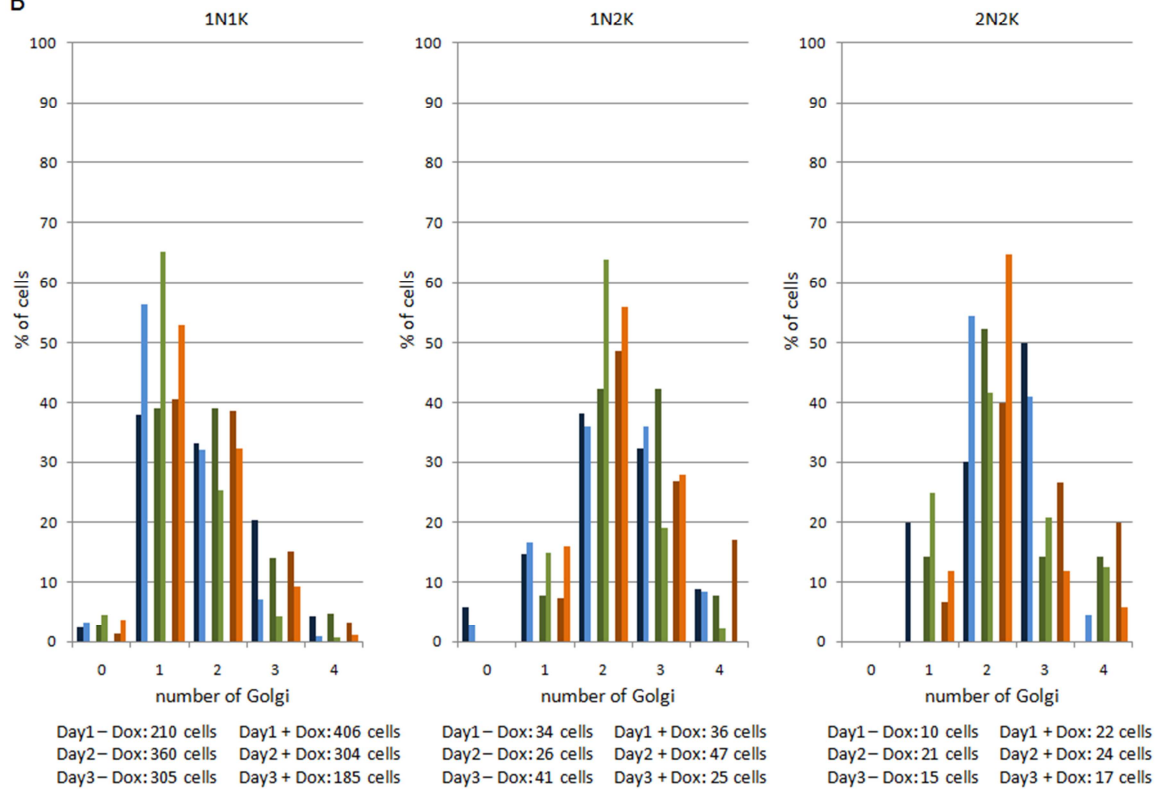
TbSec24.1 depletion the majority of cells showed no distinct TbGRASP positive Golgi.

Furthermore, depletion of TbSec24.2 (Figure 26B) showed a constant increase of about 15 to 25 % in cells with one TbGRASP positive Golgi structure and a simultaneously decrease in cells with two and three (5 to 10 %) in 1N1K cells. With the caveat of low sample size, TbSec24.2 depletion resulted in an increase of 1N2K and 2N2K cells with one and two TbGRASP labeled Golgi and a decrease of 1N2K and 2N2K cells with three and four (Figure 26B). This result after TbSec24.2 RNAi was comparable to TbGRIP70 labeling (Figure 24B).

A



B



■ Day1 - Dox ■ Day2 - Dox ■ Day3 - Dox
■ Day1 + Dox ■ Day2 + Dox ■ Day3 + Dox

Figure 26: Effects of TbSec24 isoforms on total number of TbGRASP labeled Golgi in different cell cycle stages. Cells were analyzed on day one, two and three after RNAi induction. A) Induced TbSec24.1 RNAi cells showed a strong increase of mislocalized TbGRASP from day one to day three compared to uninduced cells in all cell cycle stages. B) Inducing TbSec24.2 RNAi led to a constant increase in the number of cells with one TbGRASP labeled Golgi and a decrease in cells with two and three in 1N1K cells. 1N2K and 2N2K cells indicated an increase in the number of cells with one and two and a decrease in cells with three TbGRASP labeled foci. Cells without a detectable Golgi remained constant. The analyzed cells were the same as in Figure 20. The numbers below the graph represents the total amount of analyzed cells.

Taken together, these results indicate that TbSec24.1 but not TbSec24.2 is required for the correct Golgi localization of TbGRASP. However, Golgi localization of TbGRIP70 is not affected by depletion of either TbSec24 isoform.

3.6 The effects of TbSec24.1 RNAi on bilobe and non-bilobe Golgi

Generally, two distinct types of Golgi can be found in *T. brucei*: a single, stacked Golgi which is located close to the bilobe structure, as well as additional non-bilobe associated ones. The non-bilobe Golgi appear and disappear during the cell cycle at random locations [198]. During cell cycle progression, separation of the old and the new bilobe Golgi is accompanied by duplication of the bilobe structure. Both duplication events occur briefly before the kinetoplast divides. Therefore, the majority of 1N1K cells should contain one bilobe Golgi and one bilobe; fewer 1N1K cells should have two bilobe Golgi and one or two bilobes. In most of the 1N2K and 2N2K cells, two bilobe Golgi and two bilobes should be found.

The impact of TbSec24.1 on Golgi localization of TbGRIP70 and TbGRASP was analyzed, with an additional distinction between bilobe and non-bilobe Golgi. This time, only TbSec24.1 RNAi cells were analyzed, as only this particular TbSec24 isoform showed selective incorporation of Golgi components into COPII vesicles. Depletion of TbSec24.1 led to the mislocalization of TbGRASP but not TbGRIP70 from the Golgi (Figures 17A, 21A).

TbSec24.1 RNAi cells were labeled with anti-TbGRIP70 (Figure 27A) or anti-TbGRASP (Figure 27B). Additionally, both samples were co-labeled with antibodies against the bilobe structure. Therefore, an anti-TbCentrin4 antibody or the pan-centrin monoclonal antibody 20H5 [223] was used. Golgi were regarded as bilobe

associated Golgi if they were located adjacent the bilobe and the gap between Golgi and the bilobe structure was not bigger than the size of the Golgi itself. Otherwise they were counted as non-bilobe Golgi.

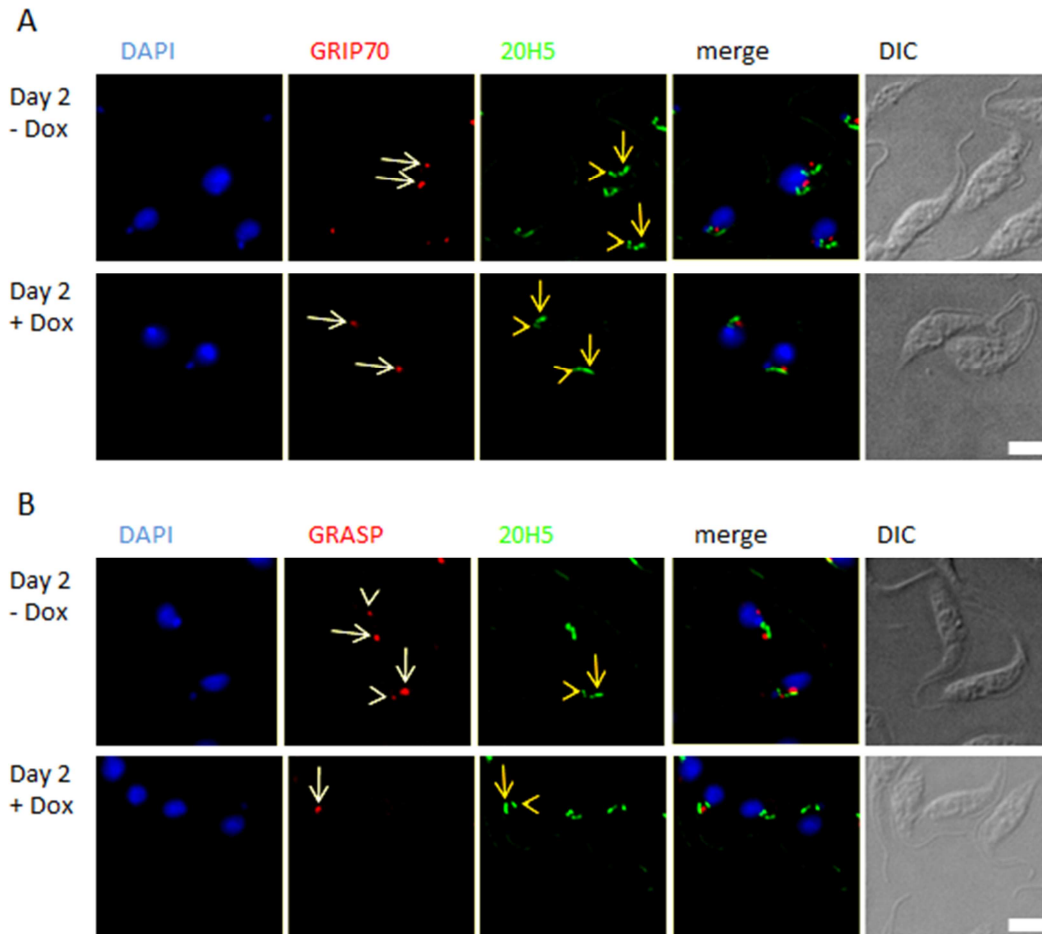


Figure 27: Effects of TbSec24.1 RNAi on bilobe and non-bilobe Golgi. Immunofluorescence microscopy of methanol fixed TbSec24.1 RNAi cells illustrated distinct Golgi structures (anti-TbGRIP70 (A) or anti TbGRASP (B) antibody, red; white arrow: bilobe Golgi, white arrowhead: non-bilobe Golgi) and the nucleus and kinetoplast (DAPI, blue). Additionally, bilobe (yellow arrow) and basal bodies (yellow arrowheads) were labeled with the pan-Centrin2 antibody 20H5 (green). Sample pictures showed cells two days after RNAi induction compared to uninduced cells. A) Distinct TbGRIP70 labeled Golgi could be seen in induced and uninduced cells. B) Depletion of TbSec24.1 led to a mislocalization of TbGRASP. Bar = 5 μ m.

3.6.1 The effect of TbSec24.1 RNAi on TbGRIP70 labeled bilobe and non-bilobe Golgi

Breakdown into bilobe Golgi and non-bilobe Golgi showed that depletion of TbSec24.1 had a very weak effect on TbGRIP70 localization to bilobe Golgi. Only a

slight (about 5 %) increase in cells without or with one TbGRIP70 labeled bilobe Golgi could be seen at the expense of cells with two TbGRIP70 positive bilobe Golgi (Figure 28A). However, a quick and consistent loss of visible TbGRIP70 labeled non-bilobe Golgi occurred on all three analyzed days (about 15 to 25 %) (Figure 28B). This suggests that the bilobe Golgi might be more stable and that the transport from the ER to the Golgi might have an influence on the formation of non-bilobe Golgi.

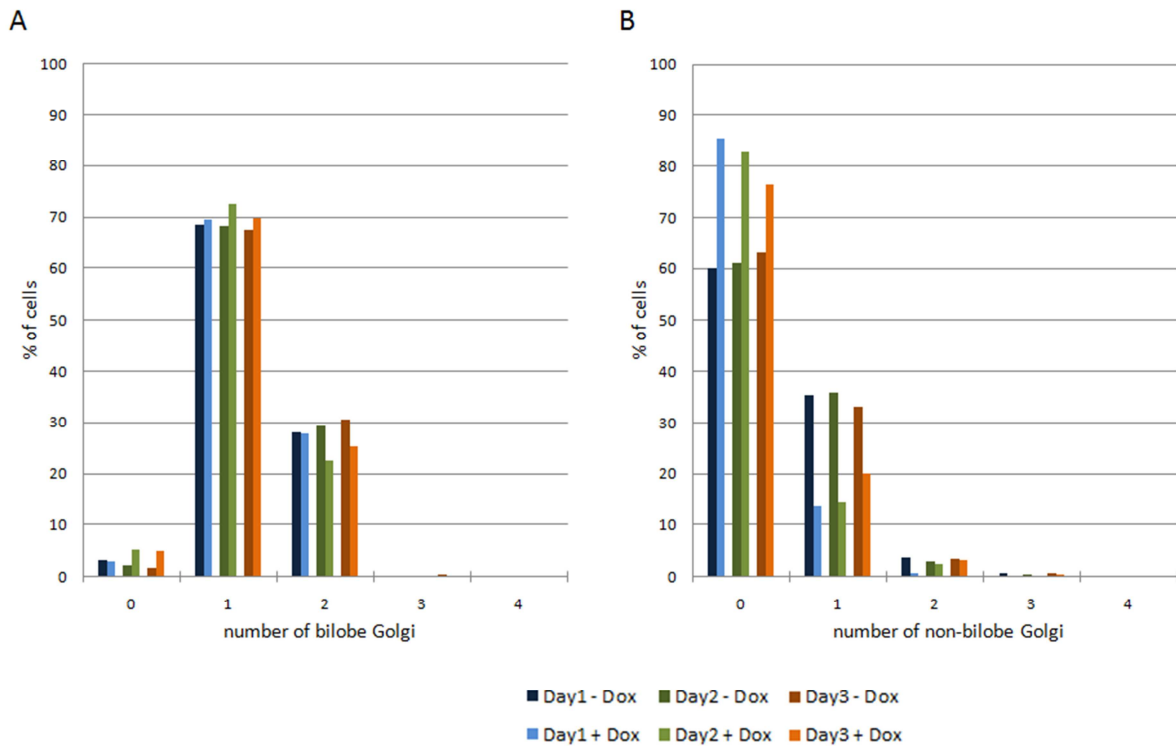


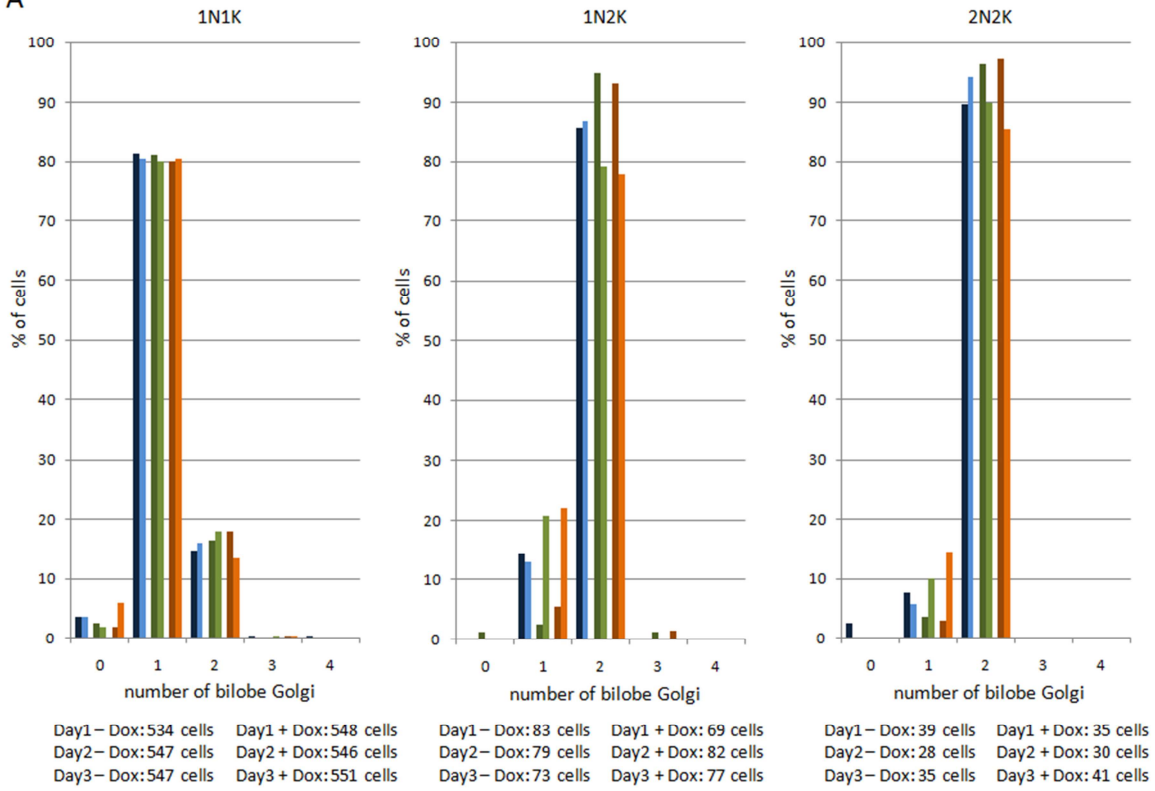
Figure 28: Quantification of TbSec24.1 effects on TbGRIP70 labeled bilobe and non-bilobe Golgi. Cells were analyzed one, two and three days after RNAi induction. A) TbGRIP70 labeling discovered a slight decrease of cells with two TbGRIP70 positive bilobe Golgi and an increase in cells without or with one after TbSec24.1 depletion. B) Cells showed a quick and constant loss of TbGRIP70 labeled non-bilobe Golgi over three days after RNAi induction. The graph was compiled after analysis of immunofluorescence microscopy pictures as shown in Figure 26. It shows the pooled data of all cell cycle stages.

Analysis of the different cell cycle stages showed that depletion of TbSec24.1 had no influence on the formation of TbGRIP70 labeled bilobe Golgi in 1N1K cells (Figure 29A). A slight decrease in the number of cells with two TbGRIP70 labeled bilobe Golgi and an increase in cells with one TbGRIP70 positive bilobe Golgi were observed in the 1N2K and 2N2K cells. However, TbSec24.1 depletion led to a quick and constant loss of cells with TbGRIP70 labeled non-bilobe Golgi in all cell cycle

stages (Figure 29B). A decrease of TbGRIP70 positive non-bilobe Golgi up to 25 % was found.

It has been described that non-bilobe Golgi appear only late in the cell cycle [211]. In contrast, my analysis highlighted an earlier appearance of non-bilobe Golgi. They were observed in already about 40 % of all uninduced 1N1K cells.

A



B

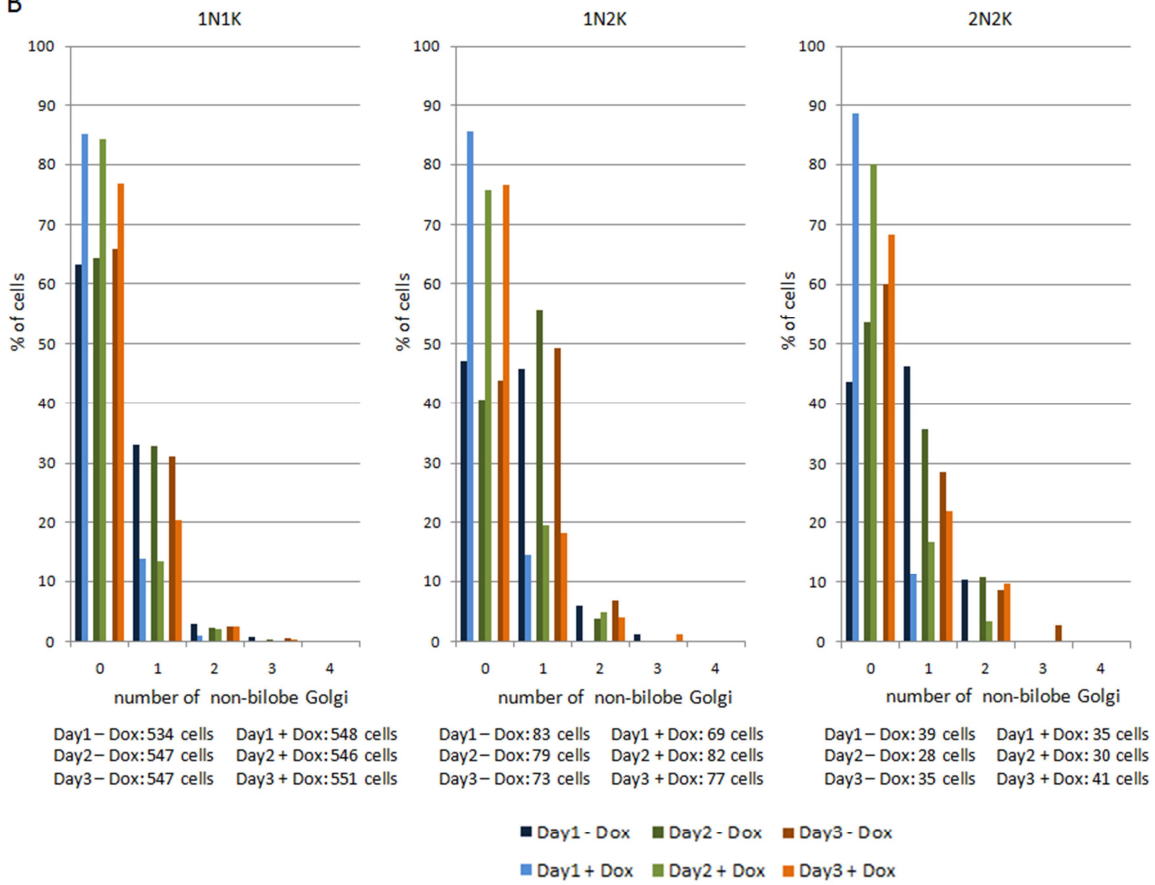


Figure 29: Effects of TbSec24.1 RNAi on TbGRIP70 labeled bilobe and non-bilobe Golgi in different cell cycle stages. Cells were analyzed one, two and three days after RNAi induction. A) 1N1K cells indicated no effect after TbSec24.1 depletion in the number of TbGRIP70 labeled bilobe Golgi, whereas 1N2K and 2N2K cells showed a slight increase in cells with one TbGRIP70 positive foci instead of two. B) A constant loss of cells with TbGRIP70 labeled non-bilobe Golgi was detected in all cell cycle stages after RNAi induction. The analyzed cells were treated as shown in Figure 26. The number of analyzed cells in each cell cycle stage is shown below the graph.

3.6.2 The effect of TbSec24.1RNAi on TbGRASP labeled bilobe and non-bilobe Golgi

After TbSec24.1 RNAi, a progressive loss of visible bilobe Golgi was indicated by TbGRASP labeling (Figure 30A). In parallel, TbGRASP labeled non-bilobe Golgi were lost as early as one day after depletion of TbSec24.1. This latter effect was maintained over the entire three-day time course (Figure 30B). The loss of TbGRASP positive non-bilobe Golgi was comparable to the analysis of the TbGRIP70 labeled non-bilobe Golgi (Figure 28B) although the effect seemed to be a little bit more drastic. A decrease of TbGRASP labeled non-bilobe Golgi (30 %) could be detected.

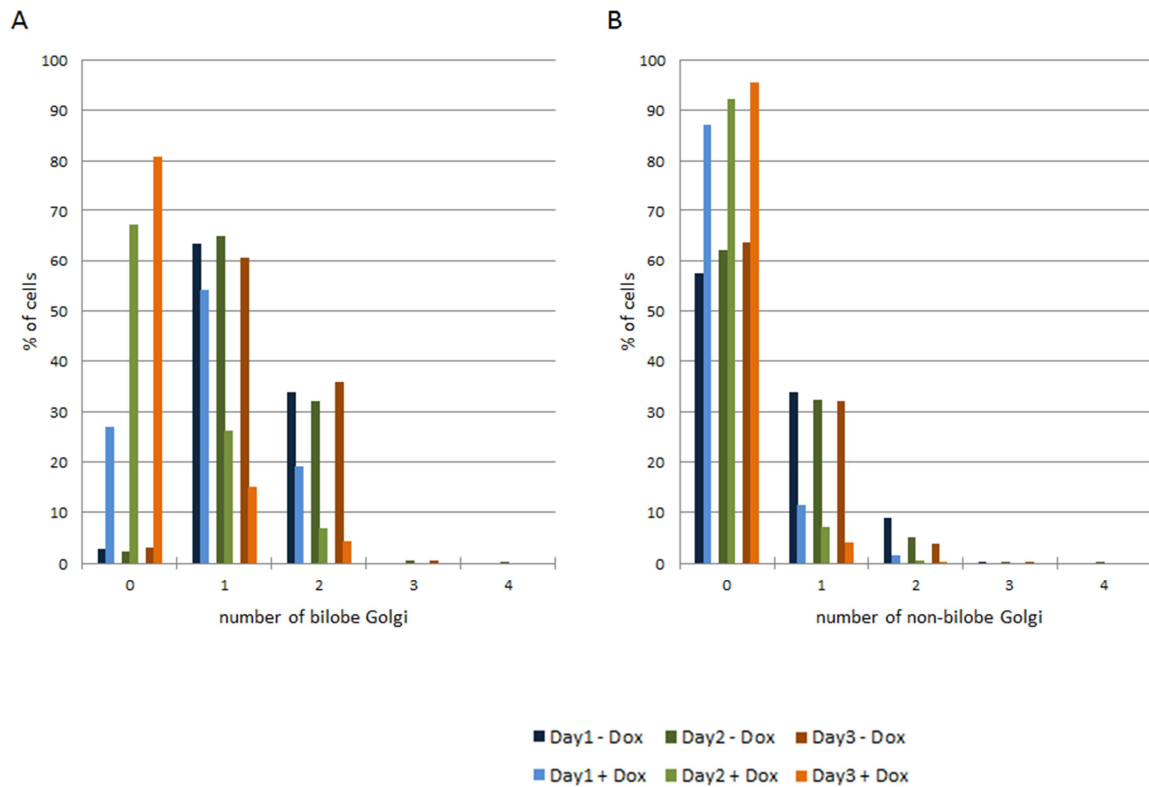
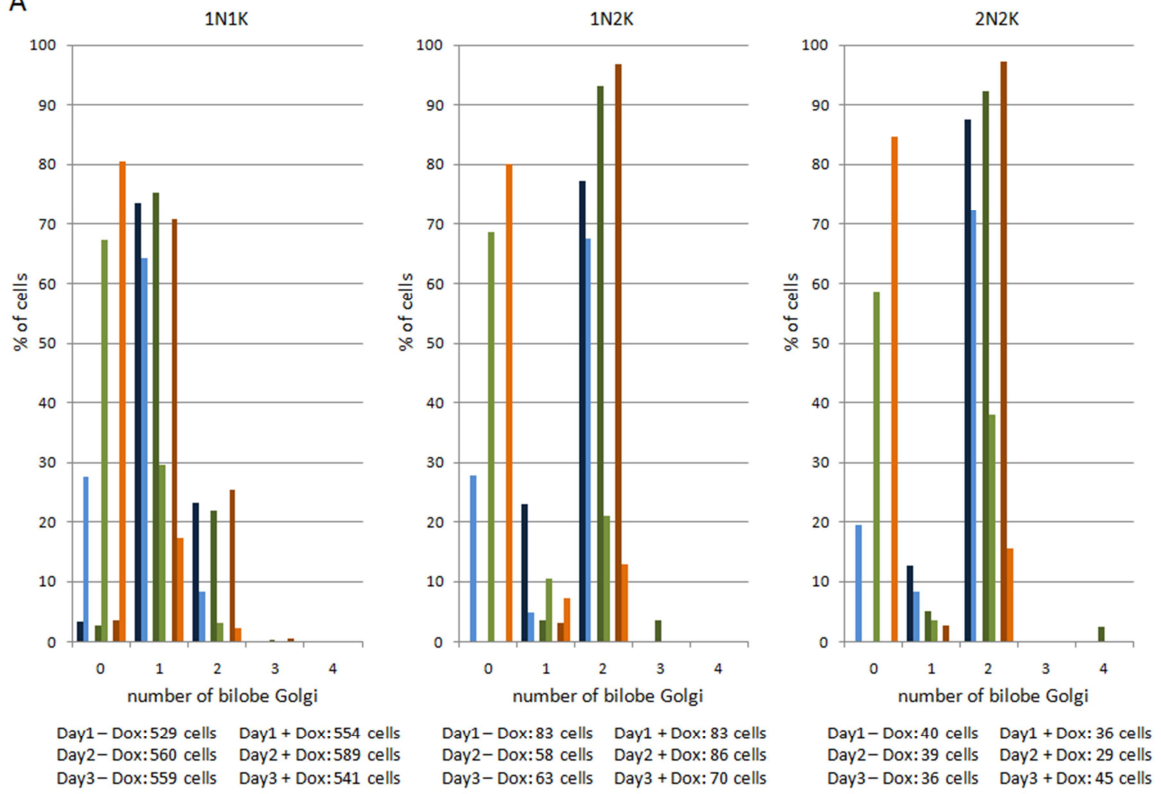


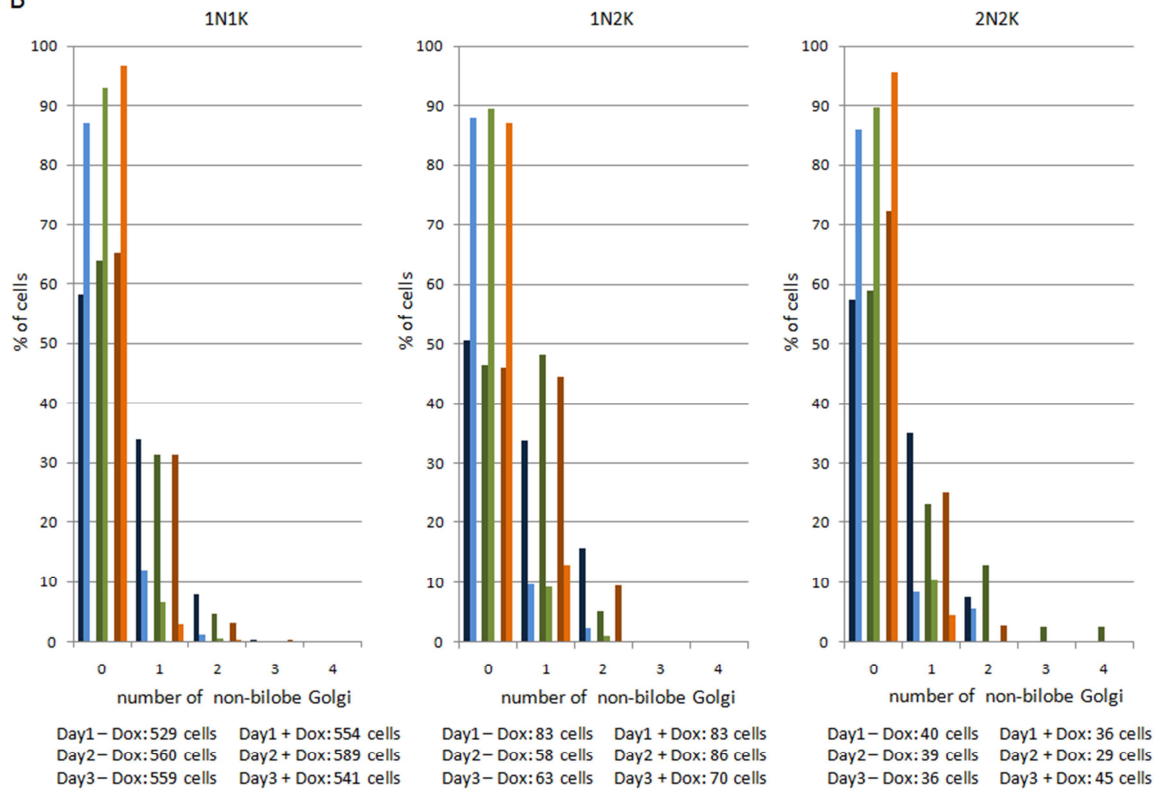
Figure 30: Quantification of TbSec24.1 effects on TbGRASP labeled bilobe and non-bilobe Golgi. Cells were analyzed on day one, two and three after RNAi induction. TbGRASP labeling showed an increasing loss of visible bilobe Golgi over three days after depletion of TbSec24.1 (A) and a rapid and constant decrease of TbGRASP labeled non-bilobe Golgi (B). The cells were treated for immunofluorescence microscopy as shown in Figure 26. The graph illustrates the pooled data of all cell cycle stages.

TbSec24.1 RNAi led to a strong increase of cells with mislocalized TbGRASP in both, bilobe and non-bilobe associated Golgi through all cell cycle stages. The RNAi effect on TbGRASP positive bilobe Golgi increased over three days after induction (Figure 31A). Only about 20 % of all analyzed cells showed distinct TbGRASP labeled Golgi on day three after depletion of TbSec24.1. However, the loss of TbGRASP labeled non-bilobe Golgi after depletion of TbSec24.1 reached its maximum one day after RNAi induction and did not increase remarkably on day two and day three (Figure 31B). The extent of the decrease of visible non-bilobe Golgi was comparable to the decrease of TbGRASP labeled bilobe Golgi one day after TbSec24.1 depletion. On day three, TbGRASP positive non-bilobe Golgi could be seen in only 5 to 10 % of 1N1K, 1N2K and 2N2K cells.

A



B



■ Day1 - Dox ■ Day2 - Dox ■ Day3 - Dox
■ Day1 + Dox ■ Day2 + Dox ■ Day3 + Dox

Figure 31: Effects of TbSec24.1 RNAi on TbGRASP labeled bilobe and non-bilobe Golgi in different cell cycle stages. Cells were analyzed one, two and three days after RNAi induction. A gradual loss of cells with TbGRASP labeled bilobe Golgi (A) and a constant loss of cells with TbGRASP positive non-bilobe Golgi (B) was observed. The analyzed cells were treated as shown in Figure 26. The numbers below the graph represents the total amount of analyzed cells.

3.7 The effect of TbSec24.1 RNAi on the formation of the paraflagellar rod

To exclude general effects of TbSec24.1 RNAi on all internal replicative processes, it was determined if depletion of TbSec24.1 affects the formation of the flagellum. A close relationship between duplication of the Golgi and the basal bodies was assumed [198, 224]. The basal body in turn nucleates the formation of the flagellum [193]. Therefore, flagellum synthesis might be an indicator if TbSec24.1 RNAi causes general malfunctions within *T. brucei* cells during cell biogenesis, manifesting aberrations in other organelles.

The number of flagella was analyzed one, two and three days after TbSec24.1 depletion by immunofluorescence microscopy. Anti-paraflagellar rod protein A (TbPFRA) antibodies were used for flagellum labeling. TbPFRA is one of the two major components of the PFR [225]. The lattice-like PFR runs adjacent to the axonemal structure within the flagellum [201].

During the *T. brucei* cell cycle, the flagellum starts to duplicate briefly before the kinetoplast divides. Thus, control cells showed one or two flagella in 1N1K cells and two flagella in 1N2K and 2N2K cells (Figure 32A). Analysis of immunofluorescence microscopy pictures after depletion of TbSec24.1 did not highlight effects of TbSec24.1 RNAi on flagella formation (Figure 32B). No differences between control cells and induced cells could be obtained.

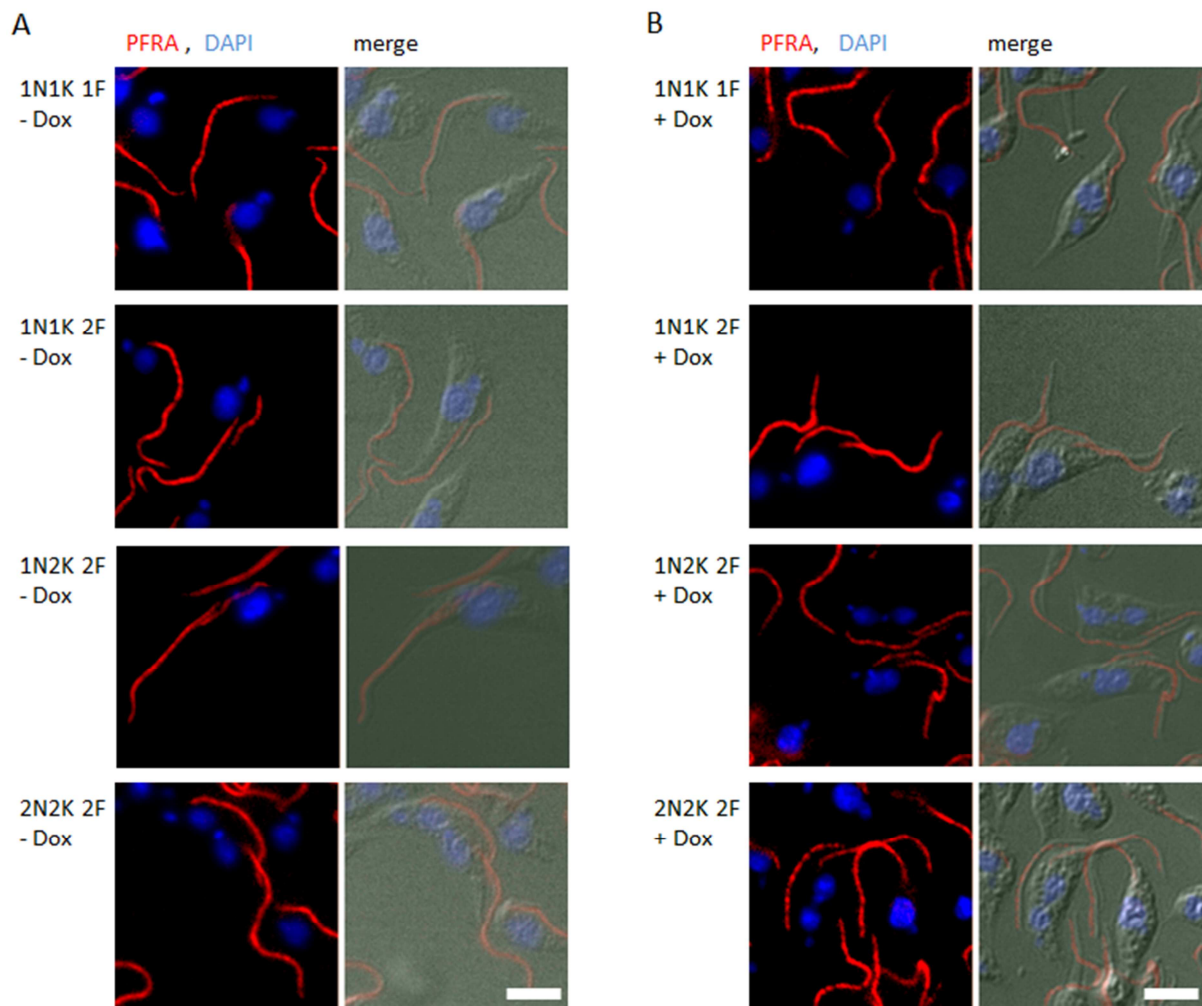


Figure 32: The effect of TbSec24.1 RNAi on the paraflagellar rod. Immunofluorescence microscopy of methanol fixed RNAi induced TbSec24.1 RNAi cells (B) indicated no differences in formation of the flagellum (anti-TbPFRA antibody, red) compared to uninduced cells (A). 1N1K cells with one (1N1K 1F) or two flagella (1N1K 2F) and 1N2K and 2N2K cells with two flagella (1N2K 2F, 2N2K 2F) could be observed. DNA is shown in blue (DAPI). The pictures illustrate samples of day two after depletion of *tbSec24.1* compared to uninduced cells. Bar = 5 μm .

3.8 Cell recovery after TbSec24.1RNAi and TbSec24.2 RNAi

It was additionally examined if TbSec24.1 and TbSec24.2 RNAi leads to irreversible defects within *T. brucei*, or if cells can recover from diminished COPII vesicle transport. Therefore both TbSec24.1 and TbSec24.2 RNAi was induced over six days. On day six, Dox was removed by washing cells with tetracycline free medium. Cell cultures were allowed to grow afterwards for another six days without Dox.

3.8.1 The effect of switching off RNAi on the growth rate and cell cycle stages of *T. brucei*

Comparable growth defects after depletion of either TbSec24.1 or TbSec24.2 RNAi occurred. RNAi induction led to a gradual decrease in the growth rate of both RNAi cell lines (Figure 12). Switching off RNAi also showed comparable effects in both RNAi cell lines. TbSec24.1 (Figure 33A) and TbSec24.2 RNAi cells (Figure 33B) demonstrated immediate growth recovery within one day after removing Dox. Cells reached again the same growth rate as the uninduced control cells four to five days after drug removal.

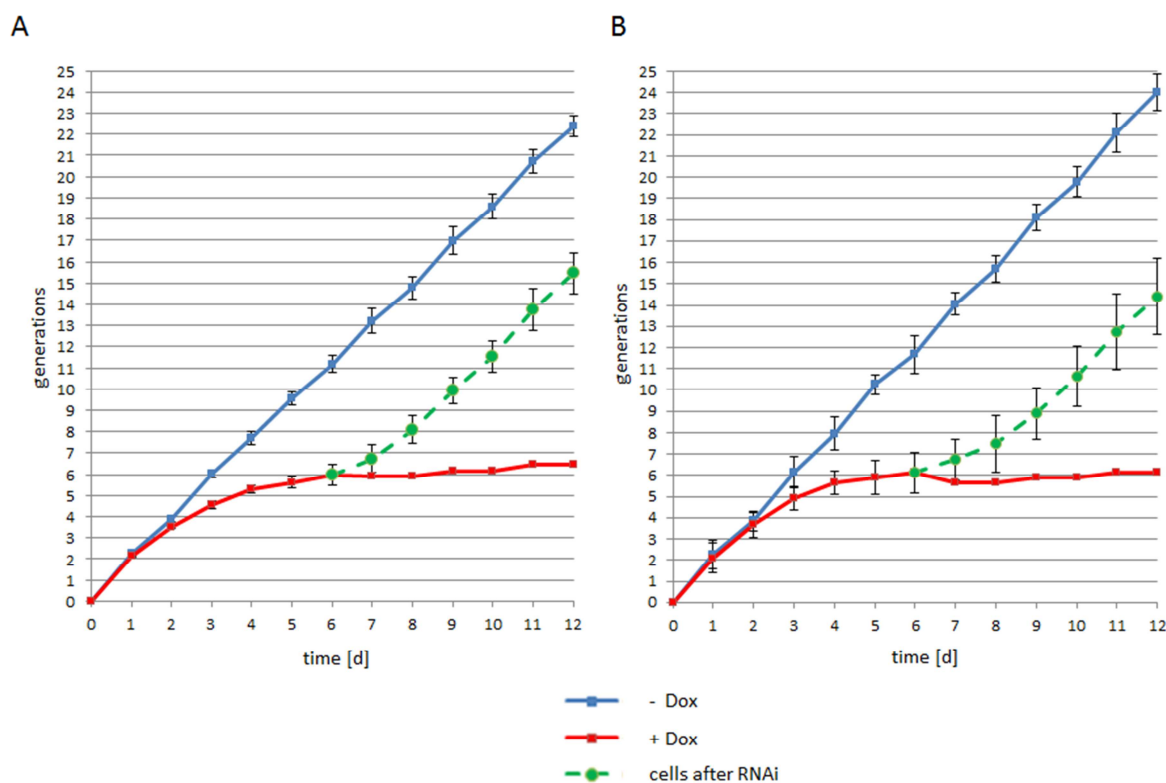


Figure 33: Cell growth and growth recovery after switching off RNAi. TbSec24.1 RNAi cells (A) and TbSec24.2 RNAi cells (B) were grown in the absence or presence of Dox to induce RNAi. Samples for cell counting were taken every 24 hours. The results are presented as mean \pm SD, $n = 2$. The growth rate of uninduced control cells is shown in blue; the red line indicates the rate of RNAi induced cells. Six days after RNAi induction, Dox was removed in an aliquot of induced cells by washing them with Dox free medium. Afterwards, cells continued to grow without Dox (green) for six more days. The cells show immediate recovery of growth rate after removing Dox.

The effect on the different cell cycle stages after TbSec24.1 RNAi was analyzed by immunofluorescence microscopy. Samples were taken on the day, where the recovering cells reached about the same growth rate again as uninduced cells, which corresponded to day five after Dox removal. No differences in cell cycle stages after switching off TbSec24.1 RNAi were observed (Figure 34). About 85 % were 1N1K cells, about 10 % 1N2K cells, and about 5 % were 2N2K cells (see Figure 13A, B).

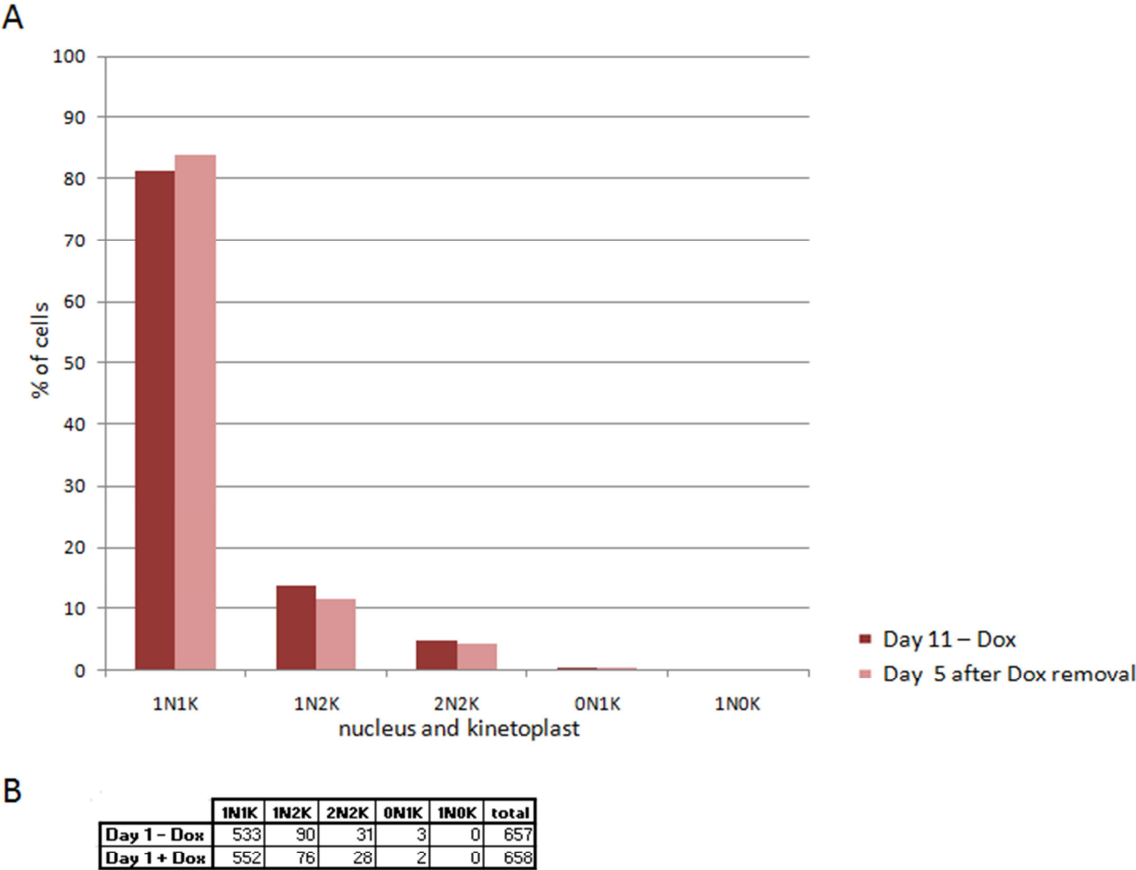


Figure 34: Recovery after TbSec24.1 RNAi of the cell cycle stages. A) Switching off TbSec24.1RNAi did not show significant effects on cell cycle stages comparing induced and control cells. DNA was stained with DAPI in induced cells five days after removing of Dox. Uninduced cells were stained in a similar fashion. B) The absolute numbers of analyzed cells are shown.

The results showed that RNAi of both TbSec24 isoforms did not generally lead to irreversible effects. Cells were able to recover from TbSec24.1 and TbSec24.2 RNAi caused growth defects.

3.8.2 The effect of switching off TbSec24.1 RNAi and TbSec24.2 RNAi on protein levels

It was shown that cells can return to their normal growth rate after switching off RNAi of both TbSec24 isoforms. The next step was to determine if the protein levels of TbSec24.1 and TbSec24.2 also recover after removing Dox from the medium. Immunoblotting showed depletion of TbSec24.1 protein level after TbSec24.1 RNAi (Figure 35A). A decrease in the level of TbSec24.2 was observed in TbSec24.2 RNAi cells after RNAi induction (Figure 35B). Compared to day six, a slight increase in the protein level could already be detected one day after switching off RNAi (day seven). These effects could be observed in both TbSec24 RNAi cell lines. Five days after removing Dox (day eleven), the levels of both TbSec24 isoforms were still lower than in the uninduced controls. However, a remarkable increase of protein levels comparing day six and day eleven could be seen clearly. This continuing augmentation in the protein level of the depleted TbSec24 isoform provides evidence for successful abortion of the induced RNAi. TbGRIP70 and TbGRASP protein levels were affected neither by depletion of either TbSec24 isoforms nor by RNAi relaxation.

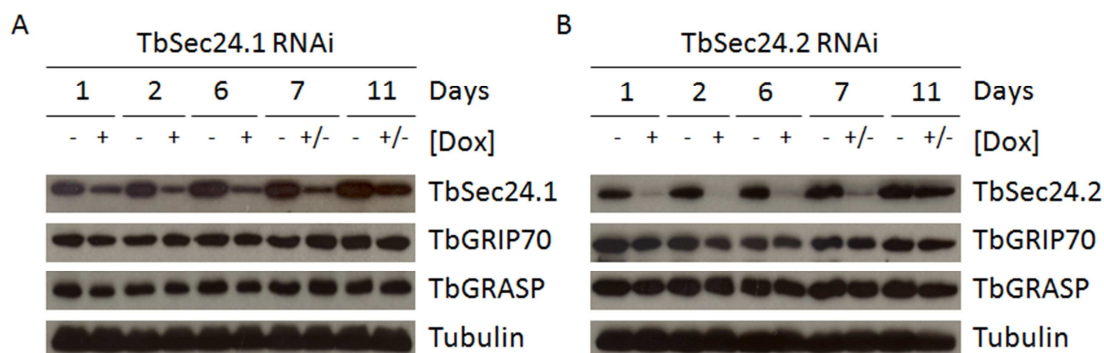


Figure 35: Recovery of protein levels after TbSec24.1 and TbSec24.2 RNAi. Protein levels were assessed in TbSec24.1 RNAi cells (A) and TbSec24.2 RNAi cells (B) before and after switching off RNAi by immunoblotting. +: RNAi induced cells, -: uninduced controls, +/-: induced cells after Dox removal. Removing Dox after six days led to a recovery of TbSec24 protein levels in both cell lines. The amount of detected protein seemed to recover immediately after switching off RNAi. Five days after Dox removal (day 11), only a slight difference in the signal of induced cells compared to the control lysate could be seen. The levels of the Golgi markers TbGRIP70 and TbGRASP were not affected in both TbSec24 RNAi cells, neither by induction nor by switching off RNAi. Lysate: 2×10^6 cells per lane were used. Anti-tubulin antibodies were used as control for equal loading.

3.8.3 The effect of switching off TbSec24.1 RNAi on the total number of TbGRIP70 and TbGRASP labeled Golgi

Immunofluorescence microscopy pictures were taken and analyzed to determine, if the effects of TbSec24.1 RNAi on TbGRIP70 and TbGRASP localization are reversible as well. Cells were harvested five days after removing Dox and treated equally to Figure 27.

It was determined that Dox removal by washing RNAi induced cells with Dox free medium led to a recovery of the correct localization of the Golgi markers TbGRIP70 (Figure 36A) and TbGRASP (Figure 36B). The effect was observed throughout all cell cycle stages after switching off TbSec24.1 RNAi (data not shown).

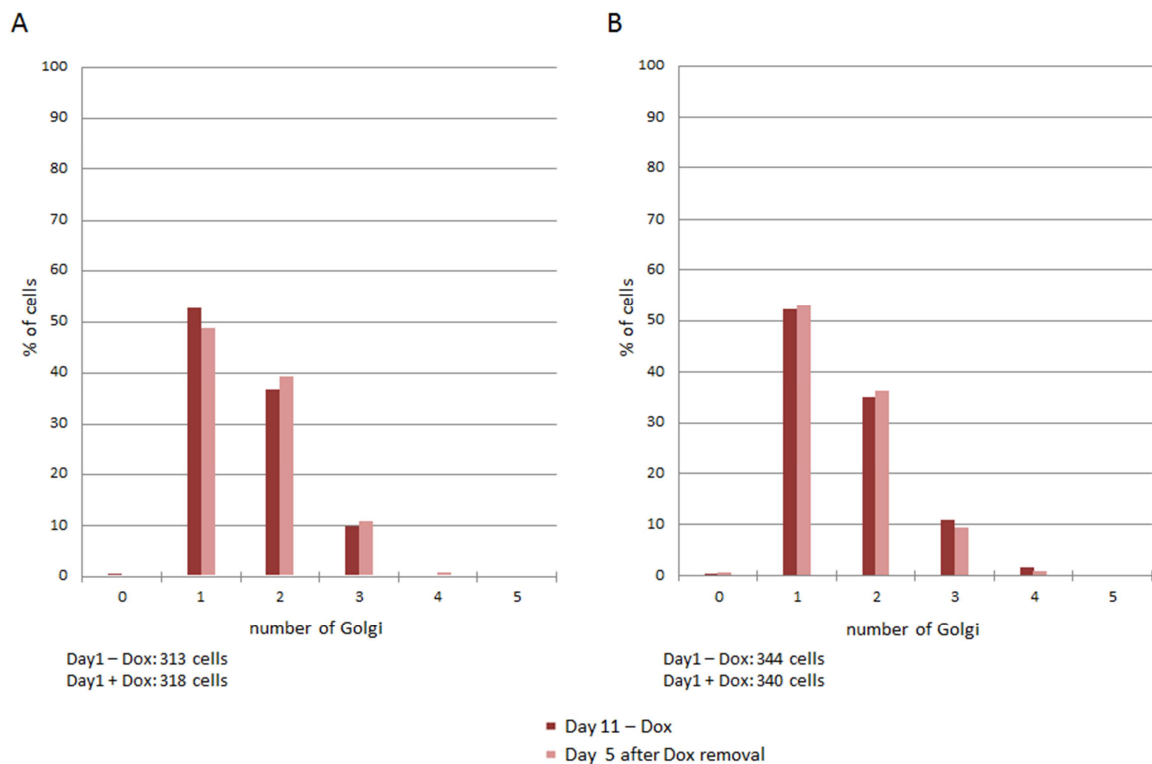


Figure 36: Recovery of the total number of Golgi after TbSec24.1 RNAi. Cells were analyzed five days after removing Dox. The total Golgi analysis did not show striking differences in induced and uninduced cells five days after removal of Dox in TbGRIP70 (A) and TbGRASP (B) labeling. The absolute numbers of analyzed cells are shown below the graph.

3.8.4 The effect of switching off TbSec24.1 RNAi on TbGRIP70 and TbGRASP labeled bilobe and non bilobe Golgi

It was examined if removal of Dox had an equal recovery effect on both, bilobe and non-bilobe Golgi after TbSec24.1 RNAi. The analysis remarked a complete rescue of the effects of TbSec24.1 RNAi on the number of bilobe Golgi in TbGRIP70 (Figure 37A) and TbGRASP (Figure 37C) labeling. TbGRASP labeling showed slightly more cells with one visible bilobe Golgi and less with two TbGRASP positive bilobe Golgi but the effect was not striking compared to the mislocalization during TbSec24.1 RNAi. Analysis of the visible non-bilobe Golgi also indicated full recovery in both, TbGRIP70 (Figure 37B) and TbGRASP labeling (Figure 37D) after switching off RNAi.

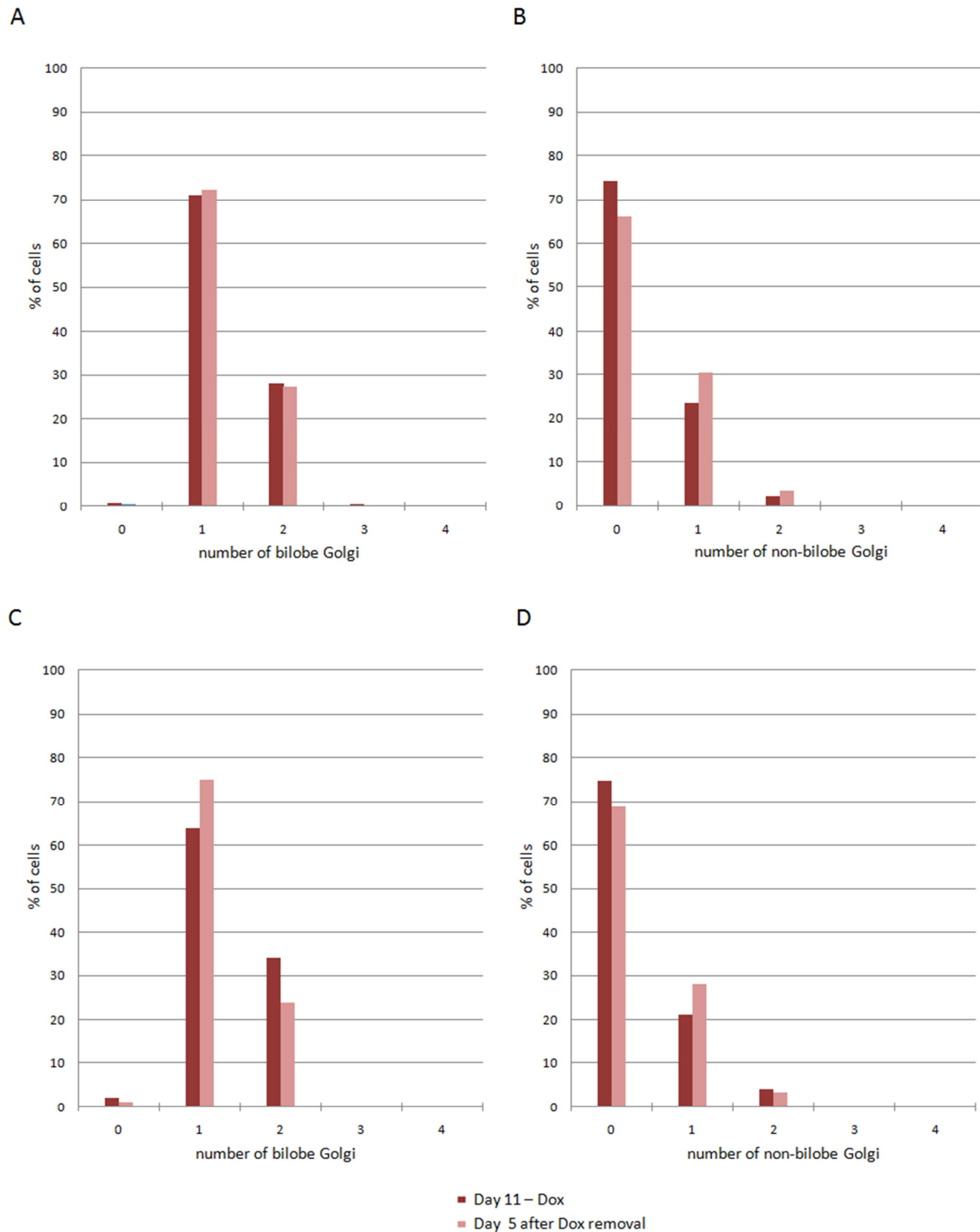


Figure 37: Recovery of the number of TbGRIP70 and TbGRASP labeled bilobe and non-bilobe Golgi after TbSec24.1 RNAi. Cells were analyzed five days after removing Dox. Bilobe labeling was obtained by using anti-Centrin4 antibodies. The graph displays the pooled data of all cell cycle stages. The absolute numbers of analyzed cells were shown in Figure 36. Both analyzed Golgi markers (TbGRIP70: A, B; TbGRASP: C, D) showed recovery of the TbSec24.1 effects on bilobe (A, C) and non-bilobe (B, D) Golgi.

These results indicated that TbGRIP70 (data not shown) and TbGRASP (Figure 38) re-localize correctly to both, bilobe and non-bilobe Golgi after switching off TbSec24.1 RNAi. However, our findings did not indicate if re-localization to both types of Golgi recover co-instantaneously, or successively.

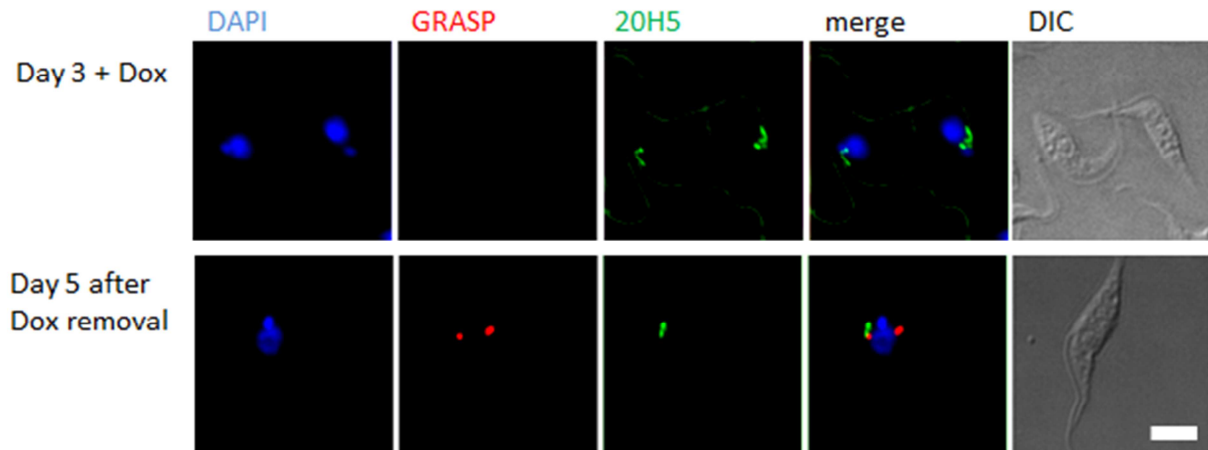


Figure 38: Recovery of TbGRASP localization to the Golgi after TbSec24.1 RNAi. The figure illustrates pictures of methanol fixed TbSec24.1 RNAi cells three days after RNAi induction and five days after switching off RNAi. Bilobe structures were labeled anti-TbCen4 (green). Nucleus and kinetoplast were stained with DAPI (blue). Depletion of TbSec24.1 led to a mislocalization of TbGRASP, whereas distinct Golgi structures (anti-GRASP antibody, red) could be seen five days after removing Dox. Bar = 5 μ m.

3.9 Biochemical analysis of TbGRASP interaction with TbGolgin63

Immunofluorescence microscopy has shown that the transmembrane protein TbGolgin63 colocalizes with TbGRASP (Figure 39). This was already described in [226]. Additionally, TbGolgin63 behaves similarly to TbGRASP upon RNAi of the TbSec24 isoforms (data not shown). TbGolgin63 also mislocalized after inducing TbSec24.1 RNAi but remained localized to the Golgi after inducing TbSec24.2 RNAi. Identical to TbGRASP, the protein levels of TbGolgin63 remained stable upon RNAi of both TbSec24 isoforms over three days after RNAi induction (data not shown). These experiments were done by Lars Demmel.

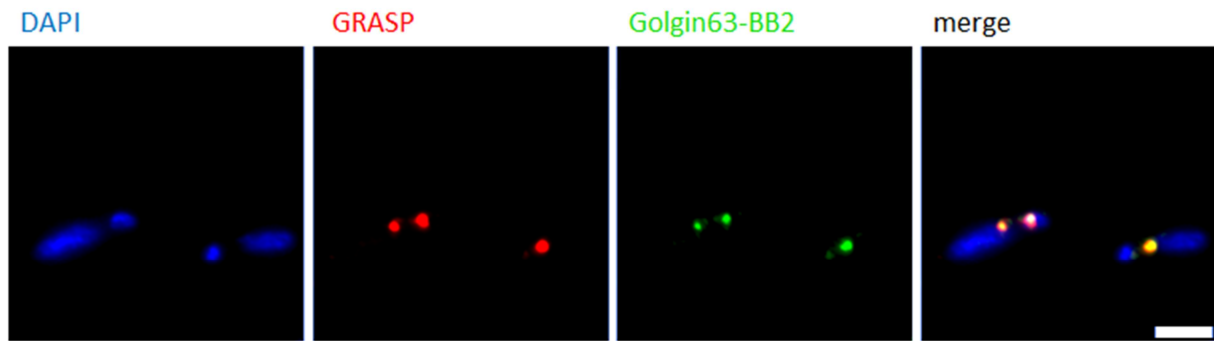


Figure 39: Localization of stably expressed TbGolgin63-BB2 and TbGRASP-GST. Immunofluorescence microscopy images of methanol fixed Lister 427 cells stably expressing TbGolgin63-BB2 and TbGRASP-GST show distinct Golgi structures (green: observed using antibodies to BB2; red: observed using antibodies to TbGRASP). Merged images indicated colocalization of TbGolgin63-BB2 and TbGRASP-GST. Bar = 5 μ m.

The colocalization of TbGolgin63 and TbGRASP and their similar behavior upon TbSec24.1 RNAi led to the idea of an interaction between these proteins. Furthermore, TbGolgin63 might be a required factor for the Golgi recruitment and Golgi association of TbGRASP.

To examine a possible interaction between TbGRASP and TbGolgin63, a GST-pulldown (Figure 40A) and a co-immunoprecipitation assay (Figure 40B) were executed. Therefore, *T. brucei* strain Lister 427 was stably transfected with C-terminal glutathione S-transferase (GST) tagged TbGRASP and C-terminal BB2 tagged TbGolgin63.

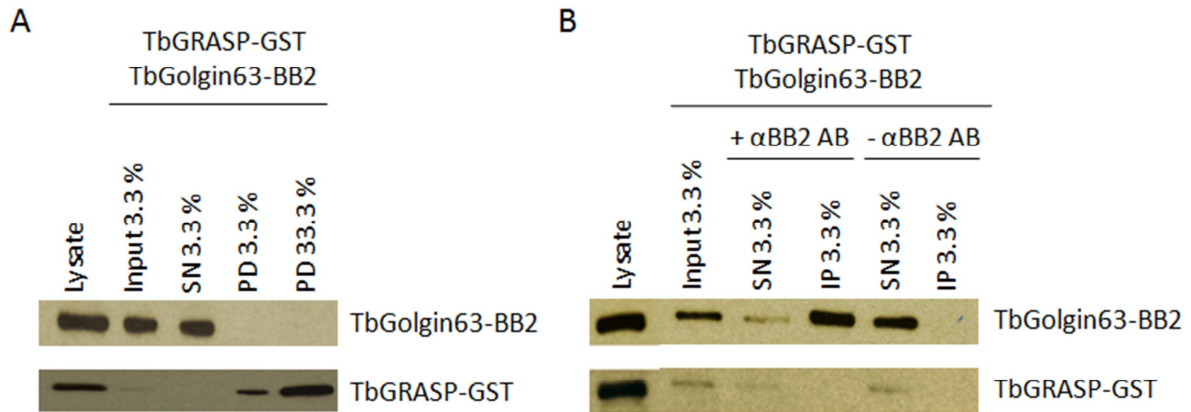


Figure 40: TbGolgin63 does not interact with TbGRASP. Lister 427 cells were stably transfected with TbGRASP-GST and TbGolgin63-BB2. Anti-GST and anti-BB2 antibodies were used. A) Immunoblotting of the GST-pulldown assay. Cleared cell lysate (Input) was mixed with glutathion sepharose beads. Afterwards, the mix was separated into supernatant (SN) and beads by centrifugation. Beads were washed and resuspended in 2 x SB (PD). Equal fractions were loaded on a SDS-PAGE. PD lane showed purified TbGRASP-GST but no TbGolgin63 signal. TbGolgin63, but not TbGRASP could be detected in the SN. Lysate: 4×10^6 cells of TbGRASP-GST/TbGolgin63-BB2 cells are used as control for the blot and the cell line. B) Immunoblotting of the co-immunoprecipitation assay. Anti-BB2 antibodies and protein A sepharose beads were added to cleared cell lysate (Input). Slurry was separated into supernatant (SN) and beads afterwards. Beads were resuspended in 2 x SB (IP). Equal fractions of the Input, SN and IP were loaded on a SDS-PAGE. The same procedure without using anti-BB2 antibody was executed additionally as a control for unspecific binding. TbGolgin63-BB2 signal was detected in IP (+ anti-BB2 antibody) and in SN (- anti-BB2 antibody). A weak signal was observed in the SN (+anti-BB2 antibody), indicating a small unbound amount of TbGolgin63-BB2. TbGRASP-GST could only be detected in the SN. Lysate: 4×10^6 cells of TbGRASP-GST/TbGolgin63-BB2 cells are used as control for the blot and the cell line. Both assays do not show any interactions of TbGRASP and TbGolgin63.

The analysis of both, GST-pulldown and co-immunoprecipitation assay, did not provide evidence of interaction between TbGolgin63 and TbGRASP. However, the results of these assays should be interpreted very carefully, as their execution revealed technical inaccuracies. For example, the Input signal normally has to be as strong as the summation of the SN and PD signal. Here, the Input signal for unknown reasons was weaker than estimated.

4. Discussion

4.1 Both isoforms of the COPII component TbSec24 are essential

In eukaryotes, the COPII machinery is necessary for the trafficking of cargo from the ER to the Golgi by means of transport vesicles. During vesicle formation at the ERES, membrane bound cargo or receptors for luminal soluble proteins are captured by interaction with multiple cargo binding sites of the COPII coat subunit Sec24 [52, 53]. Most organisms contain multiple isoforms of Sec24, which are thought to differ in their recognition of ER export signals on secretory cargo [53, 70]. The isoforms also vary in terms of functional redundancy and whether or not they are essential for cell viability [70].

In contrast to other organisms in which either none or only one Sec24 isoform is essential for growth [70, 82-84], it was recently shown in the Lister 427 bloodstream form of *T. brucei* that both TbSec24 isoforms, TbSec24.1 and TbSec24.2, are indispensable for cell viability [219]. RNAi silencing of either isoform led to an arrest in cell growth about twelve hours after RNAi induction, followed by cell death approximately six hours later [219]. This indicates that both isoforms are essential for the transport of cellular key components required for internal replicative processes. However, only little is known about the identity of these components and their sorting into COPII vesicles. Another possibility for decelerated cell division is that degradation of one TbSec24 isoform might simply result in a reduction of the total transport capacity of cellular components.

Here we show in the procyclic form of *T. brucei* that depletion of either TbSec24 isoforms also leads to an arrest in cell growth at about 48 hours after RNAi induction. However, the depletion of TbSec24.1 or TbSec24.2 is not lethal in procyclic *T. brucei*. After switching off the RNAi machinery the growth rate in both RNAi cell lines recovered and no continuing growth defects could be detected.

The difference in the observed growth phenotypes between the procyclic form to the bloodstream form might be a consequence of a different vector used for RNAi or a different RNAi targeting sequence. It might also simply reflect the fact that the

bloodstream form of *T. brucei* commonly exhibits more severe phenotypes than the procyclic form [227].

It was also tested if depletion of either TbSec24 isoforms has an impact on the cell cycle progression of *T. brucei*. Normally, cells need a greater amount of membrane material and other cellular components to carry out cytokinesis. However, as deficient formation of COPII components might result in diminished supply of material, it is quite possible that cytokinesis is inhibited but nuclear division continues unaffected. Hence, it might be assumed that restricted COPII transport could lead to an accumulation of multinucleated cells. This circumstance has been frequently described in the literature to be common for a failure to complete cytokinesis [228-231]. However, no accumulation of cells in a specific cell cycle stage could be detected after TbSec24.1 or TbSec24.2 RNAi over a period of three days. It seems that cells arrest growth as soon as the level of either TbSec24 isoforms falls below a certain threshold. This quiescent state is similar to a G₀-like cell cycle stage.

Recently, it was shown in the bloodstream form that knockdown of one TbSec24 isoform leads to an increase of the mRNA transcript of the other. TbSec24.1 mRNA increased approximately 70 % after TbSec24.2 RNAi and TbSec24.2 mRNA about 40 % after TbSec24.1 RNAi [219]. This would suggest that lack of one TbSec24 isoform is compensated with transcript upregulation of the other. However, no appreciable upregulation could be observed at the protein level in the procyclic form. It has not been investigated so far if there is a difference between the bloodstream and the procyclic form of *T. brucei* in this matter, or if the rising mRNA level does not subsequently entail increased translation. As the protein level is more functionally relevant than the mRNA level it can be concluded that, at least in the procyclic form, cells do not compensate for depletion of one TbSec24 isoform by upregulating expression of the other.

4.2 Golgi components are differentially selected by COPII vesicles

Recently, a selective dependence on TbSec24.1 for loading of VSG, a GPI-anchored protein into COPII vesicles was described in *T. brucei* [219]. Here, a specific TbSec24 isoform dependency on the localization of several Golgi proteins was investigated. After depletion of either TbSec24 isoform, effects on the localization of

the TGN marker TbGRIP70, the COPI coatomer subunit Tb ϵ -COP, and TbGRASP were assessed by immunofluorescence microscopy.

Depletion of TbSec24.1 by RNA interference silencing led to a striking mislocalization of TbGRASP. Three days after TbSec24.1 RNAi induction, only about 20 % of the cells showed TbGRASP localization to the Golgi. In the majority of cells, no TbGRASP labeled Golgi could be detected by immunofluorescence microscopy. On the contrary, TbSec24.2 RNAi did not result in TbGRASP mislocalization. The other investigated proteins, TbGRIP70 and Tb ϵ -COP showed consistent Golgi localization after both TbSec24.1 RNAi and TbSec24.2 RNAi. These findings suggest that TbSec24 isoforms not only differ in trafficking of GPI-anchored cargo to the cell surface [219], but also in the selective recruitment of Golgi localized proteins. More precisely, TbSec24.1 is specifically required for the localization of TbGRASP to the Golgi. This is further affirmed by the fact that full recovery of TbGRASP localization to the Golgi was observed after TbSec24.1 RNAi relaxation.

Immunoblotting experiments indicated that neither TbSec24.1 RNAi nor TbSec24.2 RNAi have any effect on the protein levels of the investigated Golgi markers. Thus, the inability to detect TbGRASP at the Golgi by immunofluorescence microscopy was not the result of diminished translation or protein degradation.

Mammalian GRASP proteins are peripherally associated on the cytosolic site of the cis- and medial Golgi membrane by an N-terminal myristoyl moiety [163]. However, the specific targeting mechanism of GRASP homologues to the Golgi membrane is still unclear. GRASP55 and GRASP65 are dependent on interaction with other proteins to localize to the Golgi. GRASP65 was shown to require interaction with the coiled-coil golgin protein GM130 for Golgi recruitment, whereas GRASP55 interacts with Golgin45 [156, 159-161]. The yeast GRASP65 related protein Grh1p lacks a myristoylation site but features instead an acetylated N-terminal amphipathic helix which mediates Golgi association. Golgi localization of Grh1p in *S. cerevisiae* additionally is dependent on its interaction with the coiled-coil protein Bug1p. Bug1p shows some structural analogy to GM130, although no homologue of GM130 could be identified so far outside of multicellular organisms [162].

Presumably, the Golgi localization of TbGRASP in *T. brucei* is also dependent on one or more yet unidentified additional binding partners. These proteins might bind

preferentially to TbSec24.1 for subsequent packaging into COPII vesicles and delivery to the Golgi. This would account for the differences in TbGRASP localization, observed after TbSec24.1 or TbSec24.2 depletion.

Contrary to TbGRASP the other investigated Golgi components, TbGRIP70 and Tb ϵ -COP, localize to the Golgi even after depletion of either TbSec24 isoforms. This might be due to the fact that TbGRIP70 and Tb ϵ -COP require different binding partners than TbGRASP to be peripherally anchored to the Golgi surface. Both Golgi markers are dependent on small GTPases for their Golgi anchoring. In mammalian cells and yeast, proteins containing a GRIP domain are recruited to the Golgi by Arf-related GTPases [232-234]. COPI vesicle formation and subsequent ϵ -COP recruitment were shown to be dependent on the small GTPase Arf1 [235].

It is reasonable to assume that the putative binding partners of TbGRASP, needed for its Golgi association, might be members of the golgin family. However, no interaction between TbGRASP and the only so far identified Golgin in *T. brucei*, TbGolgin63 has been detected in biochemical assays.

Another possibility is that Golgi recruitment of TbGRASP might be dependent on members of the p24 type I transmembrane cargo receptor family. These proteins can interact directly with GRASP, but only if the p24s form oligomers [236]. It is assumed that Golgi located p24 proteins are present in a higher oligomeric state compared to ER localized ones [163]. Therefore, oligomeric p24s might be able to recruit GRASP specifically to the Golgi membranes. The genome of *T. brucei* contains six putative p24 orthologues [219].

Further experiments have to be carried out to identify putative interaction partners of TbGRASP, needed for its Golgi association. A possibility would be implementation of a tandem affinity purification assay. TbSec24.1 RNAi cells will be transfected with C-terminally TAP-tagged TbGRASP. In control cells, TbGRASP-TAP localizes to the Golgi, presumably dependent on interaction with other proteins whose delivery to the Golgi depends on TbSec24.1. Upon TbSec24.1 RNAi induction, the putative TbGRASP interaction partner might be retained in the ER. Hence, TbGRASP is unable to bind to its partner and cannot be recruited to the Golgi. TAP-tagged TbGRASP, together with interacting proteins, will be purified from RNAi induced and control cells, followed by SDS-PAGE and coomassie blue staining. Comparison of

the protein bands from control and RNAi induced cells should reveal bands only present in the control lane and might represent putative binding partners of TbGRASP, involved in its recruitment to the Golgi.

So far, it also has not been determined where TbGRASP specifically localizes after induction of TbSec24.1 RNAi. As GRASP proteins lack a transmembrane domain and are known to localize peripherally to the Golgi membrane [159, 160], it is very likely that TbGRASP localizes to the cytosol upon TbSec24.1 depletion. Due to the high dilution of TbGRASP within the cytoplasm, it cannot be detected by immunofluorescence microscopy.

Additionally, it cannot not be excluded that defective COPII mediated transport leads to severe defects in the structural and enzymatic composition of the Golgi. It might be that at least TbSec24.1 RNAi causes defects in the formation of the Golgi as it results in mislocalization of TbGRASP, which is thought to play a role in maintaining the morphology of the Golgi. For instance it was shown in mammalian cells that depletion of either GRASP55 or GRASP65 reduces the number of cisternae per Golgi stack. Depletion of both GRASP proteins at the same time leads to disassembly of the entire Golgi stack [237]. Therefore, it will be crucial to carry out corresponding EM studies of the Golgi in *T. brucei*, as light microscopy lacks the resolution to determine if the Golgi maintains its correct morphology and function after depletion of either TbSec24.1 or TbSec24.2.

4.3 Depletion of both TbSec24 isoforms shows differential effects on Golgi labeling and the number of discriminative Golgi populations

There are two Golgi populations in a *T. brucei* cell. The first appears as single copy and lies between the nucleus and the kinetoplast. This 'main Golgi' is closely located to the previously discovered bilobe structure [198]. Usually, wild type *T. brucei* have one or two bilobe associated Golgi at an early cell cycle stage (1N1K), whereas 1N2K and 2N2K cells have two [198]. The bilobe structure was suggested to play a role in defining the construction site of the new ERES and to provide a scaffold to regulate the position and the size of the new assembled Golgi [198, 216]. The second Golgi population occurs at random locations in variable numbers within the cell and is not associated to the bilobe [198, 211]. Previous studies have indicated

that these non-bilobe-associated Golgi are stacked [196] and functional (unpublished data) and appear towards the end of the cell cycle [211]. According to previously done live cell imaging these Golgi disappear just before the cell undergoes cytokinesis [211]. However, in this work, TbGRIP70 or TbGRASP labeled non-bilobe Golgi could be observed in about 40 % of all control cells irrespectively of their cell cycle stage by immunofluorescence microscopy. Thereby, 1N1K cells showed about the same percentage of non-bilobe Golgi as 1N2K and 2N2K cells. This discrepancy might simply be a matter of the much larger amount of analyzed cells in the present study.

Without distinguishing between bilobe and non-bilobe Golgi, the depletion of either TbSec24 isoforms proposes a loss of non-bilobe Golgi. The total numbers of TbGRIP70- or TbGRASP-labeled foci upon depletion of TbSec24.1 or TbSec24.2 are approximately the same as the number of bilobe Golgi in uninduced cells. This is true for all cell cycle stages.

A striking mislocalization of TbGRASP from bilobe associated Golgi after depletion of TbSec24.1 occurred progressively from day one to day three. The phenotype was observed throughout all cell cycle stages. In contrast, TbGRASP labeling showed a quick and constant decrease of cells containing visible non-bilobe Golgi after TbSec24.1 depletion. In the majority of cells (up to 90 %) TbGRASP labeled non-bilobe associated Golgi could not be detected upon TbSec24.1 RNAi induction in all cell cycle stages.

TbGRIP70 labeling did not show an effect in the number of visible bilobe Golgi over three days after induction of TbSec24.1 RNAi. This suggests that TbSec24.1 RNAi has no effect on the localization of TbGRIP70 to bilobe Golgi. However, a quick and constant decrease of visible TbGRIP70 labeled non-bilobe Golgi foci could be seen after depletion of TbSec24.1. The effect showed comparable kinetics as detected by TbGRASP labeling.

TbGRIP70 and TbGRASP mislocalize from non-bilobe associated Golgi in a similar manner. As both markers show differences in their localization to bilobe Golgi on the one hand, but contrary behave nearly identical regarding non-bilobe Golgi, it is reasonable to assume that non-bilobe Golgi are not even formed upon TbSec24.1 RNAi. These findings additionally suggest that bilobe Golgi and non-bilobe Golgi

differ in their stability. Apparently, bilobe Golgi are more stable, which might be due to their association with the bilobe structure.

Nevertheless, function and formation of the additional Golgi remain unclear and still have to be determined. It was already shown that non-bilobe Golgi have an associated ERES [198, 211]. Therefore, it seems plausible that COPII components are synthesized continuously during the cell cycle of *T. brucei*. This might result in an excess of COPII components, which randomly assemble at the ER membrane and in turn form new ERES and subsequently a new Golgi. Upon depletion of either TbSec24 isoform, the surplus of COPII components might be reduced and cells would therefore be unable to form additional ERES, consequently resulting in fewer non-bilobe Golgi.

5. Materials and Methods

5.1 Buffers and Solutions

10x Running buffer:	250 mM Tris base pH 8.8 1.9 M glycine 1 % SDS
1x Sample buffer:	62.5 mM Tris HCl pH 6.8 2 % SDS 10 % Glycerol 50 mM DTT Bromphenolblue
Blotting buffer:	1 x Running buffer 20 % Methanol
10x TBS:	200 mM Tris-Cl pH 7.5 1.5 M NaCl
TBST:	1 x TBS 0.1 % Tween 20
1x TAE:	40 mM Tris-Acetate 1 mM EDTA pH 8.5

5.2 Antibody list

Antibody	Origin/Clonality	Titer	Origin
20H5	mouse monoclonal	IF 1:1000	gift from Jeff Salisbury, JCB (1994); 124: 795
BB2	mouse monoclonal	IB 1:100, IF 1:300	MBP (1996); 77 (2): 235-9
GFP	rabbit polyclonal	IB 1:8000, IF 1:5000	Warren Lab
GFP	mouse monoclonal	IB 1:500, IF 1:4000	Roche
GST	mouse monoclonal	IB 1:200	MFPL antibody facility
PFRA	mouse monoclonal	IF 1:10000	J Protozool (1998); 36 (6): 617-24
TbBip	rabbit polyclonal	IF 1:1000	gift from JD Bangs, JCS (1993); 105 (Pt4): 1101-13
TbCentrin4	mouse monoclonal	IF 1:300	Warren Lab
TbGolgin63	rabbit polyclonal	IB 1:3000, IF 1:500	Warren Lab
TbGRASP	rabbit polyclonal	IB 1:2500, IF 1:500	Warren Lab
TbGRIP70	rabbit polyclonal	IB 1:500, IF 1:500	Warren Lab
TbSec24.1	rabbit polyclonal	IB 1:5000, IF 1:400	Warren Lab
TbSec24.2	rabbit polyclonal	IB 1:500, IF 1:300	Warren Lab
TbεCOP	rabbit polyclonal	IF 1:1000	Warren Lab
Tubulin	mouse monoclonal	IB 1:25000	Sigma, T6074
Alexa Fluor 488/568 conjugated 2 nd antibody	goat	IF 1:3000	Invitrogen: Molecular Probes
Horseradish peroxidase (HRP) conjugated 2 nd antibody	goat	IB 1:10000	Goat anti-rabbit: Dianova Goat anti-mouse: Pierce

5.3 *E. coli* transformation

Selection plates were prewarmed at about 37°C on the bottom of an incubator. Ultra-competent cells were taken out of freezer and thawed on ice. Plasmid DNA (1µl) or 10 µl ligation were added to the cells, and cells were left on ice for at least 5 min. Cells were then heat-shocked at 42°C for 45 sec, directly spread onto the prewarmed LB plates and allowed to grow at 37°C overnight.

LB medium:

- 1 % Tryptone
- 0.5 % Yeast extract
- 0.5 % NaCl
- 1.2 % Agar (for plates)

For LB-Amp media 100 µg/ml Ampicillin were added.

5.4 Plasmid DNA Purification

Plasmid DNA was purified using the QIAGEN Spin Miniprep Kit or the QIAGEN HiSpeed Plasmid Midi and Maxi Kit according to manufacturer's instructions.

5.5 DNA extraction and purification from agarose gels in TAE buffer

DNA was extracted and purified using the QIAGEN QIAquick Gel Extraction Kit according to manufacturer's instructions.

5.6 *T. brucei* cell lines

Lister 427 is the most commonly used procyclic *T. brucei* strain for molecular biology and biochemistry. Cells were grown at 27°C.

Culture medium (for Lister 427 cells):

- SDM79 medium [238]
- 200 mM Glutamin
- 100 µg/ml Pen/Strep
- 6.5 µg/ml Haemin
- 20 % FBS (foetal bovine serum, Gibco)
- 10 µg/ml Gentamycin

The procyclic host cell line 29-13 is co-expressing the tetracycline repressor protein and T7 RNA polymerase. It was derived from wild-type *T. brucei* 427 procyclic forms [239]. Cells were cultured at 27°C.

Culture medium (for 29-13 cells):

- SDM79 medium [238]
- 200 mM Glutamin
- 100 µg/ml Pen/Strep
- 6.5 µg/ml Haemin
- 20 % Tet-system approved FBS (Clontech)
- 10 µg/ml Gentamycin
- 50 µg/ml Hygromycin
- 15 µg/ml Neomycin

5.7 Selection markers

Hygromycin B:	50 µg/ml
Neomycin:	15 µg/ml
Phleomycin:	5 µg/ml
Blasticidin:	10 µg/ml

5.8 Vectors and constructs

Vector	Insert	Restriction site for linearization	Purpose	Transfected into	Originated by
pZJM (Phleomycin)	TbSec24.1 (GeneDB no. Tb927.3.1210), nt 708-1251	NotI	RNAi	29-13	Lars Demmel
pZJM (Phleomycin)	TbSec24.2 (GeneDB no. Tb927.3.5420), nt 338-804	NotI	RNAi	29-13	Lars Demmel
pXS2 (Neomycin)	TbGRASP (GeneDB no. Tb11.02.0260) - GST	NotI	GST-pulldown, Co-Immuno-precipitation	427	Chris deGraffenried
pXS2 (Blasticidin)	TbGolgin63 (GeneDB no. Tb11.02.4670) – BB2	NotI	GST-pulldown, Co-Immuno-precipitation	427	Chris deGraffenried

5.9 Silencing of TbSec24.1 and TbSec24.2 expression by RNA interference (RNAi)

Cultures of TbSec24.1 or TbSec24.2 RNAi cells were seeded at 1×10^6 cells/ml and grown in the presence or absence of doxycycline (10 µg/ml). Both cultures were incubated at 27°C and re-seeded at 1×10^6 cells/ml every 48 h. Furthermore, fresh doxycycline (10 µg/ml) was added every 48 h to the RNAi induced cells. Every 24 h, the number of cells in each culture was determined using a Z2 Coulter Particle Count and Size Analyzer (Beckman Coulter).

To remove doxycycline, the induced cells were washed three times with tetracycline free medium and seeded at 1×10^6 cells/ml afterwards. The cells were incubated at 27°C and re-seeded at 1×10^6 cells/ml every 48 h.

5.10 Transfection of Trypanosomes

Cytomix:	120 mM KCl
	0.15 mM CaCl ₂
	10 mM K ₂ HPO ₄
	25 mM Hepes (pH 7.6)
	2 mM EGTA
	5 mM MgCl ₂

5×10^7 cells per transfection were spun down in a 15 ml Falcon (3000 rpm, 5 min, 4°C). The supernatant was aspirated and the pellet was washed with 15 ml Cytomix. Then, cells were resuspended pellet in 500 µl Cytomix. Afterwards, the cell suspension was added to 50 µg DNA and cells were electroporated (1500 V, 25 µF, 2 x pulses [10 seconds between], time constant ~0.4). Cells were added to 6 ml medium (without selection markers) and incubated at 27°C for 6h to overnight.

In order to create a clonal cell line, 100 µl drug-free medium was added into each well from column 1 – 11 of a 96-well plate (uncoated plates). 100 µl of cells were added into each well of column 1. The cells were mixed and 100 µl were transferred into next columns throughout entire plate. 100 µl medium (including selection markers) were added. The plate was sealed with parafilm afterwards and incubated at 27°C with 5% CO₂ until clones were visible in single wells. After incubation, putative clones were picked and transferred into a 24-well plate containing 2.5 ml medium and subsequently into a T25 flask with 4 ml medium.

5.11 Immunofluorescence microscopy

Cells were spun down (800xg, 5 min, RT) and once washed in 1 ml PBS. The pellet was resuspended in 500 µl PBS and transferred onto a coverslip in a 24 well plate. The plate was then spun (800xg, 5 min, 4°C) to settle the cells onto the coverslip.

Cells were then fixed in pre-chilled methanol for 9 min at -20°C. Next, coverslips were washed 3 x 5 min with PBS and blocked in 3 % BSA in PBS at 4°C o/n.

Coverslips were then incubated with the primary antibody at RT for 1 h. Subsequently, coverslips were washed three times for 5 min with PBS and blocked in

3 % BSA in PBS at RT for 20 min. Then, they were incubated with the secondary antibody (INVITROGEN, Alexa Fluor) at RT in the dark for 1 h. Afterwards, coverslips were incubated with DAPI at RT for 10 min in the dark.

Coverslips were then washed thrice for 5 min with PBS and once rinsed with Milli-Q H₂O, mounted on slides (mounting medium: Fluoromount-G, Southern Biotech) and dried at RT overnight.

The images were obtained using an inverted microscope (Axio Observer Z1, Carl Zeiss MicroImaging Inc.) with a PCO 1600 camera using the manufacturer's drivers in a custom C++ program. The images were processed using ImageJ and Adobe Photoshop CS4 software.

Image analysis criteria:

Dots were regarded as a Golgi, if they were explicitly observable after subtracting the background. Therefore, a threshold was set to exclude diffuse cytoplasmic staining and all dots above this threshold were counted. For a comparable image analysis, untreated control cells were analyzed first to obtain a reference. The adjusted image properties were then used for analysis of RNAi induced cells.

The Golgi was defined as bilobe associated if it was located longitudinally to the bilobe and the gap between Golgi and the bilobe structure was not bigger than the size of the Golgi itself. Otherwise it was declared as non-bilobe Golgi.

The different organelles (nucleus, kinetoplast, Golgi, bilobe structure, flagellum) were counted as 2 individual units only when they were separated by a clearly visible gap. Otherwise they were considered as one.

5.12 Co-Immunoprecipitation

Lysis buffer: 20 mM Tris-HCl pH 7.5
 150 mM KCl
 5 mM MgCl₂
 1 % Triton TX-100
 Complete protease inhibitor cocktail
 1mM PMSF

10^8 cells expressing TbGolgin63-BB2 and TbGRASP-GST were harvested by centrifugation (800xg, 5 min, 4°C), washed with PBS, resuspended in 1 ml lysis buffer and lysed on ice for 30 min. The lysate was cleared by centrifugation (14000xg, 5 min, 4°C). 750 µl of the cleared lysate were mixed with 20 µl anti-BB2 antibody and 50 µl of washed protein A sepharose beads (Sigma). The mix was incubated for 2 h at 4°C on a rotator. Subsequently, the beads were spun down (3000 rpm, 3 min, 4°C). The SN was collected. Beads were washed three times with lysis buffer and thrice with lysis buffer lacking Triton TX-100. Then, beads were resuspended in 75 µl of 2x sample buffer and boiled for 5 min. Equal fractions of input, post-IP-SN and beads were loaded on a SDS-PAGE and analyzed by immunoblotting.

5.13 GST-pulldown

The GST-pulldown assay was executed as the Co-Immunoprecipitation, except that Glutathion Sepharose beads (GE Healthcare Bio-Sciences) were used instead protein A sepharose beads and that the anti-BB2 antibody was omitted.

5.14 Cell lysate

Cells were washed twice with PBS and resuspended in 2x sample buffer and proteins were denatured 95°C for 10 minutes.

5.15 SDS-PAGE and Immunoblotting (wet blot)

Samples were loaded on 7.5 or 10 % Tris-HCl bisacrylamide gels and ran at 200V for approximately 45 min in running buffer.

Stacking gel:

Reagent	
dH ₂ O	3 ml
0.5 M Tris-HCl pH 6.8	1.25 ml
30 % Bisacrylamide	650 μ l
10 % sodium dodecyl sulfate	50 μ l
10 % ammonium persulfate	50 μ l
TEMED	5 μ l
Bromphenolblue	100 μ l

Separating gel:

Reagent	7.5 % gel	10 % gel
dH ₂ O	6 ml	5 ml
1.5 M Tris-HCl pH 8.8	3 ml	3 ml
30 % Bisacrylamide	3 ml	4 ml
10 % sodium dodecyl sulfate	120 μ l	120 μ l
10 % ammonium persulfate	120 μ l	120 μ l
TEMED	10 μ l	10 μ l

For the transfer of proteins from the gel to the nitrocellulose membrane using the wet blot system. Proteins were transferred at 400 mA for about 90 min. After the transfer the membrane was blocked in 5% milk in TBST for 45 minutes at RT. Thereafter the membrane was incubated with the primary antibody at 4°C overnight or at RT for 1 h. The membrane was washed three times 10 min with TBST and incubated for one hour with a HRP (horseradish peroxidase) conjugated secondary antibody. Finally the membranes were washed twice for 5 min and thrice for 10 min with TBST. For ECL-detection, Reagent 1 and 2 from Amersham Biosciences were mixed at equal volumes and the membrane was incubated with the ECL substrate for 1 min at RT.

5.16 Immunoblot stripping

In order to strip the immunoblot, the nitrocellulose membrane was washed three times with TBST to remove remaining ECL substrate. Then, the membrane was incubated in stripping buffer (Thermo Scientific - Restore PLUS Western Blot Stripping Buffer) at RT for 30 min. The membrane was washed thrice for 5 min and blocked in 5% milk in TBST for 45 minutes at RT. The following incubation in the antibodies was executed as described before.

References

1. Mowbrey, K. and J.B. Dacks, *Evolution and diversity of the Golgi body*. FEBS Lett, 2009. 583(23): p. 3738-45.
2. Short, B. and F.A. Barr, *The Golgi apparatus*. Curr Biol, 2000. 10(16): p. R583-5.
3. Rambourg, A., et al., *Tridimensional structure of the Golgi apparatus of nonciliated epithelial cells of the ductuli efferentes in rat: an electron microscope stereoscopic study*. Biol Cell, 1987. 60(2): p. 103-15.
4. Matthews, K.R., *The developmental cell biology of Trypanosoma brucei*. J Cell Sci, 2005. 118(Pt 2): p. 283-90.
5. Jamieson, J.D. and G.E. Palade, *Intracellular transport of secretory proteins in the pancreatic exocrine cell. II. Transport to condensing vacuoles and zymogen granules*. J Cell Biol, 1967. 34(2): p. 597-615.
6. Palade, G., *Intracellular aspects of the process of protein synthesis*. Science, 1975. 189(4206): p. 867.
7. Bonifacino, J.S. and B.S. Glick, *The mechanisms of vesicle budding and fusion*. Cell, 2004. 116(2): p. 153-66.
8. Barlowe, C., et al., *COPII: a membrane coat formed by Sec proteins that drive vesicle budding from the endoplasmic reticulum*. Cell, 1994. 77(6): p. 895-907.
9. Palmer, D.J., et al., *Binding of coatomer to Golgi membranes requires ADP-ribosylation factor*. J Biol Chem, 1993. 268(16): p. 12083-9.
10. Stamnes, M.A. and J.E. Rothman, *The binding of AP-1 clathrin adaptor particles to Golgi membranes requires ADP-ribosylation factor, a small GTP-binding protein*. Cell, 1993. 73(5): p. 999-1005.
11. Hammer, J.A., 3rd and X.S. Wu, *Rabs grab motors: defining the connections between Rab GTPases and motor proteins*. Curr Opin Cell Biol, 2002. 14(1): p. 69-75.
12. Letourneur, F., et al., *Coatomer is essential for retrieval of dilysine-tagged proteins to the endoplasmic reticulum*. Cell, 1994. 79(7): p. 1199-207.
13. Pearse, B.M., *Coated vesicles from pig brain: purification and biochemical characterization*. J Mol Biol, 1975. 97(1): p. 93-8.
14. Roth, T.F. and K.R. Porter, *Yolk Protein Uptake in the Oocyte of the Mosquito Aedes Aegypti. L*. J Cell Biol, 1964. 20: p. 313-32.
15. Redman, C.M., P. Siekevitz, and G.E. Palade, *Synthesis and transfer of amylase in pigeon pancreatic micromosomes*. J Biol Chem, 1966. 241(5): p. 1150-8.
16. Hughes, H. and D.J. Stephens, *Assembly, organization, and function of the COPII coat*. Histochem Cell Biol, 2008. 129(2): p. 129-51.
17. Orci, L., et al., *Mammalian Sec23p homologue is restricted to the endoplasmic reticulum transitional cytoplasm*. Proc Natl Acad Sci U S A, 1991. 88(19): p. 8611-5.
18. Ladinsky, M.S., et al., *Golgi structure in three dimensions: functional insights from the normal rat kidney cell*. J Cell Biol, 1999. 144(6): p. 1135-49.
19. Martinez-Menarguez, J.A., et al., *Vesicular tubular clusters between the ER and Golgi mediate concentration of soluble secretory proteins by exclusion from COPI-coated vesicles*. Cell, 1999. 98(1): p. 81-90.

20. Appenzeller-Herzog, C. and H.P. Hauri, *The ER-Golgi intermediate compartment (ERGIC): in search of its identity and function*. J Cell Sci, 2006. 119(Pt 11): p. 2173-83.
21. Presley, J.F., et al., *ER-to-Golgi transport visualized in living cells*. Nature, 1997. 389(6646): p. 81-5.
22. Griffiths, G., et al., *Immunocytochemical localization of beta-COP to the ER-Golgi boundary and the TGN*. J Cell Sci, 1995. 108 (Pt 8): p. 2839-56.
23. Malhotra, V., et al., *Purification of a novel class of coated vesicles mediating biosynthetic protein transport through the Golgi stack*. Cell, 1989. 58(2): p. 329-36.
24. Friend, D.S. and M.G. Farquhar, *Functions of coated vesicles during protein absorption in the rat vas deferens*. J Cell Biol, 1967. 35(2): p. 357-76.
25. Dancourt, J. and C. Barlowe, *Protein sorting receptors in the early secretory pathway*. Annu Rev Biochem, 2010. 79: p. 777-802.
26. Heilker, R., M. Spiess, and P. Crottet, *Recognition of sorting signals by clathrin adaptors*. Bioessays, 1999. 21(7): p. 558-67.
27. Jackson, M.R., T. Nilsson, and P.A. Peterson, *Identification of a consensus motif for retention of transmembrane proteins in the endoplasmic reticulum*. EMBO J, 1990. 9(10): p. 3153-62.
28. Lewis, M.J. and H.R. Pelham, *Ligand-induced redistribution of a human KDEL receptor from the Golgi complex to the endoplasmic reticulum*. Cell, 1992. 68(2): p. 353-64.
29. Munro, S. and H.R. Pelham, *A C-terminal signal prevents secretion of luminal ER proteins*. Cell, 1987. 48(5): p. 899-907.
30. Barlowe, C., *Signals for COPII-dependent export from the ER: what's the ticket out?* Trends Cell Biol, 2003. 13(6): p. 295-300.
31. Zerial, M. and H. McBride, *Rab proteins as membrane organizers*. Nat Rev Mol Cell Biol, 2001. 2(2): p. 107-17.
32. Cai, H., K. Reinisch, and S. Ferro-Novick, *Coats, tethers, Rabs, and SNAREs work together to mediate the intracellular destination of a transport vesicle*. Dev Cell, 2007. 12(5): p. 671-82.
33. Sollner, T., et al., *SNAP receptors implicated in vesicle targeting and fusion*. Nature, 1993. 362(6418): p. 318-24.
34. Grosshans, B.L., D. Ortiz, and P. Novick, *Rabs and their effectors: achieving specificity in membrane traffic*. Proc Natl Acad Sci U S A, 2006. 103(32): p. 11821-7.
35. Chavrier, P. and B. Goud, *The role of ARF and Rab GTPases in membrane transport*. Curr Opin Cell Biol, 1999. 11(4): p. 466-75.
36. Pfeffer, S. and D. Aivazian, *Targeting Rab GTPases to distinct membrane compartments*. Nat Rev Mol Cell Biol, 2004. 5(11): p. 886-96.
37. Whyte, J.R. and S. Munro, *Vesicle tethering complexes in membrane traffic*. J Cell Sci, 2002. 115(Pt 13): p. 2627-37.
38. Sollner, T., et al., *A protein assembly-disassembly pathway in vitro that may correspond to sequential steps of synaptic vesicle docking, activation, and fusion*. Cell, 1993. 75(3): p. 409-18.
39. Sutton, R.B., et al., *Crystal structure of a SNARE complex involved in synaptic exocytosis at 2.4 Å resolution*. Nature, 1998. 395(6700): p. 347-53.
40. Bannykh, S.I., T. Rowe, and W.E. Balch, *The organization of endoplasmic reticulum export complexes*. J Cell Biol, 1996. 135(1): p. 19-35.
41. Bevis, B.J., et al., *De novo formation of transitional ER sites and Golgi structures in Pichia pastoris*. Nat Cell Biol, 2002. 4(10): p. 750-6.

42. Rossanese, O.W., et al., *Golgi structure correlates with transitional endoplasmic reticulum organization in Pichia pastoris and Saccharomyces cerevisiae*. J Cell Biol, 1999. 145(1): p. 69-81.
43. Nakano, A. and M. Muramatsu, *A novel GTP-binding protein, Sar1p, is involved in transport from the endoplasmic reticulum to the Golgi apparatus*. J Cell Biol, 1989. 109(6 Pt 1): p. 2677-91.
44. Hicke, L., T. Yoshihisa, and R. Schekman, *Sec23p and a novel 105-kDa protein function as a multimeric complex to promote vesicle budding and protein transport from the endoplasmic reticulum*. Mol Biol Cell, 1992. 3(6): p. 667-76.
45. Salama, N.R., J.S. Chuang, and R.W. Schekman, *Sec31 encodes an essential component of the COPII coat required for transport vesicle budding from the endoplasmic reticulum*. Mol Biol Cell, 1997. 8(2): p. 205-17.
46. Salama, N.R., T. Yeung, and R.W. Schekman, *The Sec13p complex and reconstitution of vesicle budding from the ER with purified cytosolic proteins*. EMBO J, 1993. 12(11): p. 4073-82.
47. Budnik, A. and D.J. Stephens, *ER exit sites--localization and control of COPII vesicle formation*. FEBS Lett, 2009. 583(23): p. 3796-803.
48. Barlowe, C. and R. Schekman, *SEC12 encodes a guanine-nucleotide-exchange factor essential for transport vesicle budding from the ER*. Nature, 1993. 365(6444): p. 347-9.
49. Nakano, A., D. Brada, and R. Schekman, *A membrane glycoprotein, Sec12p, required for protein transport from the endoplasmic reticulum to the Golgi apparatus in yeast*. J Cell Biol, 1988. 107(3): p. 851-63.
50. Bielli, A., et al., *Regulation of Sar1 NH2 terminus by GTP binding and hydrolysis promotes membrane deformation to control COPII vesicle fission*. J Cell Biol, 2005. 171(6): p. 919-24.
51. Yoshihisa, T., C. Barlowe, and R. Schekman, *Requirement for a GTPase-activating protein in vesicle budding from the endoplasmic reticulum*. Science, 1993. 259(5100): p. 1466-8.
52. Miller, E., et al., *Cargo selection into COPII vesicles is driven by the Sec24p subunit*. EMBO J, 2002. 21(22): p. 6105-13.
53. Miller, E.A., et al., *Multiple cargo binding sites on the COPII subunit Sec24p ensure capture of diverse membrane proteins into transport vesicles*. Cell, 2003. 114(4): p. 497-509.
54. Lederkremer, G.Z., et al., *Structure of the Sec23p/24p and Sec13p/31p complexes of COPII*. Proc Natl Acad Sci U S A, 2001. 98(19): p. 10704-9.
55. Stagg, S.M., et al., *Structure of the Sec13/31 COPII coat cage*. Nature, 2006. 439(7073): p. 234-8.
56. Lee, M.C., et al., *Sar1p N-terminal helix initiates membrane curvature and completes the fission of a COPII vesicle*. Cell, 2005. 122(4): p. 605-17.
57. Oka, T. and A. Nakano, *Inhibition of GTP hydrolysis by Sar1p causes accumulation of vesicles that are a functional intermediate of the ER-to-Golgi transport in yeast*. J Cell Biol, 1994. 124(4): p. 425-34.
58. Connerly, P.L., et al., *Sec16 is a determinant of transitional ER organization*. Curr Biol, 2005. 15(16): p. 1439-47.
59. Novick, P., C. Field, and R. Schekman, *Identification of 23 complementation groups required for post-translational events in the yeast secretory pathway*. Cell, 1980. 21(1): p. 205-15.
60. Supek, F., et al., *Sec16p potentiates the action of COPII proteins to bud transport vesicles*. J Cell Biol, 2002. 158(6): p. 1029-38.

61. Espenshade, P., et al., *Yeast SEC16 gene encodes a multidomain vesicle coat protein that interacts with Sec23p*. J Cell Biol, 1995. 131(2): p. 311-24.
62. Gimeno, R.E., P. Espenshade, and C.A. Kaiser, *COPII coat subunit interactions: Sec24p and Sec23p bind to adjacent regions of Sec16p*. Mol Biol Cell, 1996. 7(11): p. 1815-23.
63. Ivan, V., et al., *Drosophila Sec16 mediates the biogenesis of tER sites upstream of Sar1 through an arginine-rich motif*. Mol Biol Cell, 2008. 19(10): p. 4352-65.
64. Bhattacharyya, D. and B.S. Glick, *Two mammalian Sec16 homologues have nonredundant functions in endoplasmic reticulum (ER) export and transitional ER organization*. Mol Biol Cell, 2007. 18(3): p. 839-49.
65. Watson, P., et al., *Sec16 defines endoplasmic reticulum exit sites and is required for secretory cargo export in mammalian cells*. Traffic, 2006. 7(12): p. 1678-87.
66. Iinuma, T., et al., *Mammalian Sec16/p250 plays a role in membrane traffic from the endoplasmic reticulum*. J Biol Chem, 2007. 282(24): p. 17632-9.
67. Kappeler, F., et al., *The recycling of ERGIC-53 in the early secretory pathway. ERGIC-53 carries a cytosolic endoplasmic reticulum-exit determinant interacting with COPII*. J Biol Chem, 1997. 272(50): p. 31801-8.
68. Nishimura, N. and W.E. Balch, *A di-acidic signal required for selective export from the endoplasmic reticulum*. Science, 1997. 277(5325): p. 556-8.
69. Nufer, O., et al., *Role of cytoplasmic C-terminal amino acids of membrane proteins in ER export*. J Cell Sci, 2002. 115(Pt 3): p. 619-28.
70. Wendeler, M.W., J.P. Paccaud, and H.P. Hauri, *Role of Sec24 isoforms in selective export of membrane proteins from the endoplasmic reticulum*. EMBO Rep, 2007. 8(3): p. 258-64.
71. Appenzeller, C., et al., *The lectin ERGIC-53 is a cargo transport receptor for glycoproteins*. Nat Cell Biol, 1999. 1(6): p. 330-4.
72. Nichols, W.C., et al., *Mutations in the ER-Golgi intermediate compartment protein ERGIC-53 cause combined deficiency of coagulation factors V and VIII*. Cell, 1998. 93(1): p. 61-70.
73. Schweizer, A., et al., *Identification, by a monoclonal antibody, of a 53-kD protein associated with a tubulo-vesicular compartment at the cis-side of the Golgi apparatus*. J Cell Biol, 1988. 107(5): p. 1643-53.
74. Jenne, N., et al., *Oligomeric state and stoichiometry of p24 proteins in the early secretory pathway*. J Biol Chem, 2002. 277(48): p. 46504-11.
75. Muniz, M., et al., *The Emp24 complex recruits a specific cargo molecule into endoplasmic reticulum-derived vesicles*. J Cell Biol, 2000. 148(5): p. 925-30.
76. Stamnes, M.A., et al., *An integral membrane component of coatamer-coated transport vesicles defines a family of proteins involved in budding*. Proc Natl Acad Sci U S A, 1995. 92(17): p. 8011-5.
77. Foley, D.A., H.J. Sharpe, and S. Otte, *Membrane topology of the endoplasmic reticulum to Golgi transport factor Erv29p*. Mol Membr Biol, 2007. 24(4): p. 259-68.
78. Hauri, H.P., et al., *ERGIC-53 and traffic in the secretory pathway*. J Cell Sci, 2000. 113 (Pt 4): p. 587-96.
79. Otte, S. and C. Barlowe, *The Erv41p-Erv46p complex: multiple export signals are required in trans for COPII-dependent transport from the ER*. EMBO J, 2002. 21(22): p. 6095-104.
80. Strating, J.R. and G.J. Martens, *The p24 family and selective transport processes at the ER-Golgi interface*. Biol Cell, 2009. 101(9): p. 495-509.

81. Mossesso, E., L.C. Bickford, and J. Goldberg, *SNARE selectivity of the COPII coat*. Cell, 2003. 114(4): p. 483-95.
82. Kurihara, T., et al., *Sec24p and Iss1p function interchangeably in transport vesicle formation from the endoplasmic reticulum in Saccharomyces cerevisiae*. Mol Biol Cell, 2000. 11(3): p. 983-98.
83. Shimoni, Y., et al., *Lst1p and Sec24p cooperate in sorting of the plasma membrane ATPase into COPII vesicles in Saccharomyces cerevisiae*. J Cell Biol, 2000. 151(5): p. 973-84.
84. Esaki, M., Y. Liu, and B.S. Glick, *The budding yeast Pichia pastoris has a novel Sec23p homolog*. FEBS Lett, 2006. 580(22): p. 5215-21.
85. Pagano, A., et al., *Sec24 proteins and sorting at the endoplasmic reticulum*. J Biol Chem, 1999. 274(12): p. 7833-40.
86. Tang, B.L., et al., *A family of mammalian proteins homologous to yeast Sec24p*. Biochem Biophys Res Commun, 1999. 258(3): p. 679-84.
87. Roberg, K.J., et al., *LST1 is a SEC24 homologue used for selective export of the plasma membrane ATPase from the endoplasmic reticulum*. J Cell Biol, 1999. 145(4): p. 659-72.
88. Merte, J., et al., *Sec24b selectively sorts Vangl2 to regulate planar cell polarity during neural tube closure*. Nat Cell Biol, 2010. 12(1): p. 41-6; sup pp 1-8.
89. Mancias, J.D. and J. Goldberg, *Structural basis of cargo membrane protein discrimination by the human COPII coat machinery*. EMBO J, 2008. 27(21): p. 2918-28.
90. Schimmoller, F., et al., *The absence of Emp24p, a component of ER-derived COPII-coated vesicles, causes a defect in transport of selected proteins to the Golgi*. EMBO J, 1995. 14(7): p. 1329-39.
91. Peng, R., A. De Antoni, and D. Gallwitz, *Evidence for overlapping and distinct functions in protein transport of coat protein Sec24p family members*. J Biol Chem, 2000. 275(15): p. 11521-8.
92. Bonnon, C., et al., *Selective export of human GPI-anchored proteins from the endoplasmic reticulum*. J Cell Sci, 2010. 123(Pt 10): p. 1705-15.
93. Dalton, A.J. and M.D. Felix, *Cytologic and cytochemical characteristics of the Golgi substance of epithelial cells of the epididymis in situ, in homogenates and after isolation*. Am J Anat, 1954. 94(2): p. 171-207.
94. Farquhar, M.G. and G.E. Palade, *The Golgi apparatus (complex)-(1954-1981)-from artifact to center stage*. J Cell Biol, 1981. 91(3 Pt 2): p. 77s-103s.
95. Griffiths, G. and K. Simons, *The trans Golgi network: sorting at the exit site of the Golgi complex*. Science, 1986. 234(4775): p. 438-43.
96. Kirchhausen, T., *Clathrin*. Annu Rev Biochem, 2000. 69: p. 699-727.
97. Toomre, D., et al., *Dual-color visualization of trans-Golgi network to plasma membrane traffic along microtubules in living cells*. J Cell Sci, 1999. 112 (Pt 1): p. 21-33.
98. Bonifacino, J.S. and R. Rojas, *Retrograde transport from endosomes to the trans-Golgi network*. Nat Rev Mol Cell Biol, 2006. 7(8): p. 568-79.
99. Joiner, K.A. and D.S. Roos, *Secretory traffic in the eukaryotic parasite Toxoplasma gondii: less is more*. J Cell Biol, 2002. 157(4): p. 557-63.
100. Preuss, D., et al., *Characterization of the Saccharomyces Golgi complex through the cell cycle by immunoelectron microscopy*. Mol Biol Cell, 1992. 3(7): p. 789-803.
101. Morre, J., L.M. Merlin, and T.W. Keenan, *Localization of glycosyl transferase activities in a Golgi apparatus-rich fraction isolated from rat liver*. Biochem Biophys Res Commun, 1969. 37(5): p. 813-9.

102. Neutra, M. and C.P. Leblond, *Radioautographic comparison of the uptake of galactose-3H and glucose-3H in the golgi region of various cells secreting glycoproteins or mucopolysaccharides*. J Cell Biol, 1966. 30(1): p. 137-50.
103. Whur, P., A. Herscovics, and C.P. Leblond, *Radioautographic visualization of the incorporation of galactose-3H and mannose-3H by rat thyroids in vitro in relation to the stages of thyroglobulin synthesis*. J Cell Biol, 1969. 43(2): p. 289-311.
104. Ellgaard, L., M. Molinari, and A. Helenius, *Setting the standards: quality control in the secretory pathway*. Science, 1999. 286(5446): p. 1882-8.
105. Dunphy, W.G., et al., *Early and late functions associated with the Golgi apparatus reside in distinct compartments*. Proc Natl Acad Sci U S A, 1981. 78(12): p. 7453-7.
106. Kornfeld, R. and S. Kornfeld, *Assembly of asparagine-linked oligosaccharides*. Annu Rev Biochem, 1985. 54: p. 631-64.
107. Haltiwanger, R.S., G.D. Holt, and G.W. Hart, *Enzymatic addition of O-GlcNAc to nuclear and cytoplasmic proteins. Identification of a uridine diphospho-N-acetylglucosamine:peptide beta-N-acetylglucosaminyltransferase*. J Biol Chem, 1990. 265(5): p. 2563-8.
108. Wells, L., et al., *Mapping sites of O-GlcNAc modification using affinity tags for serine and threonine post-translational modifications*. Mol Cell Proteomics, 2002. 1(10): p. 791-804.
109. Pelham, H.R., *Getting through the Golgi complex*. Trends Cell Biol, 1998. 8(1): p. 45-9.
110. Glick, B.S., *Organization of the Golgi apparatus*. Curr Opin Cell Biol, 2000. 12(4): p. 450-6.
111. Balch, W.E., et al., *Reconstitution of the transport of protein between successive compartments of the Golgi measured by the coupled incorporation of N-acetylglucosamine*. Cell, 1984. 39(2 Pt 1): p. 405-16.
112. Balch, W.E., B.S. Glick, and J.E. Rothman, *Sequential intermediates in the pathway of intercompartmental transport in a cell-free system*. Cell, 1984. 39(3 Pt 2): p. 525-36.
113. Braell, W.A., et al., *The glycoprotein that is transported between successive compartments of the Golgi in a cell-free system resides in stacks of cisternae*. Cell, 1984. 39(3 Pt 2): p. 511-24.
114. Orci, L., B.S. Glick, and J.E. Rothman, *A new type of coated vesicular carrier that appears not to contain clathrin: its possible role in protein transport within the Golgi stack*. Cell, 1986. 46(2): p. 171-84.
115. Orci, L., et al., *Dissection of a single round of vesicular transport: sequential intermediates for intercisternal movement in the Golgi stack*. Cell, 1989. 56(3): p. 357-68.
116. Ostermann, J., et al., *Stepwise assembly of functionally active transport vesicles*. Cell, 1993. 75(5): p. 1015-25.
117. Banfield, D.K., M.J. Lewis, and H.R. Pelham, *A SNARE-like protein required for traffic through the Golgi complex*. Nature, 1995. 375(6534): p. 806-9.
118. Bergmann, J.E. and S.J. Singer, *Immunoelectron microscopic studies of the intracellular transport of the membrane glycoprotein (G) of vesicular stomatitis virus in infected Chinese hamster ovary cells*. J Cell Biol, 1983. 97(6): p. 1777-87.
119. Rothman, J.E. and F.T. Wieland, *Protein sorting by transport vesicles*. Science, 1996. 272(5259): p. 227-34.

120. Beams, H.W. and R.G. Kessel, *The Golgi apparatus: structure and function*. Int Rev Cytol, 1968. 23: p. 209-76.
121. Grasse, P.P., [*Ultrastructure, polarity and reproduction of Golgi apparatus.*]. C R Hebd Seances Acad Sci, 1957. 245(16): p. 1278-81.
122. Glick, B.S., T. Elston, and G. Oster, *A cisternal maturation mechanism can explain the asymmetry of the Golgi stack*. FEBS Lett, 1997. 414(2): p. 177-81.
123. Bonfanti, L., et al., *Procollagen traverses the Golgi stack without leaving the lumen of cisternae: evidence for cisternal maturation*. Cell, 1998. 95(7): p. 993-1003.
124. Bannykh, S.I. and W.E. Balch, *Membrane dynamics at the endoplasmic reticulum-Golgi interface*. J Cell Biol, 1997. 138(1): p. 1-4.
125. Mironov, A.A., P. Weidman, and A. Luini, *Variations on the intracellular transport theme: maturing cisternae and trafficking tubules*. J Cell Biol, 1997. 138(3): p. 481-4.
126. Losev, E., et al., *Golgi maturation visualized in living yeast*. Nature, 2006. 441(7096): p. 1002-6.
127. Shorter, J. and G. Warren, *Golgi architecture and inheritance*. Annu Rev Cell Dev Biol, 2002. 18: p. 379-420.
128. Warren, G. and W. Wickner, *Organelle inheritance*. Cell, 1996. 84(3): p. 395-400.
129. Lowe, M. and F.A. Barr, *Inheritance and biogenesis of organelles in the secretory pathway*. Nat Rev Mol Cell Biol, 2007. 8(6): p. 429-39.
130. Glick, B.S., *Can the Golgi form de novo?* Nat Rev Mol Cell Biol, 2002. 3(8): p. 615-9.
131. Yoshimura, S.I., et al., *Direct targeting of cis-Golgi matrix proteins to the Golgi apparatus*. J Cell Sci, 2001. 114(Pt 22): p. 4105-15.
132. Gleeson, P.A., *Targeting of proteins to the Golgi apparatus*. Histochem Cell Biol, 1998. 109(5-6): p. 517-32.
133. Benchimol, M., et al., *Structure and division of the Golgi complex in Trichomonas vaginalis and Tritrichomonas foetus*. Eur J Cell Biol, 2001. 80(9): p. 593-607.
134. Pelletier, L., et al., *Golgi biogenesis in Toxoplasma gondii*. Nature, 2002. 418(6897): p. 548-52.
135. Guo, Y. and A.D. Linstedt, *COPII-Golgi protein interactions regulate COPII coat assembly and Golgi size*. J Cell Biol, 2006. 174(1): p. 53-63.
136. Barr, F.A., *Golgi inheritance: shaken but not stirred*. J Cell Biol, 2004. 164(7): p. 955-8.
137. Rossanese, O.W. and B.S. Glick, *Deconstructing Golgi inheritance*. Traffic, 2001. 2(9): p. 589-96.
138. Axelsson, M.A. and G. Warren, *Rapid, endoplasmic reticulum-independent diffusion of the mitotic Golgi haze*. Mol Biol Cell, 2004. 15(4): p. 1843-52.
139. Jesch, S.A. and A.D. Linstedt, *The Golgi and endoplasmic reticulum remain independent during mitosis in HeLa cells*. Mol Biol Cell, 1998. 9(3): p. 623-35.
140. Jesch, S.A., et al., *Mitotic Golgi is in a dynamic equilibrium between clustered and free vesicles independent of the ER*. Traffic, 2001. 2(12): p. 873-84.
141. Jokitalo, E., et al., *Golgi clusters and vesicles mediate mitotic inheritance independently of the endoplasmic reticulum*. J Cell Biol, 2001. 154(2): p. 317-30.
142. Pecot, M.Y. and V. Malhotra, *Golgi membranes remain segregated from the endoplasmic reticulum during mitosis in mammalian cells*. Cell, 2004. 116(1): p. 99-107.

143. Lucocq, J.M. and G. Warren, *Fragmentation and partitioning of the Golgi apparatus during mitosis in HeLa cells*. EMBO J, 1987. 6(11): p. 3239-46.
144. Shima, D.T., et al., *An ordered inheritance strategy for the Golgi apparatus: visualization of mitotic disassembly reveals a role for the mitotic spindle*. J Cell Biol, 1998. 141(4): p. 955-66.
145. Wei, J.H. and J. Seemann, *The mitotic spindle mediates inheritance of the Golgi ribbon structure*. J Cell Biol, 2009. 184(3): p. 391-7.
146. Tang, D., Y. Xiang, and Y. Wang, *Reconstitution of the cell cycle-regulated Golgi disassembly and reassembly in a cell-free system*. Nat Protoc, 2010. 5(4): p. 758-72.
147. Shorter, J. and G. Warren, *A role for the vesicle tethering protein, p115, in the post-mitotic stacking of reassembling Golgi cisternae in a cell-free system*. J Cell Biol, 1999. 146(1): p. 57-70.
148. Farquhar, M.G. and G.E. Palade, *The Golgi apparatus: 100 years of progress and controversy*. Trends Cell Biol, 1998. 8(1): p. 2-10.
149. Cluett, E.B. and W.J. Brown, *Adhesion of Golgi cisternae by proteinaceous interactions: intercisternal bridges as putative adhesive structures*. J Cell Sci, 1992. 103 (Pt 3): p. 773-84.
150. Franke, W.W., et al., *Inter- and intracisternal elements of the Golgi apparatus. A system of membrane-to-membrane cross-links*. Z Zellforsch Mikrosk Anat, 1972. 132(3): p. 365-80.
151. Turner, F.R. and W.G. Whaley, *Intercisternal Elements of the Golgi Apparatus*. Science, 1965. 147: p. 1303-4.
152. Rabouille, C., et al., *Reassembly of Golgi stacks from mitotic Golgi fragments in a cell-free system*. J Cell Biol, 1995. 129(3): p. 605-18.
153. Slusarewicz, P., et al., *Isolation of a matrix that binds medial Golgi enzymes*. J Cell Biol, 1994. 124(4): p. 405-13.
154. Seemann, J., et al., *Matrix proteins can generate the higher order architecture of the Golgi apparatus*. Nature, 2000. 407(6807): p. 1022-6.
155. Seemann, J., et al., *Partitioning of the matrix fraction of the Golgi apparatus during mitosis in animal cells*. Science, 2002. 295(5556): p. 848-51.
156. Short, B., et al., *A GRASP55-rab2 effector complex linking Golgi structure to membrane traffic*. J Cell Biol, 2001. 155(6): p. 877-83.
157. Ward, T.H., et al., *Maintenance of Golgi structure and function depends on the integrity of ER export*. J Cell Biol, 2001. 155(4): p. 557-70.
158. Ramirez, I.B. and M. Lowe, *Golgins and GRASPs: holding the Golgi together*. Semin Cell Dev Biol, 2009. 20(7): p. 770-9.
159. Barr, F.A., et al., *GRASP65, a protein involved in the stacking of Golgi cisternae*. Cell, 1997. 91(2): p. 253-62.
160. Shorter, J., et al., *GRASP55, a second mammalian GRASP protein involved in the stacking of Golgi cisternae in a cell-free system*. EMBO J, 1999. 18(18): p. 4949-60.
161. Barr, F.A., N. Nakamura, and G. Warren, *Mapping the interaction between GRASP65 and GM130, components of a protein complex involved in the stacking of Golgi cisternae*. EMBO J, 1998. 17(12): p. 3258-68.
162. Behnia, R., et al., *The yeast orthologue of GRASP65 forms a complex with a coiled-coil protein that contributes to ER to Golgi traffic*. J Cell Biol, 2007. 176(3): p. 255-61.
163. Short, B., A. Haas, and F.A. Barr, *Golgins and GTPases, giving identity and structure to the Golgi apparatus*. Biochim Biophys Acta, 2005. 1744(3): p. 383-95.

164. Burkhard, P., J. Stetefeld, and S.V. Strelkov, *Coiled coils: a highly versatile protein folding motif*. Trends Cell Biol, 2001. 11(2): p. 82-8.
165. Nozawa, K., M.J. Fritzler, and E.K. Chan, *Unique and shared features of Golgi complex autoantigens*. Autoimmun Rev, 2005. 4(1): p. 35-41.
166. Shorter, J., et al., *Sequential tethering of Golgins and catalysis of SNAREpin assembly by the vesicle-tethering protein p115*. J Cell Biol, 2002. 157(1): p. 45-62.
167. Nakamura, N., et al., *Characterization of a cis-Golgi matrix protein, GM130*. J Cell Biol, 1995. 131(6 Pt 2): p. 1715-26.
168. Kooy, J., et al., *Human autoantibodies as reagents to conserved Golgi components. Characterization of a peripheral, 230-kDa compartment-specific Golgi protein*. J Biol Chem, 1992. 267(28): p. 20255-63.
169. Sonnichsen, B., et al., *A role for giantin in docking COPI vesicles to Golgi membranes*. J Cell Biol, 1998. 140(5): p. 1013-21.
170. Wang, Y., et al., *A direct role for GRASP65 as a mitotically regulated Golgi stacking factor*. EMBO J, 2003. 22(13): p. 3279-90.
171. Feinstein, T.N. and A.D. Linstedt, *GRASP55 regulates Golgi ribbon formation*. Mol Biol Cell, 2008. 19(7): p. 2696-707.
172. Puthenveedu, M.A., et al., *GM130 and GRASP65-dependent lateral cisternal fusion allows uniform Golgi-enzyme distribution*. Nat Cell Biol, 2006. 8(3): p. 238-48.
173. Preisinger, C., et al., *Plk1 docking to GRASP65 phosphorylated by Cdk1 suggests a mechanism for Golgi checkpoint signalling*. EMBO J, 2005. 24(4): p. 753-65.
174. Jesch, S.A., et al., *Mitotic phosphorylation of Golgi reassembly stacking protein 55 by mitogen-activated protein kinase ERK2*. Mol Biol Cell, 2001. 12(6): p. 1811-7.
175. Yoshimura, S., et al., *Convergence of cell cycle regulation and growth factor signals on GRASP65*. J Biol Chem, 2005. 280(24): p. 23048-56.
176. Lane, J.D., et al., *Caspase-mediated cleavage of the stacking protein GRASP65 is required for Golgi fragmentation during apoptosis*. J Cell Biol, 2002. 156(3): p. 495-509.
177. Nakamura, N., et al., *The vesicle docking protein p115 binds GM130, a cis-Golgi matrix protein, in a mitotically regulated manner*. Cell, 1997. 89(3): p. 445-55.
178. Allan, B.B., B.D. Moyer, and W.E. Balch, *Rab1 recruitment of p115 into a cis-SNARE complex: programming budding COPII vesicles for fusion*. Science, 2000. 289(5478): p. 444-8.
179. Malsam, J., et al., *Golgin tethers define subpopulations of COPI vesicles*. Science, 2005. 307(5712): p. 1095-8.
180. Diao, A., et al., *Coordination of golgin tethering and SNARE assembly: GM130 binds syntaxin 5 in a p115-regulated manner*. J Biol Chem, 2008. 283(11): p. 6957-67.
181. Roditi, I. and M.J. Lehane, *Interactions between trypanosomes and tsetse flies*. Curr Opin Microbiol, 2008. 11(4): p. 345-51.
182. Matthews, K.R., J.R. Ellis, and A. Paterou, *Molecular regulation of the life cycle of African trypanosomes*. Trends Parasitol, 2004. 20(1): p. 40-7.
183. Vickerman, K. and A.G. Luckins, *Localization of variable antigens in the surface coat of Trypanosoma brucei using ferritin conjugated antibody*. Nature, 1969. 224(5224): p. 1125-6.

184. Cross, G.A., *Identification, purification and properties of clone-specific glycoprotein antigens constituting the surface coat of Trypanosoma brucei*. Parasitology, 1975. 71(3): p. 393-417.
185. Ferguson, M.A., et al., *Biosynthesis of Trypanosoma brucei variant surface glycoproteins. N-glycosylation and addition of a phosphatidylinositol membrane anchor*. J Biol Chem, 1986. 261(1): p. 356-62.
186. Miller, J.K., *Variation of the soluble antigens of Trypanosoma brucei*. Immunology, 1965. 9(6): p. 521-8.
187. Pays, E., L. Vanhamme, and D. Perez-Morga, *Antigenic variation in Trypanosoma brucei: facts, challenges and mysteries*. Curr Opin Microbiol, 2004. 7(4): p. 369-74.
188. Pays, E., L. Vanhamme, and M. Berberof, *Genetic controls for the expression of surface antigens in African trypanosomes*. Annu Rev Microbiol, 1994. 48: p. 25-52.
189. Overath, P., et al., *Repression of glycoprotein synthesis and release of surface coat during transformation of Trypanosoma brucei*. EMBO J, 1983. 2(10): p. 1721-8.
190. Roditi, I., et al., *Procyclin gene expression and loss of the variant surface glycoprotein during differentiation of Trypanosoma brucei*. J Cell Biol, 1989. 108(2): p. 737-46.
191. Roditi, I. and M. Liniger, *Dressed for success: the surface coats of insect-borne protozoan parasites*. Trends Microbiol, 2002. 10(3): p. 128-34.
192. Vassella, E., et al., *A major surface glycoprotein of trypanosoma brucei is expressed transiently during development and can be regulated post-transcriptionally by glycerol or hypoxia*. Genes Dev, 2000. 14(5): p. 615-26.
193. Gull, K., *The cytoskeleton of trypanosomatid parasites*. Annu Rev Microbiol, 1999. 53: p. 629-55.
194. Woods, A., et al., *Definition of individual components within the cytoskeleton of Trypanosoma brucei by a library of monoclonal antibodies*. J Cell Sci, 1989. 93 (Pt 3): p. 491-500.
195. Robinson, D.R., et al., *Microtubule polarity and dynamics in the control of organelle positioning, segregation, and cytokinesis in the trypanosome cell cycle*. J Cell Biol, 1995. 128(6): p. 1163-72.
196. Yelinek, J.T., C.Y. He, and G. Warren, *Ultrastructural study of Golgi duplication in Trypanosoma brucei*. Traffic, 2009. 10(3): p. 300-6.
197. McConville, M.J., et al., *Secretory pathway of trypanosomatid parasites*. Microbiol Mol Biol Rev, 2002. 66(1): p. 122-54; table of contents.
198. He, C.Y., M. Pypaert, and G. Warren, *Golgi duplication in Trypanosoma brucei requires Centrin2*. Science, 2005. 310(5751): p. 1196-8.
199. Overath, P., Y.D. Stierhof, and M. Wiese, *Endocytosis and secretion in trypanosomatid parasites - Tumultuous traffic in a pocket*. Trends Cell Biol, 1997. 7(1): p. 27-33.
200. Vaughan, S. and K. Gull, *The trypanosome flagellum*. J Cell Sci, 2003. 116(Pt 5): p. 757-9.
201. Bastin, P., K.R. Matthews, and K. Gull, *The paraflagellar rod of kinetoplastida: solved and unsolved questions*. Parasitol Today, 1996. 12(8): p. 302-7.
202. Kohl, L., T. Sherwin, and K. Gull, *Assembly of the paraflagellar rod and the flagellum attachment zone complex during the Trypanosoma brucei cell cycle*. J Eukaryot Microbiol, 1999. 46(2): p. 105-9.

203. Scott, V., T. Sherwin, and K. Gull, *gamma-tubulin in trypanosomes: molecular characterisation and localisation to multiple and diverse microtubule organising centres*. J Cell Sci, 1997. 110 (Pt 2): p. 157-68.
204. Robinson, D.R. and K. Gull, *Basal body movements as a mechanism for mitochondrial genome segregation in the trypanosome cell cycle*. Nature, 1991. 352(6337): p. 731-3.
205. Shapiro, T.A. and P.T. Englund, *The structure and replication of kinetoplast DNA*. Annu Rev Microbiol, 1995. 49: p. 117-43.
206. El-Sayed, N.M., et al., *The African trypanosome genome*. Int J Parasitol, 2000. 30(4): p. 329-45.
207. Williams, R.O., J.R. Young, and P.A. Majiwa, *Genomic environment of T. brucei VSG genes: presence of a minichromosome*. Nature, 1982. 299(5882): p. 417-21.
208. McKean, P.G., *Coordination of cell cycle and cytokinesis in Trypanosoma brucei*. Curr Opin Microbiol, 2003. 6(6): p. 600-7.
209. Lacomble, S., et al., *Basal body movements orchestrate membrane organelle division and cell morphogenesis in Trypanosoma brucei*. J Cell Sci, 2010. 123(Pt 17): p. 2884-91.
210. McKean, P.G., et al., *Gamma-tubulin functions in the nucleation of a discrete subset of microtubules in the eukaryotic flagellum*. Curr Biol, 2003. 13(7): p. 598-602.
211. He, C.Y., et al., *Golgi duplication in Trypanosoma brucei*. J Cell Biol, 2004. 165(3): p. 313-21.
212. Sherwin, T. and K. Gull, *The cell division cycle of Trypanosoma brucei brucei: timing of event markers and cytoskeletal modulations*. Philos Trans R Soc Lond B Biol Sci, 1989. 323(1218): p. 573-88.
213. Cosgrove, W.B. and M.J. Skeen, *The cell cycle in Crithidia fasciculata. Temporal relationships between synthesis of deoxyribonucleic acid in the nucleus and in the kinetoplast*. J Protozool, 1970. 17(2): p. 172-7.
214. Kohl, L., D. Robinson, and P. Bastin, *Novel roles for the flagellum in cell morphogenesis and cytokinesis of trypanosomes*. EMBO J, 2003. 22(20): p. 5336-46.
215. Ralston, K.S., et al., *Flagellar motility contributes to cytokinesis in Trypanosoma brucei and is modulated by an evolutionarily conserved dynein regulatory system*. Eukaryot Cell, 2006. 5(4): p. 696-711.
216. de Graffenried, C.L., H.H. Ho, and G. Warren, *Polo-like kinase is required for Golgi and bilobe biogenesis in Trypanosoma brucei*. J Cell Biol, 2008. 181(3): p. 431-8.
217. Hammarton, T.C., *Cell cycle regulation in Trypanosoma brucei*. Mol Biochem Parasitol, 2007. 153(1): p. 1-8.
218. Field, M.C. and M. Carrington, *Intracellular membrane transport systems in Trypanosoma brucei*. Traffic, 2004. 5(12): p. 905-13.
219. Sevova, E.S. and J.D. Bangs, *Streamlined architecture and glycosylphosphatidylinositol-dependent trafficking in the early secretory pathway of African trypanosomes*. Mol Biol Cell, 2009. 20(22): p. 4739-50.
220. Vaughan, S., et al., *A repetitive protein essential for the flagellum attachment zone filament structure and function in Trypanosoma brucei*. Protist, 2008. 159(1): p. 127-36.
221. Morriswood, B., et al., *The bilobe structure of Trypanosoma brucei contains a MORN-repeat protein*. Mol Biochem Parasitol, 2009. 167(2): p. 95-103.

222. Ho, H.H., et al., *Ordered assembly of the duplicating Golgi in Trypanosoma brucei*. Proc Natl Acad Sci U S A, 2006. 103(20): p. 7676-81.
223. Sanders, M.A. and J.L. Salisbury, *Centrin plays an essential role in microtubule severing during flagellar excision in Chlamydomonas reinhardtii*. J Cell Biol, 1994. 124(5): p. 795-805.
224. Field, H., et al., *Cell-cycle and developmental regulation of TbRAB31 localisation, a GTP-locked Rab protein from Trypanosoma brucei*. Mol Biochem Parasitol, 2000. 106(1): p. 21-35.
225. Schlaeppli, K., J. Deflorin, and T. Seebeck, *The major component of the paraflagellar rod of Trypanosoma brucei is a helical protein that is encoded by two identical, tandemly linked genes*. J Cell Biol, 1989. 109(4 Pt 1): p. 1695-709.
226. Ramirez, I.B., et al., *TbG63, a golgin involved in Golgi architecture in Trypanosoma brucei*. J Cell Sci, 2008. 121(Pt 9): p. 1538-46.
227. Broadhead, R., et al., *Flagellar motility is required for the viability of the bloodstream trypanosome*. Nature, 2006. 440(7081): p. 224-7.
228. Boucher, N., et al., *An essential cell cycle-regulated nucleolar protein relocates to the mitotic spindle where it is involved in mitotic progression in Trypanosoma brucei*. J Biol Chem, 2007. 282(18): p. 13780-90.
229. LaCount, D.J., B. Barrett, and J.E. Donelson, *Trypanosoma brucei FLA1 is required for flagellum attachment and cytokinesis*. J Biol Chem, 2002. 277(20): p. 17580-8.
230. Price, H.P., et al., *The small GTPase ARL2 is required for cytokinesis in Trypanosoma brucei*. Mol Biochem Parasitol, 2010.
231. Shi, J., et al., *Centrin4 coordinates cell and nuclear division in T. brucei*. J Cell Sci, 2008. 121(Pt 18): p. 3062-70.
232. Panic, B., J.R. Whyte, and S. Munro, *The ARF-like GTPases Arl1p and Arl3p act in a pathway that interacts with vesicle-tethering factors at the Golgi apparatus*. Curr Biol, 2003. 13(5): p. 405-10.
233. Van Valkenburgh, H., et al., *ADP-ribosylation factors (ARFs) and ARF-like 1 (ARL1) have both specific and shared effectors: characterizing ARL1-binding proteins*. J Biol Chem, 2001. 276(25): p. 22826-37.
234. Setty, S.R., et al., *Golgi recruitment of GRIP domain proteins by Arf-like GTPase 1 is regulated by Arf-like GTPase 3*. Curr Biol, 2003. 13(5): p. 401-4.
235. Rothman, J.E., *Mechanisms of intracellular protein transport*. Nature, 1994. 372(6501): p. 55-63.
236. Barr, F.A., et al., *Golgi matrix proteins interact with p24 cargo receptors and aid their efficient retention in the Golgi apparatus*. J Cell Biol, 2001. 155(6): p. 885-91.
237. Xiang, Y. and Y. Wang, *GRASP55 and GRASP65 play complementary and essential roles in Golgi cisternal stacking*. J Cell Biol, 2010. 188(2): p. 237-51.
238. Brun, R. and Schonenberger, *Cultivation and in vitro cloning or procyclic culture forms of Trypanosoma brucei in a semi-defined medium. Short communication*. Acta Trop, 1979. 36(3): p. 289-92.
239. Wirtz, E., et al., *A tightly regulated inducible expression system for conditional gene knock-outs and dominant-negative genetics in Trypanosoma brucei*. Mol Biochem Parasitol, 1999. 99(1): p. 89-101.

Acknowledgements

First of all I want to say thank you to my parents and grandparents who provided me moral and financial support throughout my studies. I also owe my deepest gratitude to Thea for enduring and encouraging me during tough times and, even more, for sharing the pleasant times with me.

I am indebted to all my friends and colleagues for providing necessary and welcome balance during stressful periods.

My special acknowledgements go to my co-workers in the Warren-lab for all their help, excellent advice, the good working atmosphere and of course for taking care of my cells on a couple of weekends.

I would like to thank my advisor Lars for introducing me to the project, providing excellent assistance during my work on the thesis and upgrading my knowledge of molecular biology. I am also grateful to him for proofreading this thesis frequently and providing me helpful suggestions for improvement.

Last but not least, I would like to take the opportunity to thank my supervisor Graham Warren who made it possible to work in his lab and for reviewing my master thesis.

Curriculum Vitae

Name: Melak Michael
Date of birth: 20th March, 1981
Place of birth: Mistelbach, Austria

Education

2004 - 2010 Molecular Biology, University of Vienna
1995 - 2000 Handelsakademie Mistelbach

Work experience

06/2001 – 09/2004 Raiffeisen Zentralbank Österreich AG – Cost controlling
09/2000 – 04/2001 Military service

Research experience

02/2009 – 05/2010 Master Thesis
Max F. Perutz Laboratories, Vienna
Prof. Graham Warren
Differential effects of TbSec24 isoforms on Golgi proteins in *T. brucei*

07/2008 – 08/2008 Internship
Max F. Perutz Laboratories, Vienna
Prof. Graham Warren
Components and binding partners of the Golgi apparatus underlying bilobed structure in *T. brucei*

02/2008 – 03/2008 Internship
Nepean Hospital, Discipline of Paediatrics, Sydney
Prof. Ralph Nanan
A comparative analysis of regulatory T-Lymphocytes in healthy and pre-eclamptic pregnancies

07/2007 – 08/2007 Internship
IMBA - Institute of Molecular Biotechnology of the Austrian Academy of Sciences, Vienna
Prof. Josef Penninger
MKK7 and its role in breast cancer by generating in vitro and mouse models